To the Graduate Council:

I am submitting herewith a thesis written by Taisuke Akasaka entitled "Modelling Bone Fracture Behavior: The Case for Fuzzy Logic." I have examined the final copy of this thesis for form and content and recommend that it be accepted in partial fulfillment of the requirements for the degree of Master of Science, with a major in Engineering Science.

Jack Wasserman

J. F. Wasserman, Major Professor

We have read this thesis

and recommend its acceptance:

Accepted for the Council:

Associate Vice Chancellor

and Dean of The Graduate School

STATEMENT OF PERMISSION TO USE

In presenting this thesis in partial fulfillment of the requirements for a Master's degree at The University of Tennessee, Knoxville, I agree that the Library shall make it available to borrowers under rules of the Library. Brief quotations from this thesis are allowable without special permission, provided that accurate acknowledgement of the source is made.

Permission for extensive quotation from or reproduction of this thesis may be granted by my major professor, or in his absence, by the head of Interlibrary Service when, in the option of either, the proposed use of the material is for scholarly purposes. Any copying or use of the material in this thesis for financial gain shall not be allowed without my written permission.

Signature Taisuke Akasaka

Date December 3, 1993

Modelling Bone Fracture Behavior: The Case for Fuzzy Logic

A Thesis

Presented for the

Master of Science

Degree

The University of Tennessee, Knoxville

Taisuke Akasaka

December 1993

ACKNOWLEDGMENTS

The research contract sponsored by the Japan Automobile Manufacturers Association (JAMA), Inc. was started at the University of Tennessee in June, 1986 to study the impact fractures of human bones. This thesis, entitled "Modelling Bone Fracture Behavior: The Case for Fuzzy Logic," is the fourth thesis published for the project since 1986.

Uncountable thanks are reserved for the author's parents who have long awaited the completion of this thesis. Their financial support and unlimited love and patience have made this publication possible. The care of the author's brother-in-law, his sister, and his old school friends Wu Wei and Lai Teh must not be forgotten also. The long distance phone calls from them have always encouraged the author spiritually.

The author expresses special thanks to his project mates, Tyler Kress and David Porta, from the University of Louisville. Their help and dedication in the laboratory work for this thesis is enormous. The author especially thanks David for the detailed dissection data. The visit of Layne, his cute two-year-old daughter, was very entertaining. Tyler's frequent impersonation of Barney at the lab was a comic relief during the overnight lab work. It made the hard working hours in the lab rather short.

Other special thanks are reserved for Doug Squires from KODAK Inc. and Dr. R. C. Berkan from MODiCO Inc. in Knoxville, TN. Doug generously loaned the latest high speed video camera free of charge on his way to business travel, and the FUZZLE1.8 program locally developed by Dr. Berkan in 1992 gave the thesis the final push toward completion.

Appreciation is also extended to Eunice Hinkle, Dr. Fortey and Faye Muly. Eunice's care made it possible for the author to stay in school as a FORTRAN teaching assistant throughout his graduate school years. The author truly enjoyed the assistant work under Dr. Fortey from England for the first two years and Faye. Muly for the last two years.

A final "thank you" is reserved for Dr. Jack Wasserman, the major professor, and Dr. John Snider, the project principal investigator. The author thanks them for their consultations, generosity, and patience over the years.

ABSTRACT

This thesis, entitled "Modelling Bone Fracture Behavior: The Case for Fuzzy Logic," is based on the laboratory experiments for the research project sponsored by Japan Automobile Manufacturers' Association (JAMA). The ultimate research goal is focused to develop an advanced computer code that can simulate bone fracture behaviors under impact loading.

To seek possible approaches and determine the one best capable of describing bone fracture behaviors as efficiently and accurately as possible, a number of theories and methods are researched here. In this thesis, the basics of impact fracture mechanics, finite element method for crack simulation, and fuzzy logic theory are discussed. For its versatility, flexibility, and ease of application, the fuzzy logic approach appears to be the best approach to be used for bone fracture predictions.

To provide the data base for the fuzzy expert system, a series of impact tests were performed on intact legs under conditions as close to real auto accident cases as possible. To generate the friction force on the foot at impact, an unique leg holding device on which weights can be put was designed. To study the effect of impact shock absorption by bumpers, a new bumper system supported by air-springs was developed.

Experimental results, rules, and membership functions used for the fuzzy expert system are discussed. The designed fuzzy expert system performance can match experimental data very closely. Although the program was developed only for demonstration purposes due to its small database size, this program behaves well within the specified range of

variables on the data base. As the data base grows bigger in the future, the program's accuracy and dependability are going to improve.

PREFACE

Theoretical description of material failures caused by impact loading is a new frontier of contemporary engineering. Numerous efforts have been put into experimental research and the formulation of theories all over the world. However, impact fracture mechanics is still falls short of being called an established field because the description of criteria factors and experimental methods for basic data are not yet standardized internationally. Everyone who approaches this frontier with different ideas is a pioneer since it is a battle-field of trials and errors.

Fuzzy logic is an innovative new concept which can be used for prediction and classification. However, its application is very similar to the classic problem solving approach of engineers since it requires a series of experimental data and rich knowledge of experts rather than extensive theory. For example, the Wright brothers, the pioneers of powered flight, were neither famous scientists nor physicists. Compared to the leading scientists who were also working hard on powered flight with government funds, they lacked theoretical knowledge and financial aid. Despite their lack of resources, they were the first to be successful.

Instead of depending heavily on calculations based on theories, the Wright brothers took a trial-and-error approach. As the series of real flight experiments proceeded, their knowledge and experience were enriched. In the competition toward the first powered flight, their approach turned out to be far more accurate and efficient than the calculated predictions and designs based on theories. Their time consuming step-by-step experimental approach,

which was considered to be less efficient by many scientists, eventually succeeded better than the mathematical approach in a short time. The problem of early aviation theories was oversimplification. A number of factors operational in real life were disregarded so that the theories only worked in an ideal imaginary world. For similar reasons, the fuzzy logic approach should be taken for the development of impact bone fracture simulation.

TABLE OF CONTENTS

CHAPTER	PAGE
I. INTRODUCTION	
A. Background Information	1
B. Approach Applied	2
C. Objective of Research	4
II. LITERATURE REVIEW	
A. Basic Characteristics of Bone Structure	6
1. General Information	6
2. Cortical Bone and Trabecular (Spongy) Bone	6
3. Woven Bone and Lamellar Bone	7
4. Structure of Lamellar Bone	8
5. Bone Modeling and Remodeling	10
6. Change of the Bone Structure Due to Aging	10
7. Bone Fracture	11
8. The Dynamic Properties and Fracture	11
9. Anisotropic Characteristics	12
10. Structure of a Shaft Bone Described by Wolff's Law	14
B. Mechanical Strength of Shaft Bones	18
1. Strength Referred to Mechanics of Materials	18
2. Material Strength Under Impact	23
C. The classification of bone fractures	23
1. General Information	23
2. Fracture Types of Femur and Tibia	29
3. Fracture Situational Category Classifiction	31
D. Effect of the Impact Object Surface Shape	31
E. Relationship Between Impact Velocity and Deformations	34
F. Stress Concentration in Static and Dynamic Cases	34
III. APPROACH TO THE FRACTURE PROBLEM	

A. FINITE ELEMENT METHOD APPROACH 39

1. History of Finite Element Method and Fracture Theories 39

2. Classification of the Fracture Mechanics 40

a. General Information 40

b. Liner Elastic Fracture Mechanics 42

c. Non-linear Elastic Fracture Mechanics 43

d. Dynamic Fracture Mechanics 47

e. Probabilistic Fracture Mechanics 47

3. Modes of Fractures and Associated Parameters 48

a. General Information 48

b. The Stress Intensity Factor 51

c. The Dynamic Energy Release Rate 53

4. Problems Associated with the FEM Approach 54

a. General Information 54

b. Crack simulation by FEM 56

c. Incubation Time for Crack Start 57

d. Variance Among Specimens 60

5. Finite Element Programs Capable of Evaluating Fractures 60

B. IMPACT FRACTURE MECHANICS APPROACH

1. Impact Fracture Mechanism 62

a. General Information 62

b. Stress Wave Created by Impact 62

c. Stress Wave Behavior at Boundry 65

d. Impact Collision Between Two Bars 67

e. Collision of Bars with Different Cross Sections 69

f. Stress in the Bar with Stepped Cross Sections 72

IV. FUZZY LOGIC APPROACH

A. Introduction to Fuzzy Logic 75

1. General Information 75

2. Merits of Fuzzy Logic 76

3. Fields in which Fuzzy Logic is Applied 78
4. Expression of Fuzziness 79

B. The Basic Concept of Fuzzy Logic 79
1. Fuzzy Variable 80
2. Membership Function 82
3. Membership Cuts 84
4. Rule Composition 86
5. Implication Principle 86
6. Graphical Concept of Fuzzy Logic 89

C. Actual Example of Fuzzy Logic Application 94
1. Application to Failure Analysis 94
2. Application to Dynamic Failure Analysis 98
3. Fuzzy Data Analysis Concept 101

V. FUZZY EXPERT SYSTEM DEVELOPMENT FOR BONE FRACTURE PREDICTION

A. Bone Fracture Simulation Construction Steps 102

B. Experimental Approach 104
1. Test Set-up 104
2. Experimental Testing Devices 104
3. Impactor Cart Bumper Design 105
4. Impactor Attachments 110
5. The Leg Holding Device 110
6. Test Parameters 114
7. Specimen Preparation 114
8. Specimen Mounting 115

C. Test Objectives 116
1. Main Objective 116
2. Test Focal Points 117

D. Experimental Result and Disection Notes 119

E. Plots of Experimental Result 128

F. Rules and Variable behaviors of the TEST Program 137
1. Functions of TEST Program 151

2. Questions and Input Variables at Program Run 152
3. Subroutione Calls and Output 153
4. Sample Output 154

G. Designed Membership Functions for the TEST program 156

H. Briefing of FUZZLE 1.8 and Developed Program 158

VI. CONCLUSIONS & RECOMMENDATIONS

A. Age, Sex and Mean cortex Thickness 160
B. Leg Mass Variation 161
C. Impact Location 161
D. Friction Condition 162
E. Impact Direction 163
F. Impact Speed vs Impact Force 164
G. Effect of the Bumper Springs 165
H. Impact Surface 165
I. Bumper Surface Covering Material 166
J. Comments on Fuzzy Expert System development 166
K. Recommendations 168

BIBLIOGRAPHY 169

APPENDIX 173

A. Photographs From Impact Test Lab 174
B. Force vs. Time Plots of Each Impact Test Series 180
C. Additional Data Resource 186
D. TEST program Fortran Source Code 190

VITA 217

LIST OF TABLES

TABLE		PAGE
3-1.	Evaluation of major FEM programs.	61
5-1.	Consecutive impact force vs. speed data from specimen, TL009L.	
	10cm impact plate with air springs (A).	119
	4cm impact plate with air springs (B).	120
	4cm impact plate without air springs (C).	121
5-2.	Consecutive impact force vs. speed data from specimen, TL961R.	121
5-3.	Consecutive impact force vs. speed data from specimen, TL755L.	122
5-4.	Consecutive impact force vs. speed data from specimen, TL991L.	123
5-5.	Consecutive impact force vs. speed data from specimen, TL070L.	124
5-6.	Consecutive impact force vs. speed data from specimen, TL070R.	124
5-7.	Consecutive impact force vs. speed data from specimen, TL949L.	125
5-8.	Consecutive impact force vs. speed data from specimen, TL949R.	125
5-9.	Pre-disection notes for leg impacts.	126
5-10.	Disection notes for leg impacts.	127
5-11.	Rules and weighting factors for TEST1.	138
5-12.	TEST1 variable behavior.	140
5-13.	Rules and weighting factors for TEST2.	142
5-14.	TEST2 variable behavior.	143
5-15.	Rules and weighting factors for TEST3.	147
5-16.	TEST3 variable behavior.	148
5-17.	Rules and weighting factors for TEST4.	149
5-18.	TEST4 variable behavior.	150
APN-1.	Dynamic impedance of various materials.	189

LIST OF FIGURES

FIGURE		PAGE
2-1.	Structure of lamellar bone.	9
2-2.	Examples of green stick fractures.	13
2-3.	Nonisotropic characteristics of the cortical bone of femur.	15
2-4.	Trabecular bone structure of femur.	17
2-5.	Moments of inertia of various cross-sectional geometries.	19
2-6.	3 point bending test.	21
2-7.	Thickness changes along the shaft.	22
2-8.	Material strength under high speed loading (A) and comparison of static compression and impact compression (B).	25
2-9.	Muller's bone fracture classification.	
	Fracture location classification code (A).	27
	Basic structure of bone fracture classification tree (B).	28
	fracture classification data of tibias (C).	30
2-10.	Effects of impact object shape.	32
2-11.	Deformation of ring diameters vs. impact speed (A) and resultant ing deformation by impact (B).	35
2-12.	Strain distribution on the femur loaded at the femur head.	37
2-13.	Cross-sectional forces and cross-sectional moments on a shell.	38
3-1.	J-R curve.	44
3-2.	Crack tip parameters.	46
3-3.	3 basic fracture modes.	49
3-4.	Finite element parameters.	52
3-5.	Evaluation process of a crack by FEM.	58
3-6.	Idealized stress-strain curve in tensile impact.	59
3-7.	Stress wave created by impact.	64
3-8.	Counter wave and reflection wave at boundary.	66
3-9.	Head to head collision of two bars.	68
3-10.	Collision of two bars with different cross-sectional areas.	70
3-11.	Bar with stepped cross-sections.	73
4-1.	Fuzzy variable.	81

4-2. Membership function. 83
4-3. Membership cuts. 85
4-4. Rule composition. 87
4-5. Implication principle. 88
4-6. Graphical explanation of fuzzy inference-1, 2, 3 and 4. 90
4-7. Evaluation diagram for structure safety assessment (A), actual example of rules used (B), and actual example of designed membership functions (C). 95
4-8. Specimen data & four points loading (A) and bending strength vs. surface coarseness (B). 99

5-1. Firestone air-springs used for the new bumper system. 107
5-2. Schematic design of the air-spring bumper system (A) and photographs of the air-spring bumper system (B). 108
5-3. Schematic design of the leg holding cramp couple (A) and leg specimen mounted on the leg holding device (B). 112 113

Data Plots in Section 5-(E) PAGE

5-4. Plot of impact data from the tibia specimen, TL755L. 128
5-5. Plot of impact data from the tibia specimen, TL991L. 129
5-6 Plot of impact data from the tibia specimen TL009L. 130
5-7. Plot of impact data from tibia specimens, TL949L & TL949R. 131
5-8. Plot of impact data from tibia specimens, TL070L.& TL070R. 132
5-9. Overlay plot of impact data from TL070L/R & TL949L/R. 133
5-10. Linear interpolations (slopes) for TL991L, TL755L, and TL009L. 134
5-11. Linear interpolations (slopes) for TL070, TL949, and TL961. 135
5-12. Plots of age vs. impact force at fracture, and average cortex thickness vs. impact force at fracture. 136

Membership Functions in Section 5-(G) PAGE

5-13. Membership functions for TEST1 (radius and slope) and Membership functions for TEST2 (radius, frict, direct and slope). 156
5-14. Membership functions for TEST3 (age, sex, cortex and strng) and Membership functions for TEST4 (diffrn and possib). 157

Figures in Appendix

FIGURE		PAGE
APN-1.	Front view of the impact cart and the leg mounting device.	174
APN-2.	Experimental setting & damage checking.	175
APN-3.	Snapshots of just before the impact & during the impact.	176
APN-4.	Impact sequence filmed.by the high-speed video camera.	177
APN-5.	Force vs. time plots.	180
APN-6.	Load vs. deflection of shaft bones.	186
APN-7.	Distribution of bone fracture experiment data points.	187
APN-8.	The change of muscle thickness along the leg.	188

Chapter I

INTRODUCTION

(A)

Background Information

Since 1986, a Japan Automobile Manufacturers' Association (JAMA) project team has been collecting experimental data on human leg fractures incurred as the result of various types of impact loading. The JAMA project staff has been working on ways to use the data for research into leg injuries associated with automobile and motorcycle accidents. As a long-term objective, chief lab conductor Dr. J. Wasserman seeks to develop a program capable of predicting bone fractures realistically in a variety of dynamic conditions.

Currently available dummy programs used for research by auto manufacturers lack the ability to predict the damage to the human body because the dynamic equations in these programs assume that a body, like a dummy, is composed of rigid unbreakable parts. Additionally, these programs can only predict the reactions of major body parts such as the head, hands, and legs in response to exterior force loading. Under such limitations as these, no realistic assessment of the location, type, and severity of fracture is possible.

(B)

Approach Applied

The primary method of modeling the impact fracture behavior of bone is the use of a finite element code, a method which is widely used for structural stress analysis today. However, this type of simulation is problematic for two reasons:

(1) There are technical difficulties associated with collecting the data required to run the program. The stress intensity factors, for example, must be obtained for each element experimentally.

(2) There are theoretical difficulties associated with the current FEM codes themselves. For example, none of the theory takes the high speeds at which most impact fractures occur into consideration.

With extensive program modifications, application of the finite element method may still be useful. From a practical standpoint, however, the FEM approach takes too long to get output, and the necessary modifications of the program are complex. Besides the FEM approach, there are two other possible approaches to the bone fracture prediction problem: pure statistics and pure dynamics (impact fracture mechanics). However, both approaches also present technical difficulties. The pure statistics approach requires a large amount of experimental data. Unlike machined specimens, no two bones are exactly the same, and the strength of individual bone varies. But, each bone can only be used for a single fracture test. Bones are not reusable for another test after breaking. It is, therefore, difficult to gather sufficient comparable data for the statistics approach. Small differences that affect the fracture

outputs cannot be simulated. Strictly speaking, the statistics approach can only get a mean of outputs.

On the other hand, the impact fracture mechanics approach suffers from the gap between experimental results and calculated results caused by oversimplification of the problem. This approach requires the behavior of a model under impact to be expressed by mathematical equations, and therefore, the shape of the bone must be represented by a simple geometric model to reduce the complexity of equations.

However, there is a newer logic now available which can achieve a fairly accurate fracture prediction while avoiding theoretical and technical difficulties, and without complicating the inferring process. This is fuzzy logic, a method developed by Professor L. A. Zadeh in 1966 at the University of California. Fuzzy logic is designed to deal with the interpretation of ambiguous questions in the framework of a database, and so it is ideal for this research. Today, control logic devices using fuzzy logic inference systems have been widely applied to a variety of things, from auto-focus cameras to complex factory machineries. In fuzzy logic, the correlations between parameters are described by simple IF-THEN rules expressed in the form of human language (for example, IF the speed is high, THEN the impact is large). Based on a series of effective IF-THEN rules extracted from experimental data, known basic principles, and formulas, fuzzy logic has proven itself useful in problems too complicated (or delicate) to be described by a mathematical formula.

The effectiveness of fuzzy logic can also be seen in non-linear dynamic problems such as structural safety analysis and automobile speed control. Fuzzy logic inference can be modified very easily. Adding or subtracting a

parameter can be done smoothly without distorting the rest of the parameter relationships. In fuzzy logic, parameters such as age and sex can be factored in smoothly.

(C)

Objective of Research

This thesis investigates the feasibility of applying fuzzy logic to the problem of bone fracture prediction. This thesis consists of three major parts. Part one reviews the basic characteristics of bone structure, with particular attention to the structural characteristics that make prediction of bone's behavior under impact difficult. Part two reviews problems with two approaches currently proposed as methods for modeling bone fracture type prediction: the finite element approach and impact fracture mechanics. Part three proposes a new and potentially more successful approach based on fuzzy logic. The nature of fuzzy logic and the way it can be used to approach the bone fracture problem are described.

In my experimental testing session, the setting is focused in order to recreate a realistic as possible situation of a bumper-leg impact. The potential ability of the bumper shock absorption capability to reduce the impact fracture speed is also investigated with a newly designed bumper system using air springs.

As a conclusion to the thesis, the fuzzy logic inference method is shown to be the simplest, fastest, and easiest way to accomplish realistic bone fracture

predictions, eliminating the technical and logical difficulties associated with the finite element method and impact fracture mechanics.

By using the parameter relationships implied by the experimental data, human intuition, and impact fracture mechanics, the fuzzy logic system will predict the resultant fracture pattern for various conditions in the same manner a human would predict it. Because a fuzzy logic program is easy to modify to a more complex version without altering the entire programming code, predictions of the degree of damage to the skin, muscle, arteries, and veins will also be possible in the future with the acquisition of new data. The fuzzy logic bone fracture pattern prediction program will be primarily useful for the pre-diagnosis of auto accident patients by orthopedists. However, it will also be useful to automobile manufacturers when designing safer vehicles.

Chapter II

LITERATURE REVIEW

(A)

Basic Characteristics of Bone Structure

1. General Information.

Unlike materials whose properties can be considered uniform (isoparametric), the characteristics of bones are non-uniform, since bones consist of the numbers of living cells which are filled with biochemical substances. It is known that the collagen affects tensile strength, and hydroxyapatite affects the compressive strength. The most unique characteristic of bones is the change of hardness due to the adherence of crystals (such as hydroxyapatite and phosphorus) to collagen

2. Cortical Bone and Trabecular (Spongy) Bone.

Bones can be classified by the exterior appearance into cortical bone and spongy bone. Cortical bone has a densely packed interior structure. Spongy bone has a hollow bubbled structure. About 80% of the total bone volume in a human is cortical bone. The exterior of the limb bones is coated by a thick layer of cortical bone cells. The majority of spongy bone is found in vertebrae, trochanters (the end parts of shaft bone), and the circumference of pelvis.

According to Shimazu and Asada, the hardness of the bone is proportional to its density, so that the cortical bone is harder than the spongy bone. The formation and the ratio of the cortical bone to the spongy bone are affected by the stimulation from the exterior dynamic environment. Certain types of exercises or sports will induce thickening of the bones. To bear torsion and bending, tibias have a thick layer of cortical bone cells around the shaft. On the other hand, the trochanter areas made of the spongy bone are the most elastic and strong against distortion. They are designed to absorb sudden impact stress and allow bending stress.

3. Woven Bone and Lamellar Bone.

There are two types of immature bone, woven bone and lamellar bone. Woven bone is the primitive bone which forms the bones of embryos. The callus, which is formed between broken bone segments for fusion, is also woven bone. The woven bone is temporary, and it is later going to be replaced by lamellar bone as the skeletal structure grows. Compared to lamellar bone fibers, woven bone contains four times the bone cells in per unit volume and has a structure of fibers running in random directions. The calcification speed, the size, and the arrangement of the bone cells are not uniform in woven bone. Because of that, woven bone is easy to deform during its formation, and it is less rigid in strength compared to lamellar bone. Occasionally fractured bones, which seemed to be fusing fine on the X-ray examination after a few weeks of healing process, may deform later. This deformation is due to the fact that the woven bone has not yet been totally

replaced by the lamellar bone. As a result, the bone is susceptible to the exterior force and weak in strength.

4. Structure of Lamellar Bone.

Mature bone is mostly cortical bone. Structually, cortical bone consists of osteons with haversian canals which contain nerve fibers, blood vessels and lymph vessels (See figure 2-1). Collagen fibers spiral axially around each osteon in concentric layers. Lamellar bone results from the deposition of inorganic salts on collagen fibers. Neighboring fiber layers of the circumferential lamellae are intermeshing, just like the grains of plywood layers cross to reinforce its strength. Collagen fibers are connected to one another not only within the lamellar layers, but also across the lamellar layers. This cross-connectedness makes the structure very tough.

Between the osteon tubes, there are irregularly shaped bone called interstitial lamellae. The boundary layer which surrounds the bone units is called the cementing line. This cementing line contains almost no collagen. Since no collagen fibers come across this boundary, the continuity of the collagen is cut off here. Therefore, it is the weak link of the lamellae bone (Buckwalter, 1987).

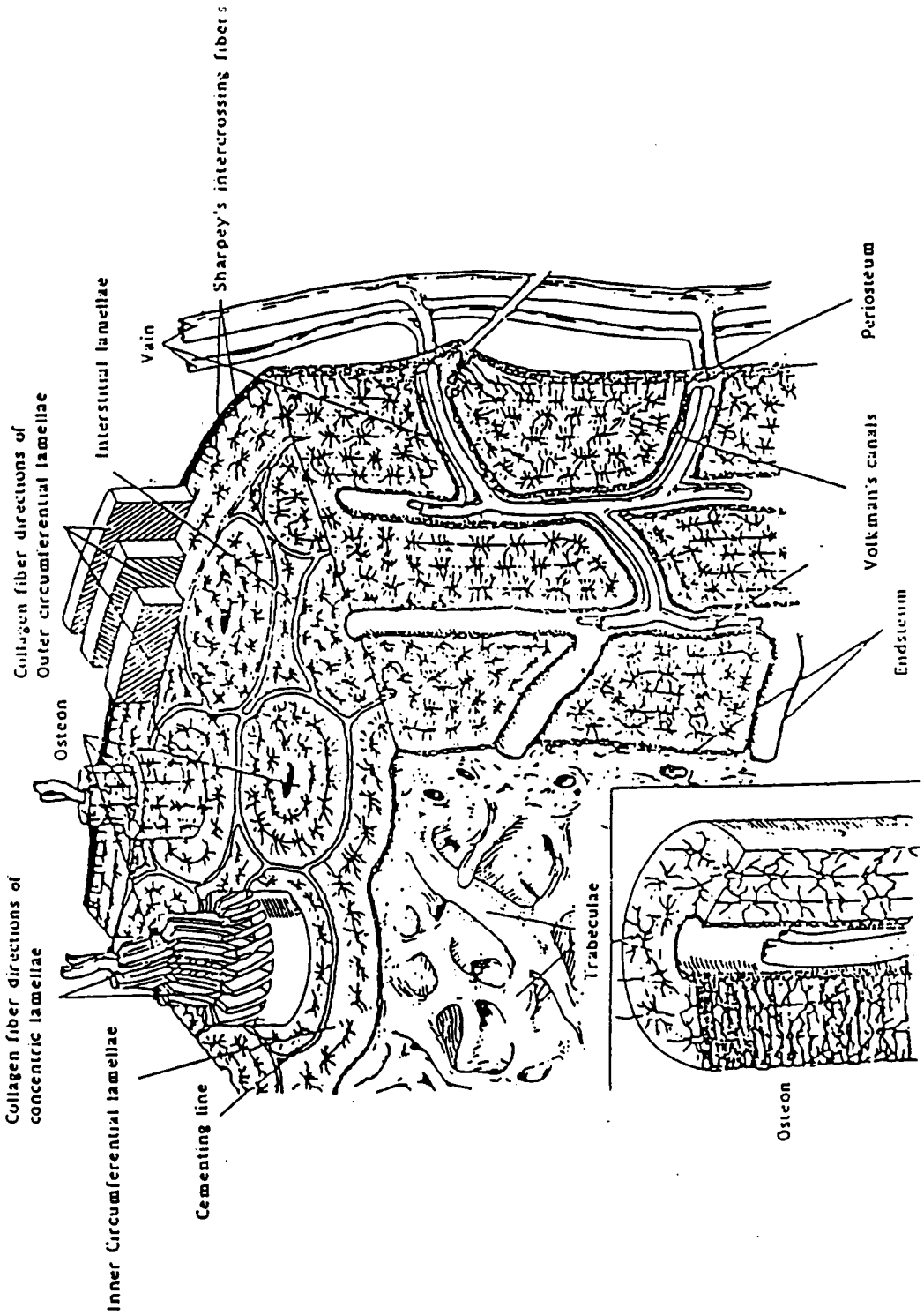


Figure 2-1.

Structure of lamellar bone.

(Backwalter, 1987)

5. Bone Modeling and Remodeling.

By the time the bones of an embryo are formed, the final shape, and size of the bones are already predetermined according to the gene information. However, the growth of bones is mainly controlled by the rate of osteoblast (the activity of generating new bone cells). Constant physical exercises during the growth period affect the rate of osteoblast. Therefore, the bone strength, size, and shape can be changed by the level of physical activity within a predetermined limit.

6. Change of the Bone Structure Due to Aging.

Bone thickness diminishes with age. The activity of removal of bone is known as resorption and is accomplished by osteoclasts. Adult cortical bone diminishes by 3% of its volume every 10 years. The spongy bone diminishes at a little higher rate, that is 6 to 8% of volume in every 10 years, and according to M. Okazima (1991), this phenomenon is more pronounced in Caucasian women. After 40 to 50 years of age, the rate of diminution increases to 9% every 10 years. As aging proceeds, the rate of osteoclast activity gradually exceeds the rate of osteoblast activity. Even though new bone is still created, it cannot keep up with the rate of absorption. As a result, bones get thinner and weaker.

7. Bone Fracture.

In biomechanics, it is important to analyze the mechanism of bone fracture from an engineering aspect. When some sort of external force is applied to a bone, the bone deforms. As the external force increases, the deformation also increases, and at some point the continuity of the bone cells is lost. As a result, the bone fractures. The relationship between load and deformation of limb bones shows a linearity. Within the elastic range, the deformation is almost proportional to the external load. As the load exceeds the yielding stress, the bone experiences permanent deformation, and at some point it finally fractures.

8. The Dynamic Properties and Fracture.

Bones can be classified into two major types, the spongy bone and the cortical bone. Carter and Hayes (1983) classified them by the percent intensity of holes. According to their classification, for the sponge bone, the density of holes is 30 to 90% of volume, and for the cortical bone, the intensity of the holes is 5 to 30%. Compared to the trabecular bone (spongy bone), the cortical bone has higher stiffness.

Although cortical bone is strong against compressive stress, it is brittle against strain deformation; it cannot sustain high strain. F. G. Evans said that most bone fractures occur in tension under both static and impact loads. According to Y. Obara (1982), the cortical bone breaks when the strain rate exceeds 2%; It is brittle. On the other hand, the spongy bone can sustain up to a

7% of strain; It is ductile. Obara said that the property of the cortical bone is similar to that of glass, and the property of the spongy bone is similar to that of a very weak metal such as aluminum.

The properties of bones change with aging as well as the patterns of fracture. The green stick fractures are seen only in infants and young children (See figure 2-2). On the other hand, the buckling fractures are seen only in elderly people. Both of the fracture styles are quite different from the fracture styles of mature adults.

The green stick fracture shows an appearance which is similar to a broken fresh branch. Unlike the fractures of adults, which totally lose the continuity of segments, green stick fractures maintain the partial continuity of the exterior bone. This is due to the fact that young bones are capable of absorbing high compliance energy without breaking up. On the other hand, the buckling fractures of aged people are due to the weakening of the bones by osteoporosis (softening of bones as aging due to absorption of exterior bone cells). Because of osteoporsis, the bone has lost its strength and stiffness. The bone is no longer hard enough to break, but buckles instead.

9. Anisotropic Characteristics.

A material which is equally elastic in all directions is called an isotropic material. Strictly speaking, materials such as plastic and steel are anisotropic because in some regions their crystals are aligned in random directions. However, the overall directional characteristics of such substances are quite uniform. Therefore, they are classified as isotropic materials. On the other

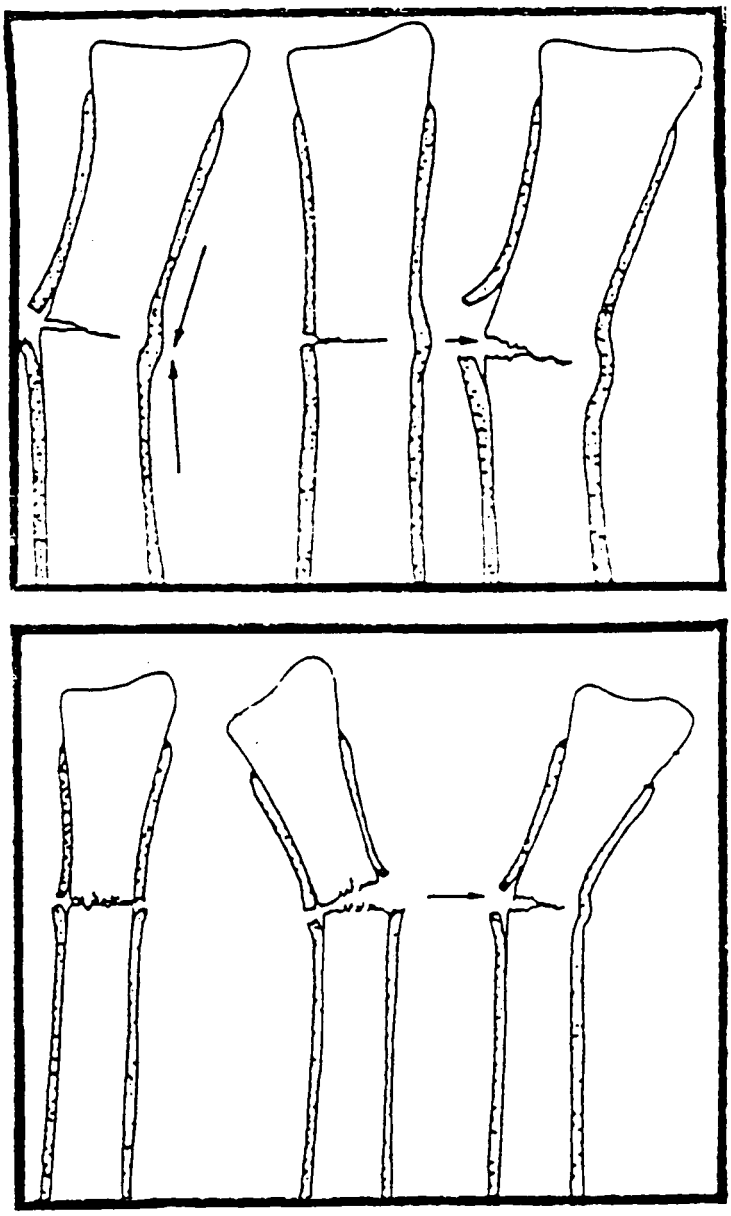


Figure 2-2.
Examples of Green Stick Fractures.

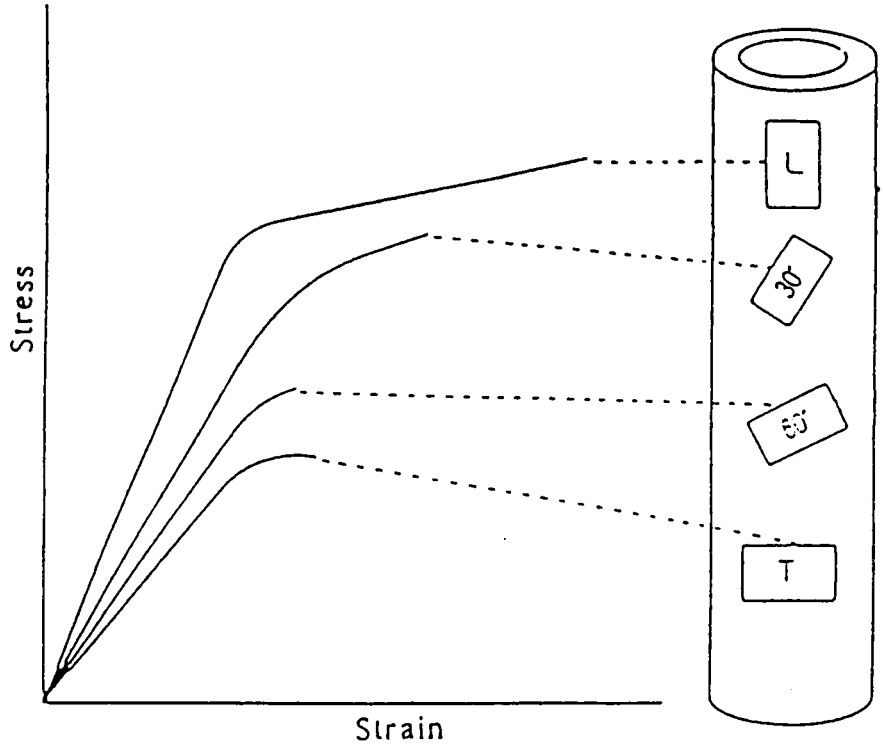
hand, living tissues are considered to be anisotropic because their elastic properties are different depending on the directions of stress. Hard tissues such as bone and the soft tissues such as veins, tendons, and muscles are all anisotropic materials.

The structure of each unit of living tissue is designed to fit the surrounding environment. For example, a bone has regions of cortical bone and spongy bone. The dynamic response of bone changes with the direction of impact. The strength and stiffness of a bone are high at the location where high external load is expected under normal physiological conditions. In 1970, Frankel experimented with the tensile strength and stiffness characteristics of the periosteum of human femurs in four different directions: axial, 30 degree, 60 degree and lateral. The tensile strength was highest in the axial direction and the lowest in the lateral direction (See figure 2-3).

10. Structure of a Shaft Bone Described by Wolff's Law.

In 1892, from detailed observations of skeletal specimens, Julius Wolff (1836-1902) found that the thinning of bone is caused by the removal of trabecular bones from the bone shaft cortex. Trabecular bones are fibrous cords of connective tissue that serves as supporting fibers by forming septums (walls which divide bone cell cavities).

Considering shaft bone as a beam with perfectly designed geometric structure, Wolff concluded that the trabecular bones mesh with one another at right angles so that they can sustain an externally applied load with a minimum volume and weight. Wolff called the layer where the compressive



L : Axial direction
30 30 degree inclination to the axis
60 60 degree inclination to the axis
T : Transverse direction

Figure 2-3.
Nonisotropic characteristics of the cortical bone of femur.
(Frankel, Burstein, 1970)

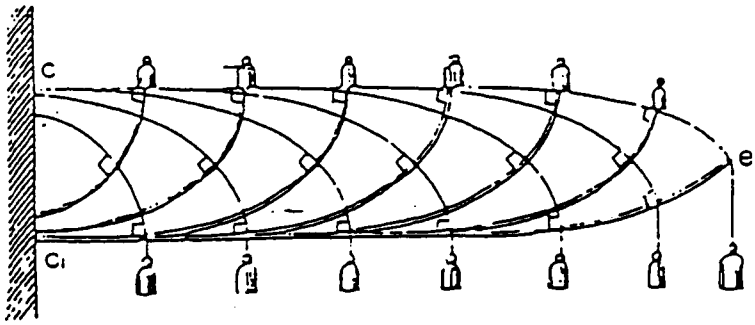
stress changes to tensile stress the neutral fibre layer. The following list is the several characteristics of the formations of trabecular bones that Wolff described.

1). The compressive stress and the tensile stress are not constant along the orbits. The stress diminishes from one end to the other along the line.

2). The fibers inter-mesh at right angles at the location where the stress caused by the external load becomes minimum.

3). At the location where the compressive stress or the tensile stress becomes maximum, orbits of fibers become parallel to the neutral fiber layer.

4). The orbits of compressive stress load and tensile stress load intersect each other at right angles, and these orbits intersect the neutral fibre layer at the angle of 45 degrees (See figure 2-4).



The orbits of the compressional stress fiber lines and the tensile stress fiber lines are crossing at right angle and are reaching to the edge at right angle (idealized bone fiber model).

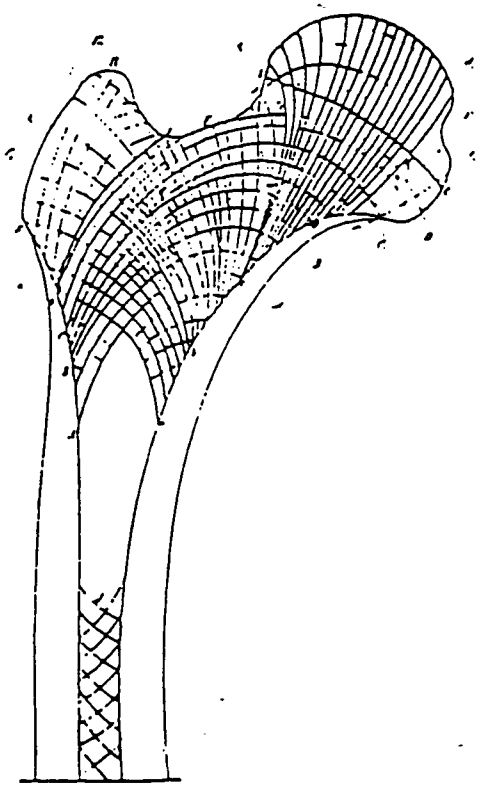


Figure 2-4.

Trabecular bone structure of femur.

(Wolf, 1892)

(B)

Mechanical Strength of Shaft Bones

1. Strength Referred to Mechanics of Materials.

The shape and the size of bones are the most important factors which affect bone strength. The larger the cross sectional area, the tougher the bone is against bending and torsion. For the beams made of isoparametric material with a constant cross sectional area, the ultimate tensile strength is proportional to the size of cross sectional area. If the cross sectional area becomes twice as large, the stress on a unit area is reduced to one half of the original stress.

The strength against bending is expressed by the moments of inertia, I. It is also known as the second moments of the area (See figure 2-5). Considering a shaft bone as a beam, the second moments of the area Ix and Iy, can be computed from the following formulas:

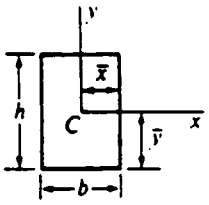
The moments of inertia of a plane with respect to the x and y axes, respectively.

$$I_x = \int x^2 \, dA \qquad I_y = \int y^2 \, dA$$

dA = the differential element of area

x, y = the coordinates of the differential element area from the neutral axis

Notation. A = area
$\bar{x}, \bar{y}$ = distances to centroid C
I_x, I_y = moments of inertia with respect to the x and y axes, respectively
I_{xy} = product of inertia with respect to the x and y axes
$I_p = I_x + I_y$ = polar moment of inertia
I_{BB} = moment of inertia with respect to axis B-B

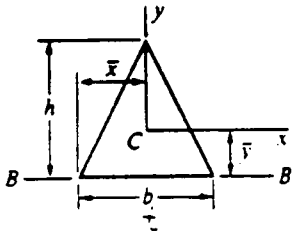


Rectangle (Origin of axes at centroid.)

$$A = bh \qquad \bar{x} = \frac{b}{2} \qquad \bar{y} = \frac{h}{2}$$

$$I_x = \frac{bh^3}{12} \qquad I_y = \frac{hb^3}{12}$$

$$I_{xy} = 0 \qquad I_p = \frac{bh}{12}(h^2 + b^2)$$



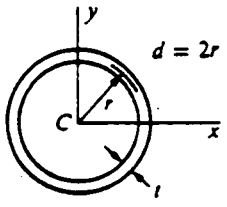
Isosceles triangle (Origin of axes at centroid.)

$$A = \frac{bh}{2} \qquad \bar{x} = \frac{b}{2} \qquad \bar{y} = \frac{h}{3}$$

$$I_x = \frac{bh^3}{36} \qquad I_y = \frac{hb^3}{48} \qquad I_{xy} = 0$$

$$I_p = \frac{bh}{144}(4h^2 + 3b^2) \qquad I_{BB} = \frac{bh^3}{12}$$

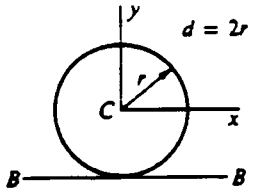
(Note: For an equilateral triangle, $h = \sqrt{3}b/2$.)



Circular ring (Origin of axes at center.)
Approximate formulas for case when t is small.

$$A = 2\pi rt = \pi dt \qquad I_x = I_y = \pi r^3 t = \frac{\pi d^3 t}{8}$$

$$I_{xy} = 0 \qquad I_p = 2\pi r^3 t = \frac{\pi d^3 t}{4}$$



Circle (Origin of axes at center.)

$$A = \pi r^2 = \frac{\pi d^2}{4} \qquad I_x = I_y = \frac{\pi r^4}{4} = \frac{\pi d^4}{64}$$

$$I_{xy} = 0 \qquad I_p = \frac{\pi r^4}{2} = \frac{\pi d^4}{32} \qquad I_{BB} = \frac{5\pi r^4}{4} = \frac{5\pi d^4}{64}$$

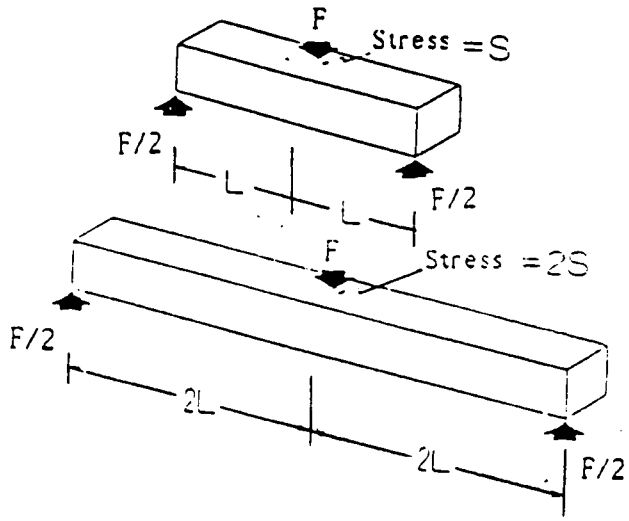
Figure 2-5.

Moments of inertia of various cross-sectional geometries.

(Gore & Timoshenko)

The multiplication of the second moments and the the modulus of elasticities (also known as Young's modulus), IE, is called bending stiffness, and it is often used as an indicator of bending strength. The neutral axis is the intersection of the cross sectional plane, and the neutral surface is the plane which does not change in length. As the second moment increases, the bone stiffness also increases. Consider two beams which are made of the same material with the same cross-sectional area. The first beam has the unit length of L, and the other one has the length of 2L (See figure 2-6). If the same bending load is applied at the center of each beam, the beam which has twice the length is subjected to twice the bending moment. The longer the bone is, the greater the bending moment. For beams made of uniform material, the magnitude of the cross sectional stress created by the bending is proportional to the length of the beam.

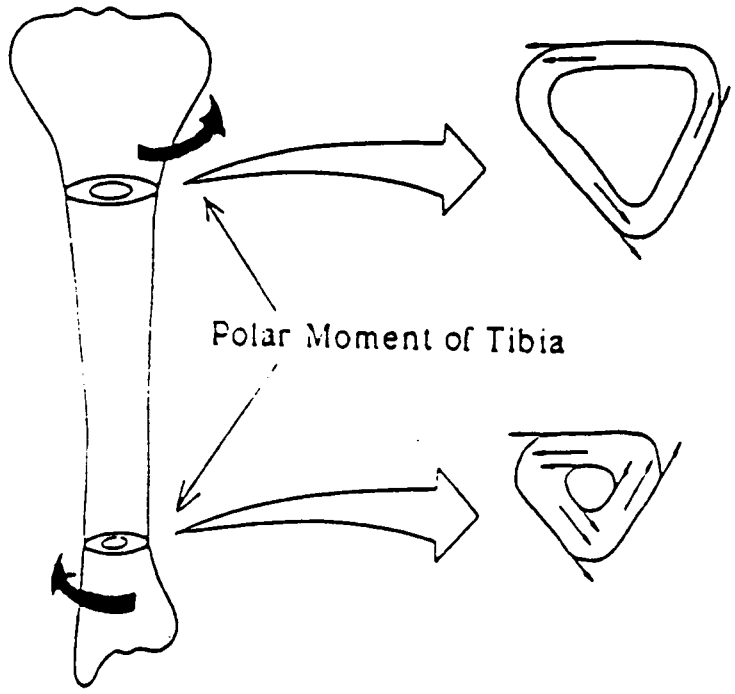
In reality, the shape of a cross-sectional area of a limb bone is not uniform throughout the axial direction (See figure 2-7). The bone gets slender toward the middle of the shaft; however, the thickness increases in order to compensate. This thickness distribution along the axial direction can be referred to the biological adoption due to evolution to endure bending stress without increasing the weight and the volume. The area of cross section and the allocation of the surface cortical bone (hard bone cell) are two of the most important factors which directly affect strength and stiffness. The polar moment of inertia J is applicable to express the strength against twisting. The more the cortical bone cells are distributed on the exterior surface away from the cross sectional center, the stiffer the bone is.



If the length of the beam becomes twice as long, the stress normal to the cross-sectional area becomes twice as big. For the beam with uniform properties, the normal stress generated by the bending moment is proportional to its length.

Figure 2-6.

3 point bending test.



Bone is thin on the large diameter part and is think on the small diameter part in order to endure the torsional moment with minimum weight.

Figure 2-7.

Thickness change along the shaft.

(Frankel, 1980, p. 15)

2. Material Strength Under Impact.

The stress-strain relationship under impact loading is quite different from that of static loading cases (See figure 2-8). According to research performed on cattle bone by Saha and Hayes, tensile strength under impact loading is about 20% higher than static strength. They also noted that statistically significant correlations can be seen among elastic properties, impact strength, and impact energy. The tensile strength and energy required for rupture and percentage elongation under dynamic conditions are higher than the static values.

(C)

The Classification of Bone Fractures

1. General Information.

In the early 1970's, as orthopedists' needs for guidelines on bone fracture operations grew, demand for an organized classification system became gradually higher. Although there were many attempts at bone fracture classification systems before the 1970's, almost all the classifications focused only on a particular location of a particular bone, and none of the classification systems had ever held the human skeletal structure as an entity.

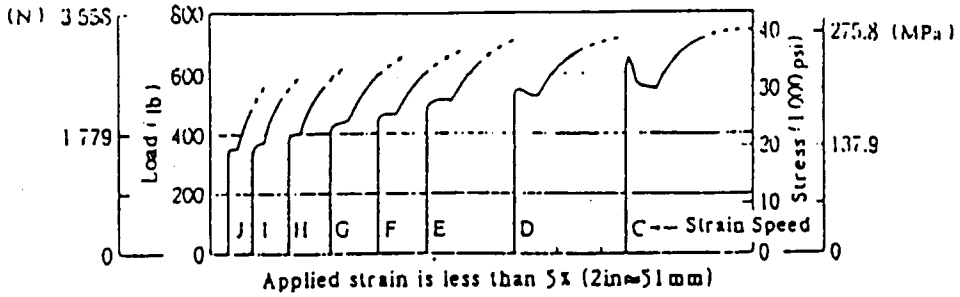
In the early 1980's, at the AO/ASIF record center in Bern, where over one million X ray photographs and fifteen-thousand operation records of bone injuries are gathered, E. Muller, P. Koch and associates started a project to classify hundreds of actual injury cases in order to find some kind of

commonality or universal characteristics that would be applicable for all types of fracture.

In the system they developed, all the fractured bones are first classified into three types (Simple, Wedge and Complex), then into three groups (Simple fracture, Spiral, Oblique and Transverse), and then into three subgroups according to the degree of damage. The types of fractures are expressed by alpha-numerical code. There are three ranks in each division (type, group and subgroup), which are arranged in the order of complexity and severity of the fracture. Parts of the skeletal structure are numbered from 1 to 9 (See figure 2-9A). In this figure, 3 is for the femur, and 4 is for the tibia and fibula as a couple. The locations of the fracture on long shaft bones are classified into three major segments (an upper bone head area, a lower bone head area and a shaft area).

Since the system utilizes 29 subdivided locations (on 9 basic skeletal parts) with 3 types, 3 groups and 3 subgroups, a total of 783 (29 x 3 x 3 x 3) types of classifications are possible (See figure 2-9B). With the additional condition codes, over 1500 types of different classifications are also possible by this classification system.

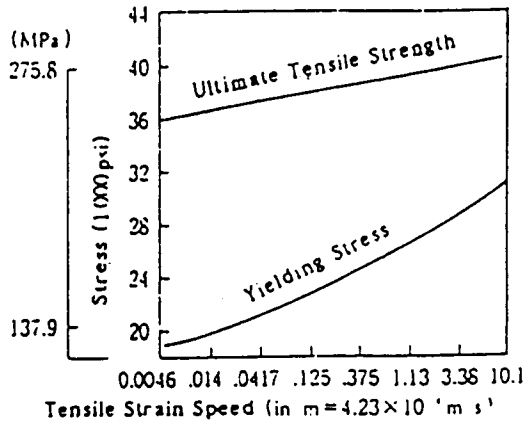
This system has the structure of an inverted tree, just like a DOS directory. By checking the fracture conditions (types, severity and location) at each branching point of classification tree, all the bone fractures are classified into one of the 783 different fracture types. Muller's classification system adequately covers all the necessary fracture types. It can be used for an expert system data base to predict fractures. His bone classification system is very straightforward and can be easily converted into a computer code.



Applied strain is less than 5% (2in≈51mm)

	J	I	H	G	F	E	D	C
Strain Speed (in/in/m)	0.002	0.006	0.018	0.056	0.166	0.50	1.50	4.44

Material Tensile Strength Under High Speed Loading



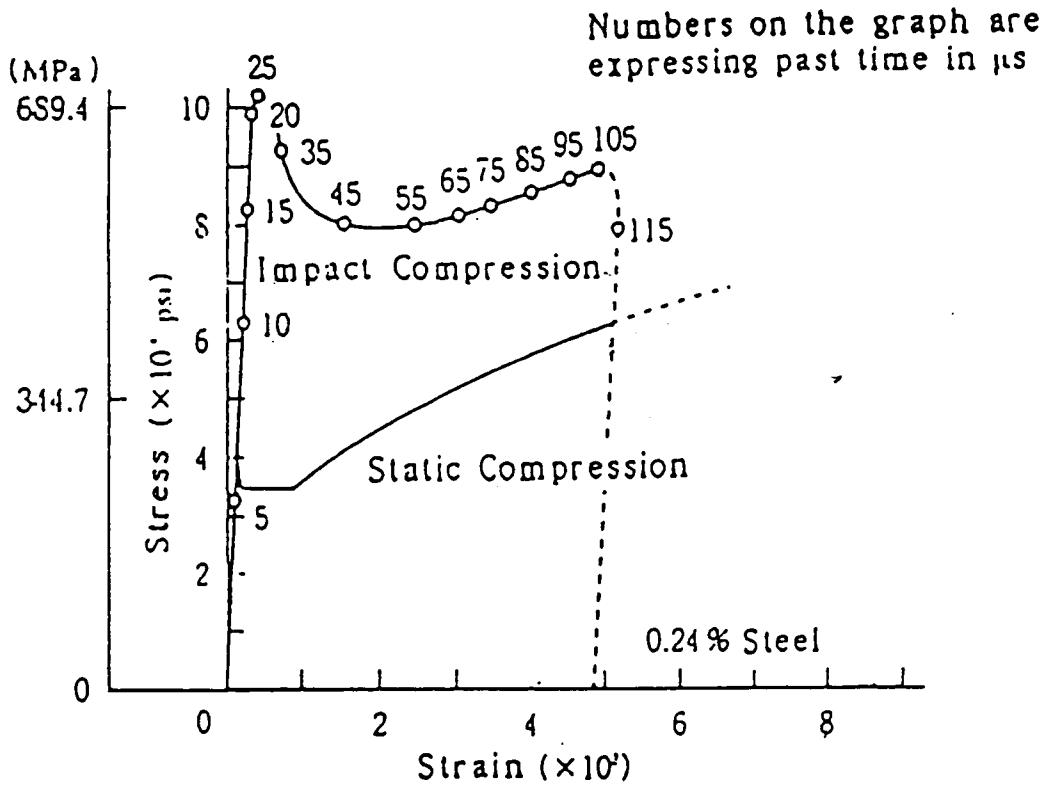
Stress VS. Strain Speed Diagram for a 0.05% Carbon Steel

(A)

Figure 2-8.

Material strength under high speed loading (A) and comparison of static compression and impact compression (B).

(Source: "Impact Fracture Mechanics" published by Japan Mechanical Engineering Academy in 1990.)



(B)

Figure 2-8. (continued)

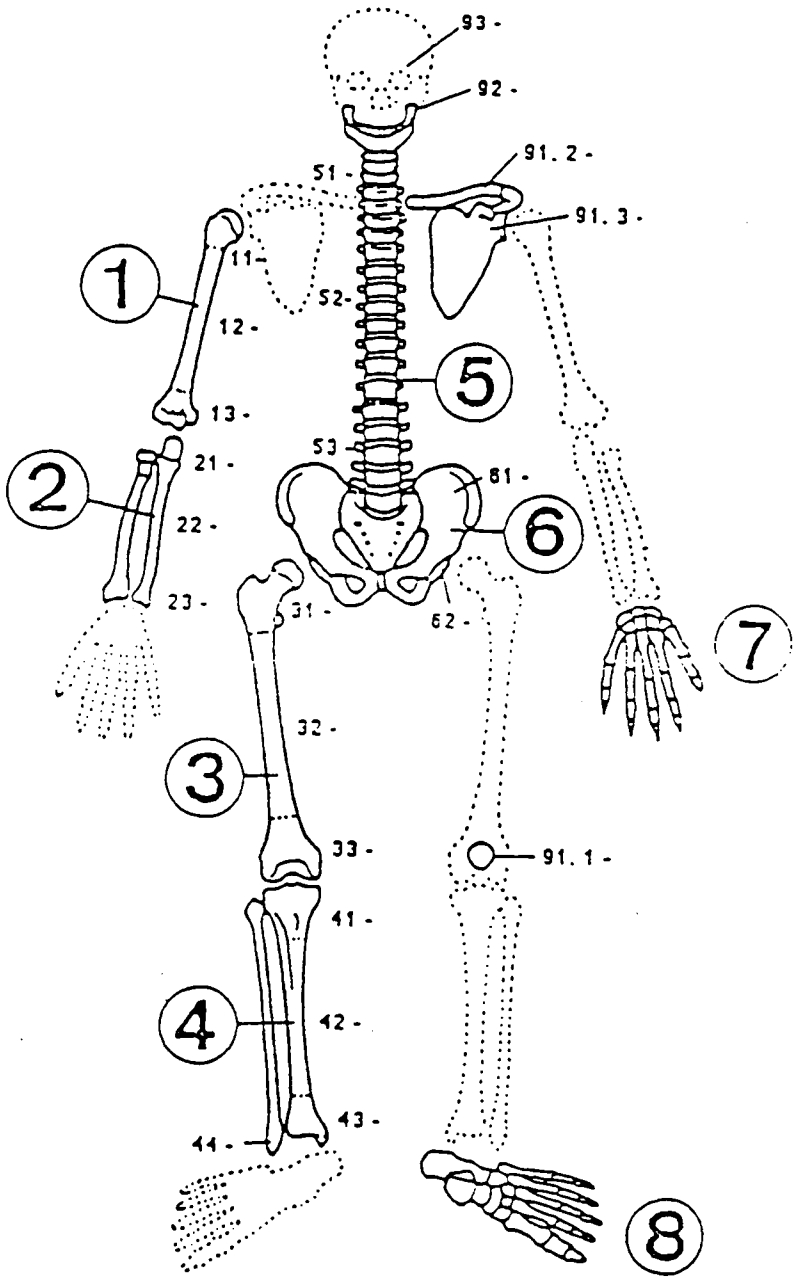


Figure 2-9.

Muller's bone fracture classification.

(A). Fracture location classification code.

(Muller, 1990)

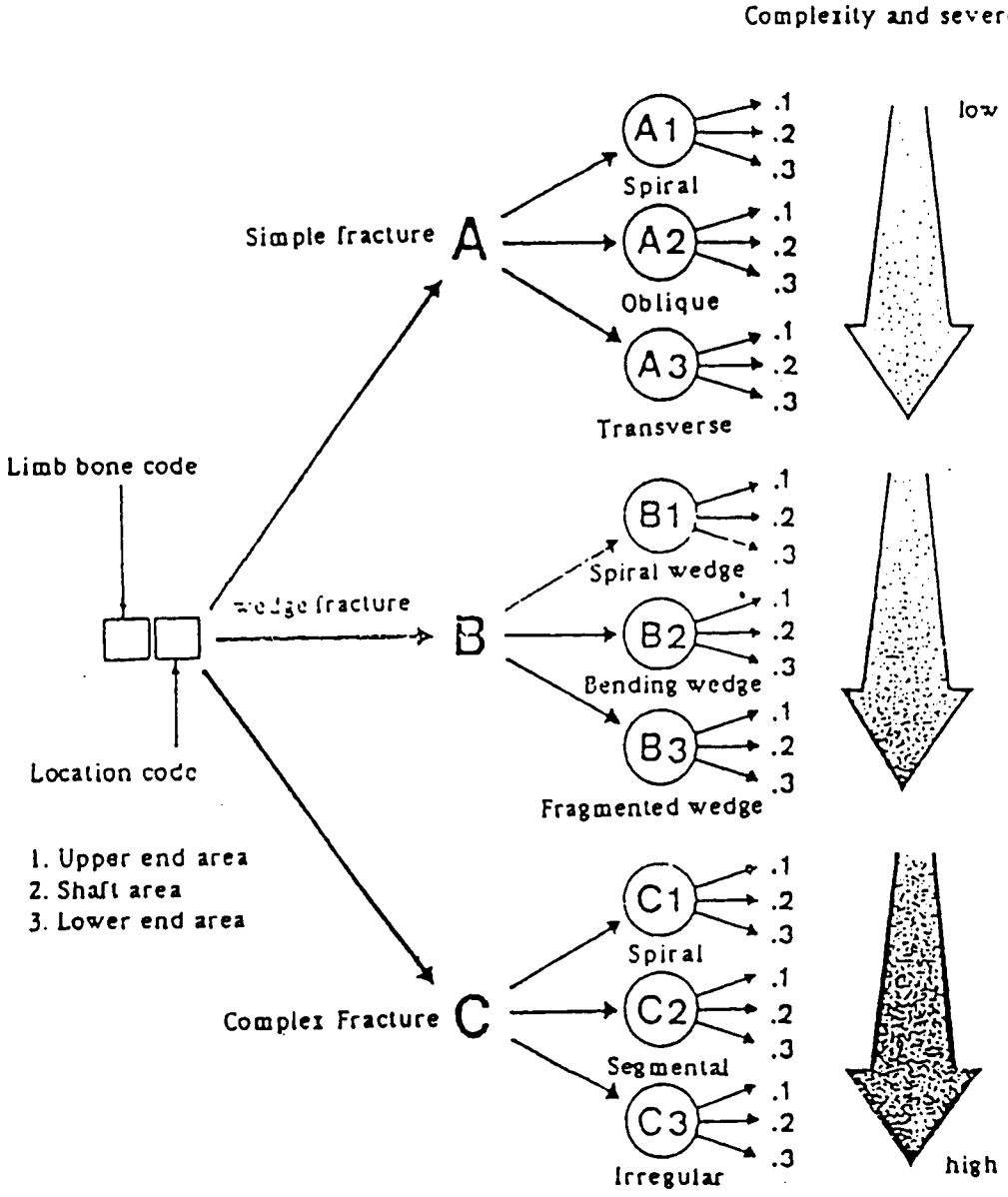


Figure 2-9. (continued)

(B). Basic structure of bone fracture classification tree.

(Muller, 1990)

One problem associated with the fracture pattern classification is that there are numerous cases which lie in between categories. This is where fuzzy logic must be used. Unfortunately, since Muller's classification system was developed purely for the purpose of providing operation guidelines, it lacks vital engineering information (such as the magnitude, direction, and time duration of the force which caused the fracture).

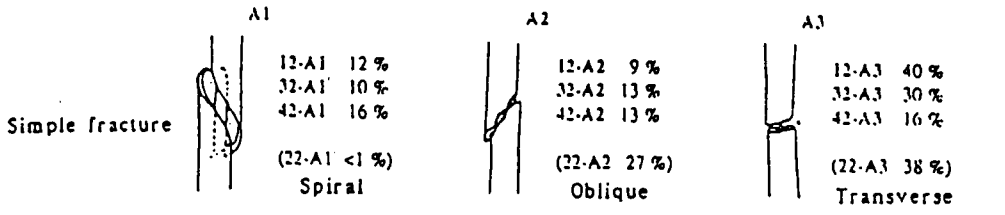
2. Fracture Types of Femur and Tibia.

According to Muller's classification, A type is a simple fracture; B type is a wedge fracture; and C type is a complex fracture. Among the 1000 tibia fracture cases, which Muller's research staff classified, 45% were A type fractures (simple fractures), 46% were B type fractures (wedge fractures), and 9% were C type fractures (complex fractures) (See figure 2-9C). The B type fracture has three subgroups, the spiral fracture, the bending fracture, and the fragmental fracture. The bending fracture corresponds to fractures which possess a major wedge-shaped fracture piece, and the fragment fracture corresponds to fracture which include fragmented pieces and axial cracks. 46% of type B fractures can be decomposed into 8% of spiral fractures, 25% of bending fractures, and 13% of fragmental fractures (46=8+25+13). 34% of Type B fractures can be decomposed into 9% of spiral fractures, 17% of bending fractures, and 8% of fragmental fractures (34=9+17+8).

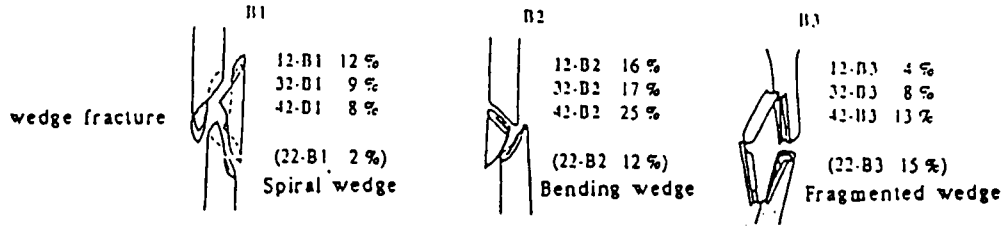
Although this statistical result does not refer to the details of loading conditions, this research shows which fracture type is most common among bone fracture types caused by real accidents.

			A	B	C	
12-	N =	200:	61 %	32 %	7 %	= 100 %
22-	N =	500:	65 %	29 %	6 %	= 100 %
32-	N =	1000:	53 %	34 %	13 %	= 100 %
42-	N =	1000:	45 %	46 %	9 %	= 100 %

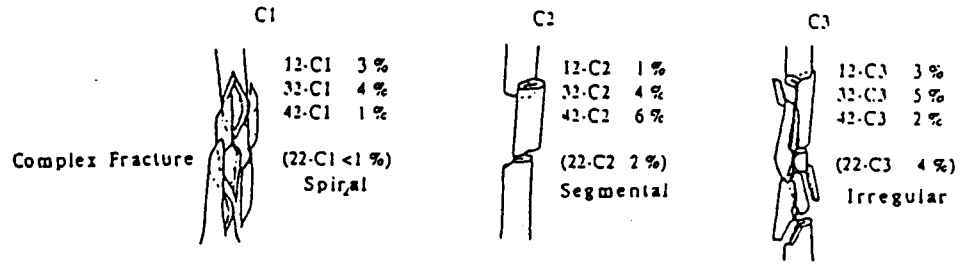
A: 12-A = 61%, 22-A = 65%, 32-A = 53%, 42-A = 45%



B: 12-B = 32%, 22-B = 29%, 32-B = 34%, 42-B = 46%



C: 12-C = 7%, 22-C = 6%, 32-C = 13%, 42-C = 9%



22-								
	A = 65%		A1	18%	A2	21%	A3	26%
	B = 29%		B1	7%	B2	8%	B3	14%
	C = 6%		C1	2%	C2	2%	C3	2%

Figure 2-9. (continued)

(C). Fracture classification data of tibias.

(Muller, 1990)

3. Fracture Situational Category Classification.

Based on the type of loading conditions, the fracture situation can be classified into three categories.

1). The fracture caused by a small high speed object.
2). The fracture caused by a twisting motion.
3). The fracture caused by a crushing motion.

For case (1), the speed of the colliding object can vary from several meter/sec to up to several hundreds meter/s. If a high speed object such as a bullet hits a bone, it causes a localized plastic deformation (sinking or penetration). In this case, the behavior of the fracture is quite different from the other fracture types. Case (2) fractures are usually seen on sports injuries. For example, an over twisting motion of the tibia can occur in skiing and cause a spiral fracture. In case (3), a bone is smashed into several pieces by crushing.

(D)

Effect of the Impact Object Surface Shape

The contact surface shape of an impacting object is closely related to the impact pressure in the vicinity of the impact point. Johnson (1972) said that a sharp impact object simply cuts material, and blunt impact object tend to give rise to predominantly radial compression and to general stress and strain distribution (See figure 2-10). This distribution is created by high internal pressure in a very thick cylinder or sphere. He also mentioned the following relationships:

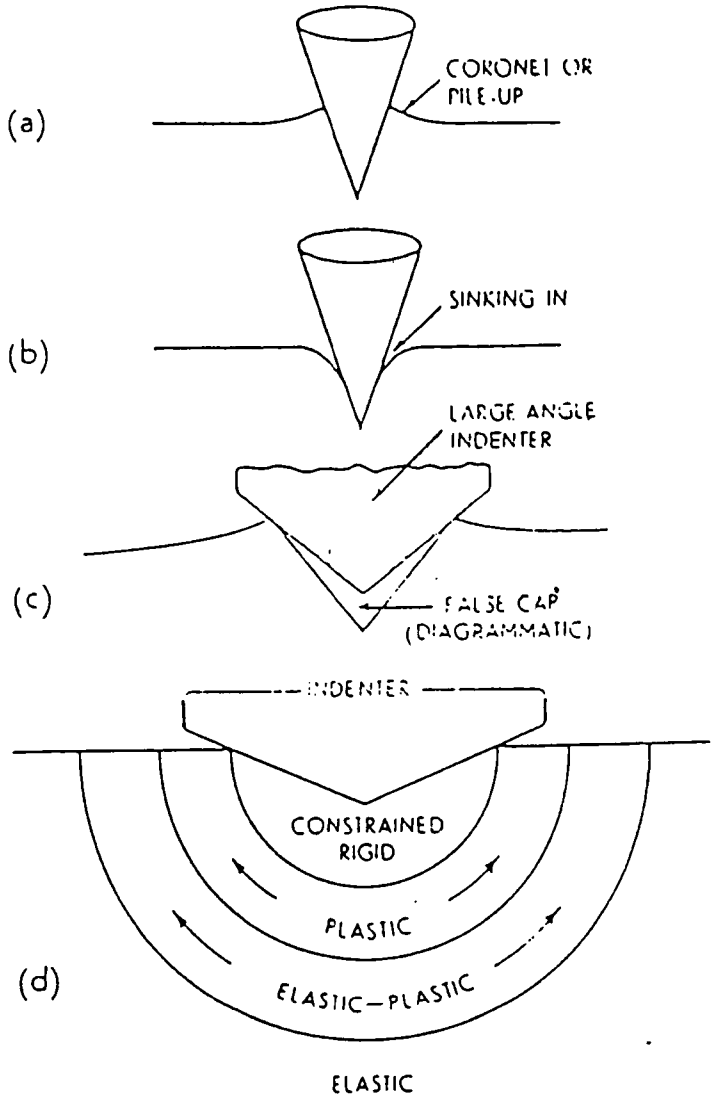


Figure 2-10.
Effects of impact object shape.

(Johnson, 1972, p. 169)

1) As the impact pressure increases, the extent of the zone of deformation increases, but is entirely contained by surrounding ela material.

2) When the impact pressure attains a value of approximately three times that of the yielding stress, the material is plastic across the whole of the impact object and may flow grossly along the sides of the impact object.

3) The severity of surface displacement depth done by a sharp impact object depends heavily on the work hardening characteristic (increase of ultimate fracture strength in high speed impact) of the impacted material.

The impact stress transmitted to the bone increases as the contact surface shape of the impact object increases. If the shape of the contact surface is dull (for example, a pipe or a plate), the impact pressure in the impact point vicinity and the extent zone of plastic deformation increase. If the impact object is blunt, the chance of preventing initiation of the impact crack is higher. But the chance of creating a large fracture piece is also higher because the range of plastic deformation is extended.

Although Johnson's conclusion is based on experimental data from industrial materials such as metals and bricks, this concept can also be extended to research on bone fractures because bones also show the characteristics of impact strain hardening and plastic deformation.

(E)

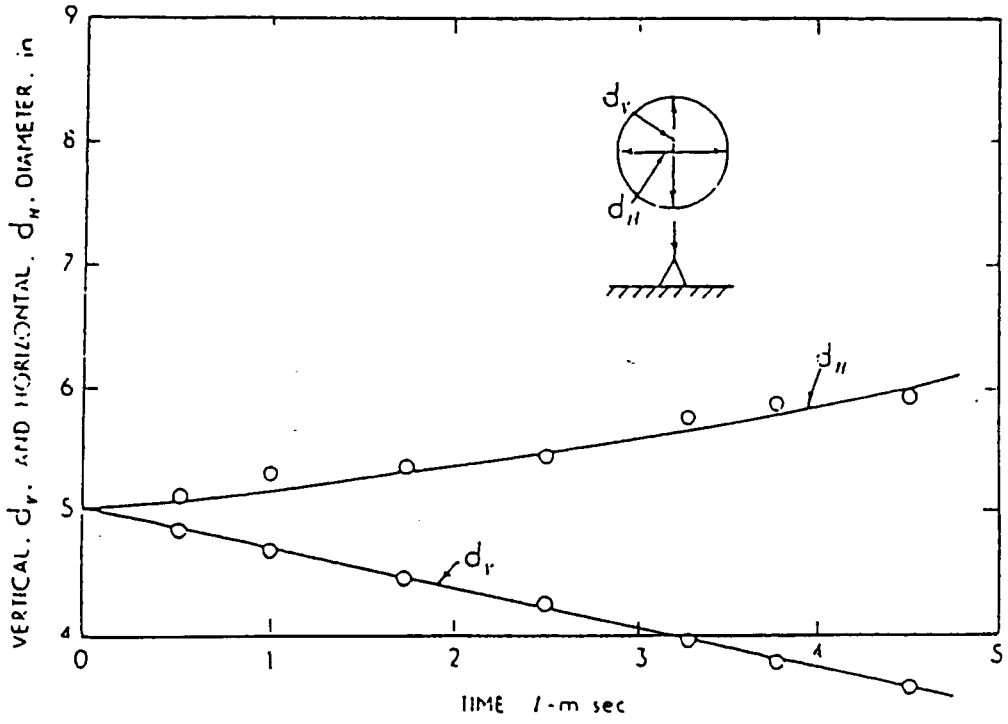
Relationship Between Impact Velocity and Deformations

Johnson simulated the effect of impacts caused by sharp objects and flat objects by testing the impact deformation of a free-falling lead ring onto a flat rigid base and sharp indenter (See figure 2-11). During impact, the vertical diameter of a ring contracts and the horizontal diameter of a ring extends, and as a result, the ring becomes an ellipse. Johnson discovered that there is a simple linear relationship between impact speed and deformations. The vertical diameter of a ring after impact linearly decreases with the impact velocity. On the other hand, the horizontal diameter of a ring increases linearly with the impact speed.

(F)

Stress Concentration in Static and Dynamic Cases

For static axial loading at the top of femur, the tensile, or compressive stress on a femur is concentrated approximately 2/3 of the way from the top end (See figure 2-12). In impact fractures, the stress and deformation are highly localized and are not distributed uniformly because the impact stress is highly concentrated in a small region. For impact fractures, a portion of the impact energy is absorbed by localized deformation in the form of strain energy. The potential energy and the kinetic energy of the shell when placed under deformation by vertical impact on the surface are expressed as follow (See figure 2-13).

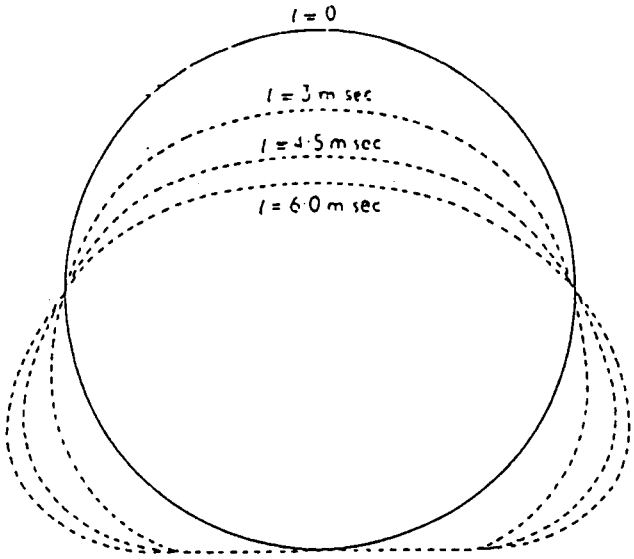


Showing how the horizontal and vertical diameters of the ring
alter with time when freely falling on to a sharp indenter of 40° nose angle, with an initial speed

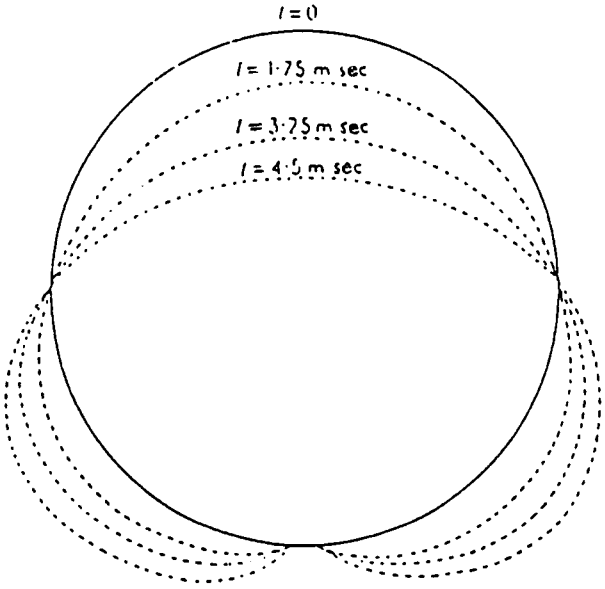
(A)

Figure 2-11.
Deformation of ring diameters vs. impact speed (A) and resultant ring deformation by. impact speed (B).

(Johnson, 1972, p. 285)



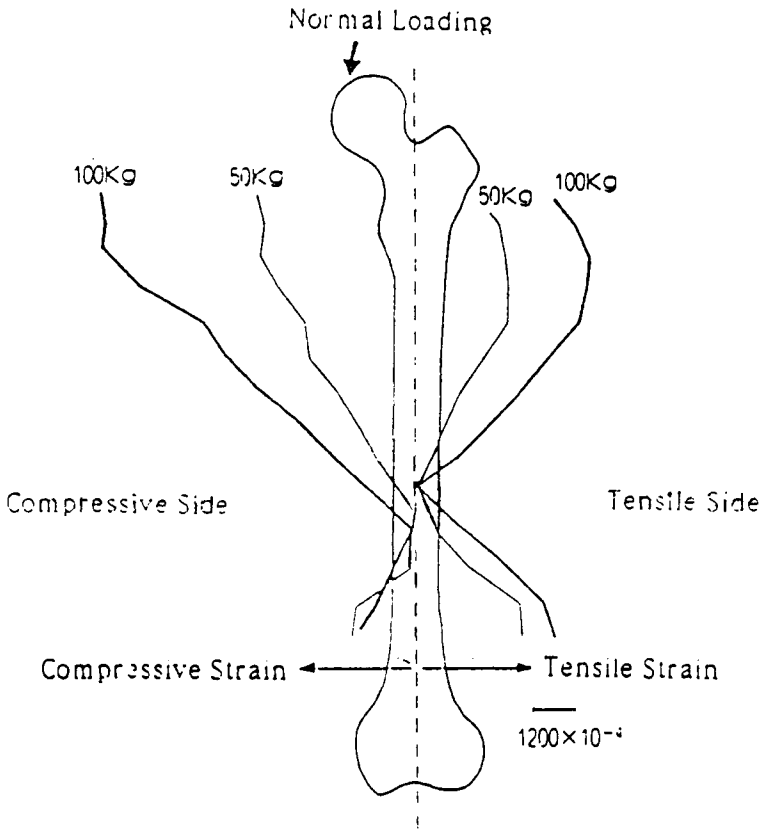
Showing the instantaneous profiles of a 2·5 in radius lead ring at various times after first impact when falling freely on to a flat rigid anvil; initial speed at $t = 0$ is 24 ft/sec.



Showing the instantaneous profile of a lead ring at various times t after impact, when falling freely and encountering a sharp indenter (5·0 in outer diameter; $\frac{1}{8}$ in radial thickness).

(B)

Figure 2-11. (continued)

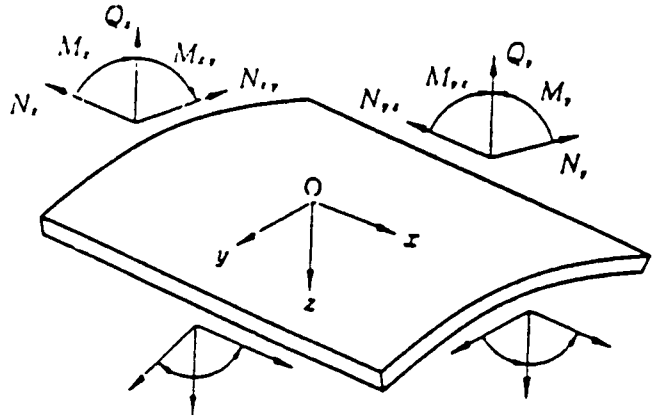


Vertical loading at the ball joint head generates a compression force inside and tensile force outside. These forces concentrate at the location approximately 2/3 of the length from the ball joint end.

Figure 2-12.

Strain distribution on the femur loaded at the femur head.

(Akaishi, 1988)



Strain Energy

$$U = \frac{1}{2}\int_0^{l}\int_0^{2\pi R}\int_{-h/2}^{h/2}(\sigma_x\varepsilon_x + \sigma_y\varepsilon_y + \tau_{xy}\gamma_{xy})\,dx\,dy\,dz$$

Figure 2-13.

Cross-sectional forces and cross-sectional moments on a shell.

(Source: "Impact fracture Mechanics" published by Japan Mechanical Engineering Academy in 1990.)

Chapter III

APPROACH TO THE FRACTURE PROBLEM

(A)

Finite Element Method Approach

1. History of Finite Element Method and Fracture Theories.

Finite Element Method (FEM) is a relatively young field of study. Its origin came in 1920 when Griffith proposed a basic theory of energy release rate for brittle materials (such as concrete and glass). During the 1940's and 50's, the number of accidents resulting from the failures of material strength had increased. During World War II, demands for computational stress failure assessment methods that could be substituted for actual failure tests had risen. In order to design large scale war planes and ships in less time, cutting down the number of trivial failure tests was desired by using theoretical predictions. In late 1940's, Orowan and Irwin modified Griffith's basic theory to be able to apply for steel materials. In 1950, Irwin proposed the stress intensity factor K which is still the most basic assessment parameter in fracture mechanics today. During the 1960's and 70's, some other modified assessment parameters were introduced. In 1963, Paris proposed the δK parameter for fatigue cracks. In 1972, Rice proposed the C parameter for creeping cracks. After 1970, efforts of standardizing measurement methods for an increasing number of assessment parameters gradually began to be led by American Society of Testing and Materials (ASTM).

Until the 1960's, the fracture theory which Griffith originally proposed (also known as deterministic fracture mechanics) was the most dominant fracture assessment theory. Current FEM codes use the theory as failure criteria. However, after 1970, a new field of fracture assessment study was established by combining the statistical point of view for fracture occurrence. Today, it is known as probabilistic fracture mechanics.

2. Classification of the Fracture Mechanics.

a. General information.

Fracture mechanics is the study of various fracture phenomena by means of experiments and mechanical theories. Some of the developed theories are adopted to failure criteria of current FEM codes. The study methods and classifications are different according to the type of fracture phenomena.

Fracture mechanics can be divided into two major categories, deterministic fracture mechanics and probabilistic fracture mechanics. Deterministic fracture mechanics can be subdevided into linear elastic fracture mechanics, non-linear elastic fracture mechanics, and dynamic fracture mechanics. In deterministic theories, the conditions of crack growth and the propagation speed of a crack are obtained directly from calculations. On the other hand, probabilistic theories are focused on the many uncertain factors associated with fractures. These theories evaluate fracture phenomena by the probability of their occurrence.

The Classification of Fracture Mechanics

Linear elastic fracture mechanics

1. Molecular fracture
   Fracture caused by separation of molecular bond.
2. Fatigue fracture
   Fracture caused by applied repetitive small strains.
3. Environment fracture
   Cracks caused by corrosion.

Non-linear elastic fracture mechanics

1. Elastic-plastic fracture
   Fractures accompanied with plastic deformation
2. High temperature creep fracture
   Crack in material under large strain which changes with time.
3. High temperature fatigue fracture
   (Plastic fracture)
   Fracture in material under large strain initiated by repetitive load.

Dynamic fracture mechanics

1. Elastic fracture
   Fracture caused by impact loading.
   Fast speed crack propagation.
2. Elastic-plastic fracture
   Time dependent crack growth associated with large plastic deformation.

Probabilistic fracture mechanics

Statistical measurement of fracture occurrence.

b. Liner Elastic Fracture Mechanics.

There are two fields of study associated with fracture problems. One field is the strength of materials, and the other is fracture mechanics. The strength of materials area puts its emphasis on materials science. This area of study focuses on the characteristics of industrial materials. On the other hand, fracture mechanics puts emphasis on the mechanism of the fracture itself. Fracture mechanics consists of two major fields of study: stress analysis and strength testing of materials. Fracture mechanics can be considered a branch of mechanics of materials.

Industrial parts are normally designed not to exceed σmax, which is the yielding stress σY divided by the safety factor F.

$$\sigma max < \frac{\sigma Y}{F}$$

The safety factor F is determined experimentally with consideration of the uncertainty of expected exterior load, the error margin of the analytical math model, and the quality tolerance of the material.

Yielding stress cannot be used for crack growth criteria, because the stress becomes infinitely large at the tip of the crack. Therefore, instead of using the maximum yielding stress, linear elastic mechanics employs the stress intensity factor, K, which characterizes the elastic stress field around the crack and the fracture toughness Kc.

$$K < \frac{Kc}{F}$$

Because the parameter K is based on linear elastic fracture theory, the parameter K can predict a result only for small scale yielding problems. To apply this theory, plastic deformation range at the crack tip should be comparatively smaller than the crack size. Therefore, linear elastic fracture mechanics is not suitable for impact crack fracture simulations.

c. Non-linear Elastic Fracture Mechanics.

On materials with large elastic-plastic deformation properties, a crack proceeds steadily at the beginning and then proceeds unstably until the total fracture occurs. To understand the crack propagation mechanism, it is important to know the conditions that lead to unstable crack growth. To describe a crack condition, the tearing modulus, which was proposed by Paris and Tada, is widely used today.

When tensile stress is applied around a sharp crack, the crack tip becomes dull due to plastic deformation (See figure 3-1, of crack propagation R v.s. J integration). When the value of J integration reaches JIC, the stable progress of the crack is started. During the stable condition, the slope of the J-R curve is constant. Therefore, the characteristics of stable crack progress can be described by the slope. The parameter which is used to express the slope is T. It is defined as follows:

$$T = \frac{E}{\sigma_0^2} \frac{dJ}{da}$$

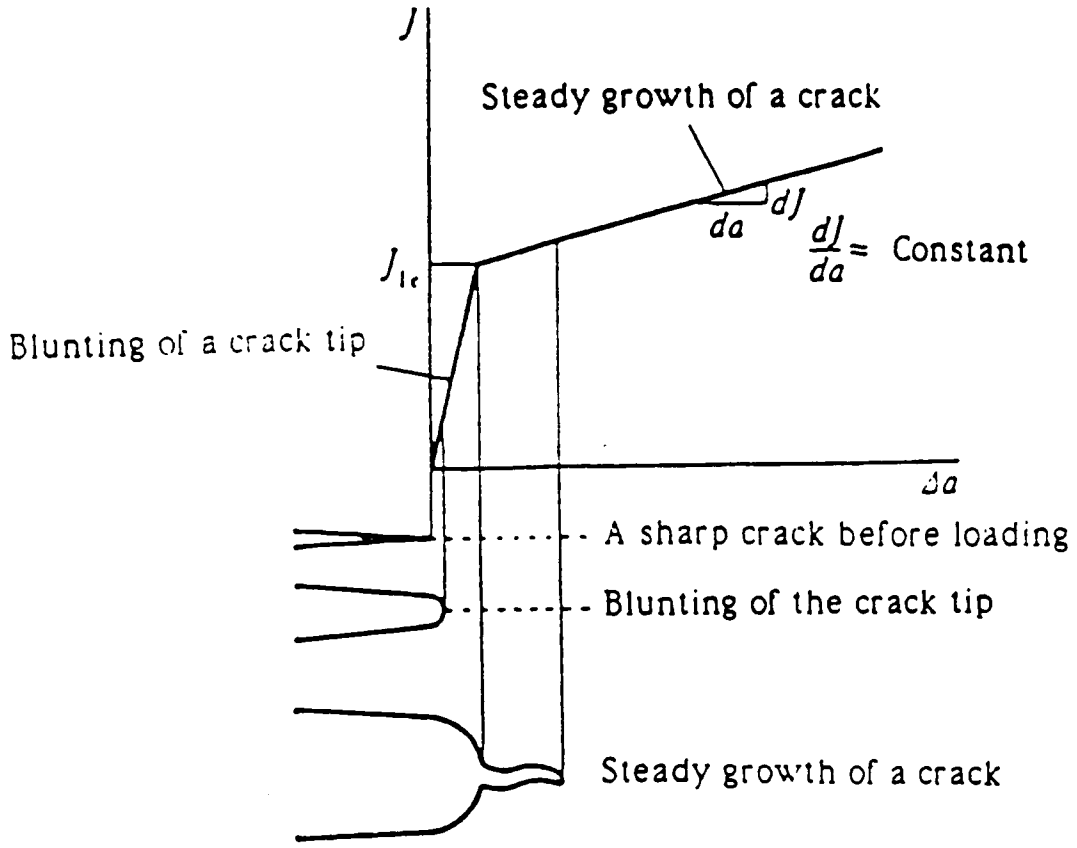


Figure 3-1.
J - R curve.

(Yagawa, 1988, p. 38)

E is Young's modulus, and $\sigma 0$ is the deformation resistance (it can be an ultimate yielding stress, σY, an ultimate compression stress, σU, or a mean value of these two, $(\sigma Y + \sigma U)/2$). A coefficient $E/\sigma 0^2$, is used to non-dimensionalize T.

When T reaches the Tmax, the stable crack growth condition changes to unstable. T max is the value which is unique for each material.

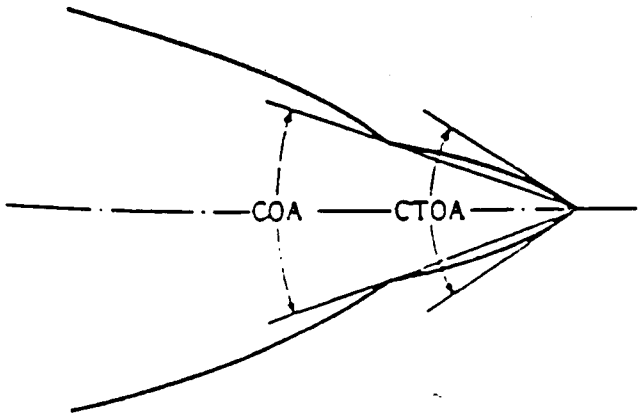
When T < Tmax, stable

When T > Tmax, unstable

In the range of small scale crack growth, the tearing modulus which is characterized by dJ/da could be one of the effective parameters to describe the elastic-plastic fracture. The effectiveness of the tearing modulus has been tested on a large number of Finite Element problems by Kanninen and Shih. They have obtained J-R curves which closely correlate to the experimental data.

Today, research on the parameters that differentiate the stable growth and unstable growth of cracks is getting more attentions. As the dominating parameters, three factors have been proposed based on the J integration theory: the tearing modulus, T, the crack tip opening angle, CTOA, and the crack opening angle, COA (See figure 3-2).

Despite the fact that many techniques have been proposed for J integration (which is the base of these parameters), the evaluation methods and criteria for the tearing modulus have not been established yet.



COA	Crack Opening Angle
CTOA	Crack Tip Opening Angle

For isotropic materials, it is reported by ASTM that the angles of COA and CTOA seem to have constant values during crack progress except for initial transition period.

Figure 3-2.

Crack tip parameters.

(Yagawa, 1988)

d. Dynamic Fracture Mechanics.

To evaluate structural safety of industrial parts, the strength of cracked parts against impact loading often needs to be considered. In high speed impacts, the stress field of the crack tip is different from that of static cases or of slow loading cases due to the inertial force. If the crack propagation speed is faster than 1/10 of the stress wave speed, the effect of the inertial force is no longer negligible. In linear elastic fracture mechanics and non-linear fracture mechanics, the stress intensity factor that expresses fracture toughness is a constant. However, in dynamic fracture mechanics, the stress intensity factor is no longer a constant because the effect of inertial force is counted. It is a function of time. The value of the stress intensity factor changes depending on the shape of the material and loading condition.

e. Probabilistic Fracture Mechanics.

Probabilistic fracture mechanics is a field of study that investigates and evaluates the fracture probability of a structure. In normal fracture mechanics (deterministic fracture mechanics), crack dimensions and material variables are treated as discrete values. However, in probabilistic fracture mechanics, these values are treated as fuzzy variables that have a range of certainty.

In deterministic fracture mechanics, the safety evaluation depends on the stress intensity factor and energy release rate, which are measured experimentally. The results are always binary (pass or fail). Unlike

deterministic fracture mechanics, probabilistic fracture mechanics measures the probability of fractures using statistical data from a large number of experiments. Therefore, the failure analysis of probabilistic fracture mechanics is not binary (pass or fail), and the resultant stress conditions are described with the degree of fracture possibility like fuzzy logic.

3. Modes of Fractures and Associated Parameters.

a. General Information.

In FEM, the applied force conditions on a crack can be classified into three basic modes. Mode I is the opening mode, and the stresses in this mode are acting to open the crack. Mode II is the sliding mode, and in mode II, one surface of the crack slides on the other in the direction of the crack line. Mode III is the tearing mode, and in mode III, the crack surfaces are sliding against each other and tear the crack (See figure 3-3).

Mode I

$$\sigma x = \frac{KI}{\sqrt{2\pi r}} \cos\frac{\theta}{2}\left(1 - \sin\frac{\theta}{2}\sin\frac{3\theta}{2}\right)$$

$$\sigma y = \frac{KI}{\sqrt{2\pi r}} \cos\frac{\theta}{2}\left(1 + \sin\frac{\theta}{2}\sin\frac{3\theta}{2}\right)$$

$$\tau xy = \frac{KI}{\sqrt{2\pi r}} \sin\frac{\theta}{2}\cos\frac{\theta}{2}\cos\frac{3\theta}{2}$$

$$\sigma z = \nu(\sigma x + \sigma y), \qquad \tau xz = \tau yz = 0$$

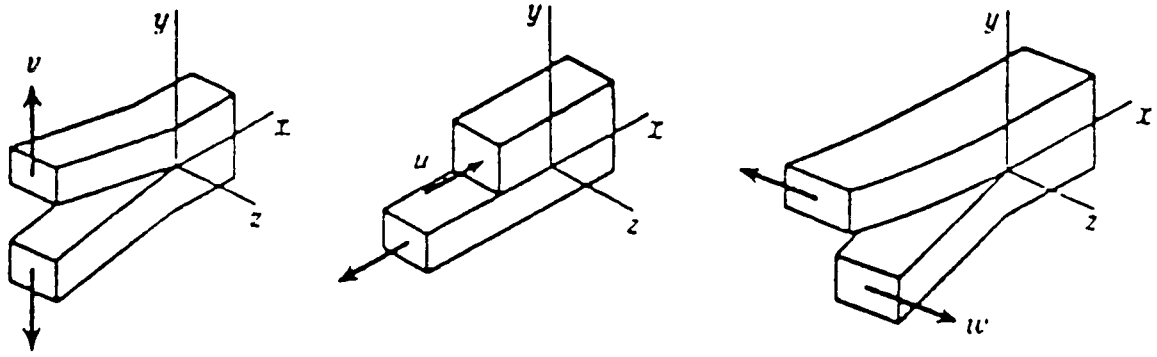


Figure 3-3.
3 basic fracture modes.

$$u = \frac{KI}{G}\sqrt{\frac{r}{2\pi}}\cos\frac{\theta}{2}\left(1 - 2\nu + \sin^2\frac{\theta}{2}\right)$$

$$v = \frac{KI}{G}\sqrt{\frac{r}{2\pi}}\sin\frac{\theta}{2}\left(2 - 2\nu - \cos^2\frac{\theta}{2}\right)$$

$$w = 0$$

Mode II

$$\sigma_x = \frac{KII}{\sqrt{2\pi r}}\sin\frac{\theta}{2}\left(2 + \cos\frac{\theta}{2}\cos\frac{3\theta}{2}\right)$$

$$\sigma_{xy} = \frac{KII}{\sqrt{2\pi r}}\sin\frac{\theta}{2}\cos\frac{\theta}{2}\cos\frac{3\theta}{2}$$

$$\tau_{xy} = \frac{KII}{\sqrt{2\pi r}}\cos\frac{\theta}{2}\left(1 - \sin\frac{\theta}{2}\sin\frac{3\theta}{2}\right)$$

$$\sigma_z = \nu(\sigma_x + \sigma_y), \qquad \tau_{xz} = \tau_{yz} = 0$$

$$u = \frac{KII}{G}\sqrt{\frac{r}{2\pi}}\sin\frac{\theta}{2}\left(2 - 2\nu + \cos^2\frac{\theta}{2}\right)$$

$$v = \frac{KII}{G}\sqrt{\frac{r}{2\pi}}\cos\frac{\theta}{2}\left(-1 - 2\nu + \sin^2\frac{\theta}{2}\right)$$

$$w = 0$$

Mode III

$$\tau_{xy} = \frac{K_{III}}{\sqrt{2\pi r}} \sin\frac{\theta}{2}$$

$$\tau_{xy} = \frac{K_{III}}{\sqrt{2\pi r}} \cos\frac{\theta}{2}$$

$$\sigma_x = \sigma_y + \sigma_z = \tau_{yz} = 0$$

$$w = \frac{K_{III}}{G}\sqrt{\frac{2r}{\pi}} \sin\frac{\theta}{2}$$

$$w = v = 0$$

See figure 3-4 for the parameter denotations.

b. The Stress Intensity Factor.

The stress intensity factor is one of the most basic factors used in linear-elastic fracture mechanics. Parameters KI, KII and KIII in the above equations are stress intensity factors. These parameters depend on the coordinate parameters, r and θ, if a material property cannot be considered linear-elastic to all directions.

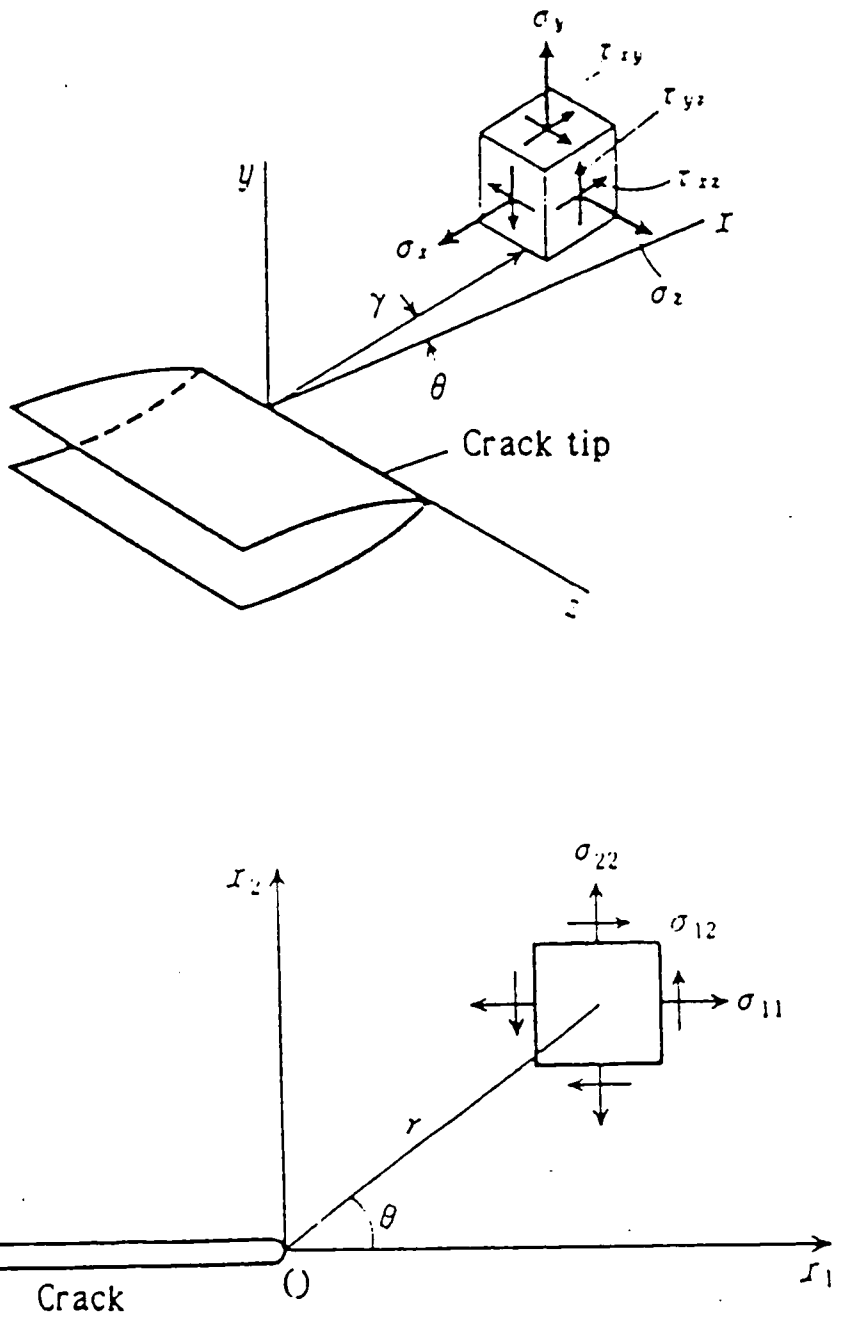


Figure 3-4.
Finite element parameters.

The stress formulas for these three modes are based on the assumption that a tested material is isoparametric. If a material does not have isoparametric properties, such as bones, the stress intensity factors are no longer constants. They are functions of the coordinate parameters. In non-linear dynamic fracture problems, the stress intensity factors are also depend on time and crack propagation speed.

The purpose of stress intensity factors is to adjust the stress distribution change caused by crack generation. The values of the stress intensity factor affect the stress magnitude passing through the crack tip and the crack type. There are several kinds of stress intensity factors depending on the type of applications and experimental settings. For example, KIC is strain fracture toughness, KIC(t) is rapid plane strain fracture toughness, and KIA is crack arrest toughness.

To eliminate the experimental data incompatibility among researchers, the American Society for Testing and Materials (ASTM) is making efforts to standardize fracture toughness data on an international scale. ASTM has already standardized the testing methods and released the table of data for KIC and KIC(t) for various materials. However, data accumulation is still mostly limited to metals, and data standardization for impact fracture is insufficient.

c. The Dynamic Energy Release Rate.

The energy release rate is an essential parameter in the crack analysis. Consider a crack proceeding in a linear elastic body. Let L be the work done by exterior force; Let W be the strain energy stored inside the body; and let K be

the dynamic energy of the body. If the energy required for crack propagation is negligible, the amount of energy that remains can be described by the following equations.

$$g(t, v) = \frac{1}{B}\frac{d}{da}\{ L - (W + K) \}$$

Here, B is the thickness of the plate, and a is the length of the crack.

4. Problems Associated with the FEM Approach.

a. General Information.

Today, with the power of advanced computer hardware, it is possible to solve repetitive mathematical computations which would have taken an enormous time to solve manually. However, there are still many obstacles to overcome. When constructing a large scale FEM model, operators often encounter the following problems.

1). Instability of the computation due to the time step size setting.

2). Increase of computational time as a number of element increases.

3). Increase of the element data as a model becomes complicated.

4). Vague reliability of solution due to the problem simplification.

These problems become more serious as the number of finite elements increases. Higher accuracy cannot be achieved simply by increasing the number of elements. If the number of elements is too few, accuracy is low. However, if the mesh elements are too many, unnecessary fluctuations or

divergence of the solution may occur. Thus, dividing a model into efficient elements is essential to each individual problem.

The output of finite element programs is digital values. Therefore, a visual check of solutions via graphical translations is necessary. Without the visual checks of experts, the chance of overlooking something important and making incorrect judgements is quite high. Even today, a final judgment of the acceptability of such solutions depends on the skills and experience of the FEM program operator.

There are many commercially available FEM programs that can handle non-linear problems. Some advanced programs are even capable of handling crack growth at relatively slow speed (up to 50 mm/s). However, FEM were not originally developed for simulating a failure process. FEM programs are only capable of approximating overall stress distributions in a model. Therefore, they are mainly used for the structural design of machine parts. Since parts are usually designed to withstand a much higher stress than a predicted stress, there is no need of accurately predicting failure point. These programs work fine for materials which can be considered uniform. But, in non-uniform materials, predicted results of stress distribution and crack propagation always suffer a high degree of uncertainty.

In finite element programs, all the elements in a model are connected together throughout the computation process unless they are intentionally separated between time frames. To mimic bone fracture patterns in the currently available finite element codes, all the possible fracture patterns must be available beforehand as crack data. Since all the fracture patterns must be predetermined to initiate a crack based on the surrounding stress

conditions, the resulting FEM outcome is not different from the prediction of an expert system, which directly relates inputs to outputs.

b. Crack Simulation by FEM.

Unlike the stress generated by static loading, the stress generated by impact transmits like a high speed wave. Under high speed wave transmission, only a single element (or a line of elements) to be subject to yielding stress in one time frame is impossible no matter how small the frame step is. A region of elements is always subjected to the yielding stress (not a line of element which can coincide with a crack line).

If a FEM program is modified to separate elements, which are subjected to the yielding stress at each time frame, these groups of elements simply disintegrate themselves. This disintegration process will be repeated like a chain reaction in the next time frame. As a result, the disintegrated region grows bigger and bigger until it penetrates through the finite element model. The simulated results are far from the actual crack behaviors. This is the reason the finite element method is incapable of accurately simulating the crack generations and propagations.

The realistic crack simulation can only be possible by manually operating the crack generations. Without setting cracks on a finite element model, stress relief along the crack edge during the impact moment cannot be accurately depicted. The crack generation possibility must be checked by visual inspection of the stress distribution at each time frame. The location and the direction of a crack must be judged and inserted manually. To preset a

crack, the initial location, direction, and penetrating speed must be obtained experimentally (See figure 3-5 for the crack parameters which are required by the finite element method).

c. Incubation Time for Crack Start.

Even under high speed impact, fractures do not occur immediately when the stress condition exceeds its limit. The stress must continue to exceed the yielding level at least a fraction of second to fracture. This time interval is known as the stress incubation time.

The stress incubation time is one of the critical factors in deciding the time step size for the failure analysis. Although the incubation time is very short, it is still approximately twice as long as the time the impact stress takes to reach the yielding limit (See figure 3-6). There is ample time for a impact stress wave to transmit into a farther region during the incubation period.

To focus on the stress condition at the moment of the fracture, the time step size must be smaller than the incubation time. If the incubation time is simply disregarded, the time delay of fracture may cause the accumulated error onto the results of overall fracture patterns. If the time step size is too small, the computation takes forever to finish. At worst, the outcome may suffer the accuracy and convergency problems which is associated with the machine's computational ability. Therefore, the time step size and the stress incubation time must be carefully managed.

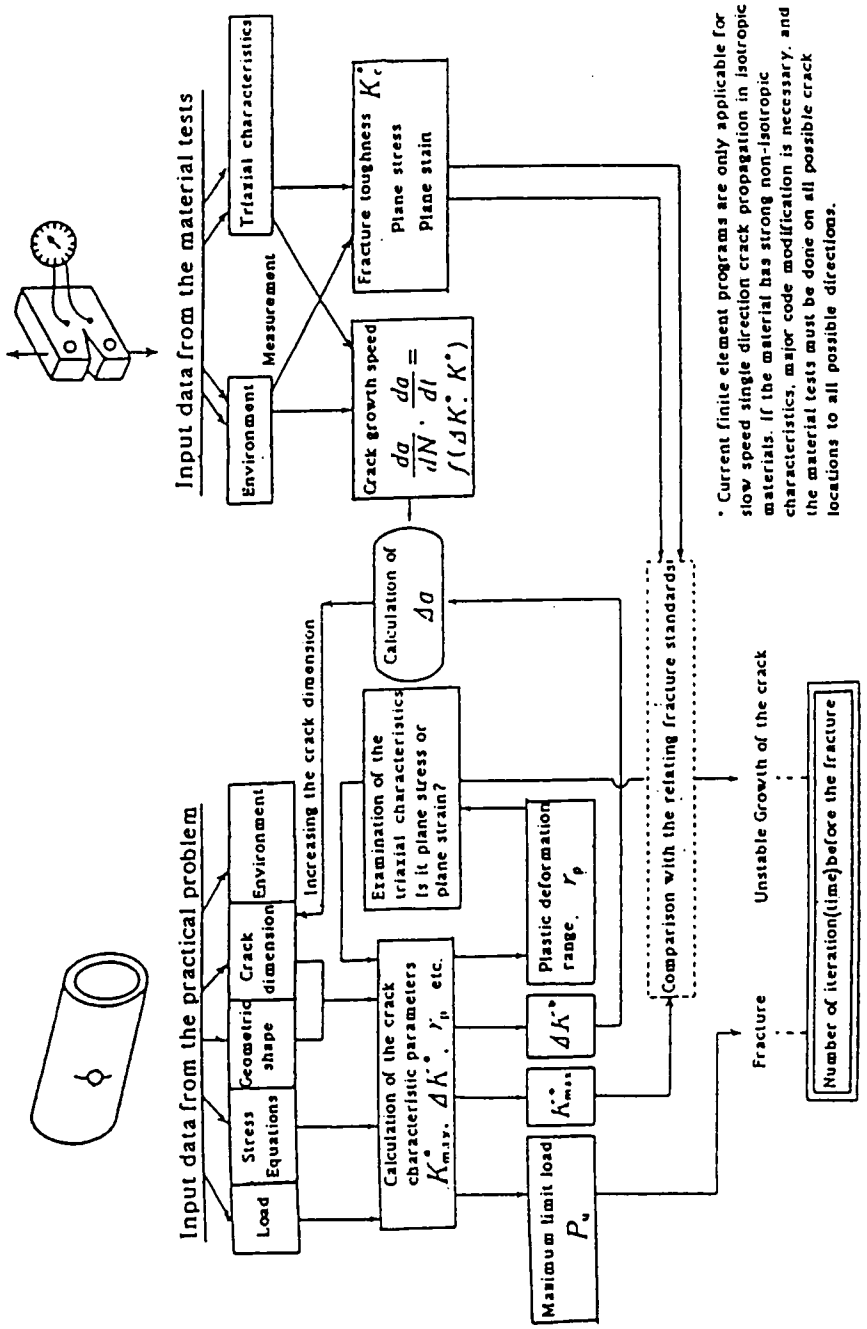
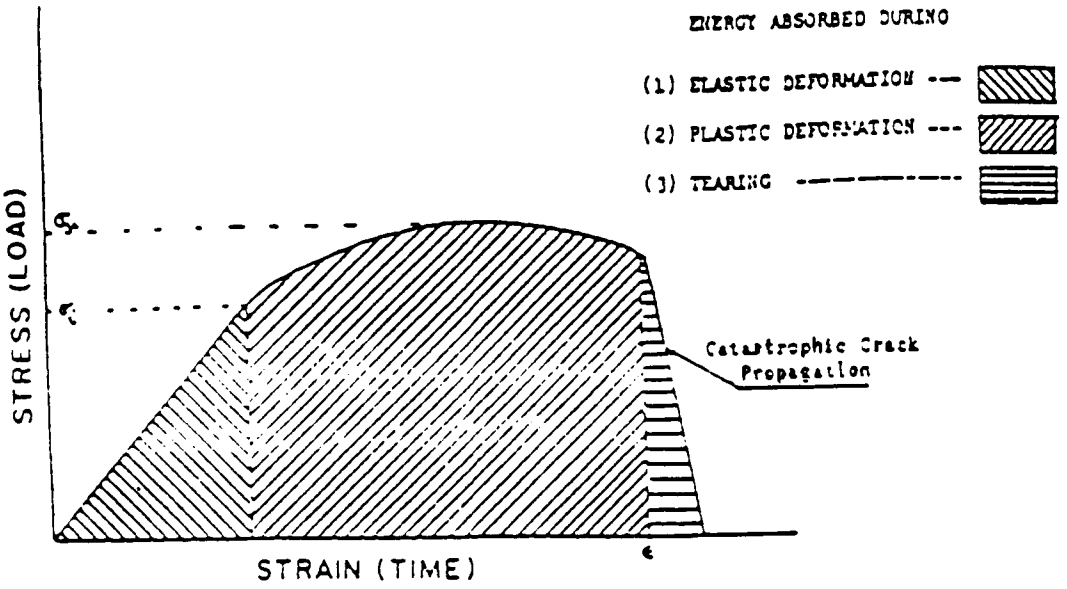


Figure 3-5.

Evaluation process of a crack by FEM.

(Gray, T. G. E, 1977)



The graph shows the energy absorbed during elastic, plastic and tearing phases.

Figure 3-6.

Idealized stress-strain Curve in tensile impact

(S. Saha and W. C. Hayes, 1974)

d. Variance Among Specimens.

Some degree of difference between simulation results and experimental results are caused by the variance among specimens. Due to the variance, yielding stress values of a composite material do not always show a constant value, even if they are machine manufactured. Therefore, the yielding stress of a composite material is always described with a tolerance. For safety design, the tolerance is not a problem. However, for the accurate fracture simulation, a large tolerance is a fatal problem. Compared to uniform materials, the properties of human bones are far more complex, and the variance among individuals is too wide to pick a constant value for the yielding stress.

5. Finite Element Programs Capable of Evaluating Fractures.

Many finite element programs are commercially available today. The most recent finite element programs are designed to be able to handle non-linear problems. Some programs capable of dealing with non-linear problems are ABAQUS, ADINA, MARC, and SIFRAM.

Recently, the Japan Mechanical Engineering Academy has formed a committee to analyze benchmark tests of the finite element programs available today for non-linear problems. Table 3-1 shows the analytical capabilities and methods of the major finite element programs.

Table 3-1

Evaluation of major FEM programs

	ABAQUS	ADINA	MARC	SIFRAM
Developer	Hibbitt, Karlsson & Sorensen,inc.	ADINA Engineering Inc.	MARC Analysis Research Corp.	Century Research Center Co.
Parameter used for computation	J integration	Energy release rate G	J integration	J,J integration
Evaluation method	Imaginary crack growth method	Imaginary crack growth method	Imaginary crack growth method	Path Integration method
Applicable dimension	2D, 3D	2D, 3D	2D, 3D	2D, 3D
Applicable problems	Elastic-plastic problems	Elastic problems	Elastic-plastic problems	Heat elastic-plastic problems
Expression of a crack by isoparametric elements	Possible	Possible	Possible	Possible
Special function	Line-spring elements			Consideration of thick shell elements
Evaluation of the crack growth				Automatic evaluation
Consideration of concrete fracture	Yes	Yes	Yes	No

(Yagawa, 1990)

(B)

Impact fracture mechanics Approach

1. Impact Fracture Mechanics.

a. General Information.

Today, the study field of impact fracture mechanics has become more and more popular as the demand for failure analysis caused by the impact force increases. A great deal of research work and theory development has been done recently in Japan. For the case of impact loading, the created stress distribution is very different from that of the static stress. Unlike static stress, impact stress transmits like a wave and changes with time. Like a sound wave, the stress wave can also reflect and refract at the material boundaries.

The formulas and figures used in this section are adapted from the *Handbook of Impact Fracture Engineering*, published by the Japan Mechanical Engineering Academy (1990). Although these formulas cannot be adapted directly to bone fractures without considerable modifications, they are adequate to show the state of impact force transmission.

b. Stress Wave Created by Impact.

Since the impact stress is treated like a wave, the impact stress spreads three-dimensionally with time. If the objects are very thick, the spreading of the stress wave is not negligible. However, to explain the basic concepts of the

stress transmission, the following examples are simplified into one-dimension by using bar problems.

When an object of mass M moving at velocity V strikes the end of the bar, a compressive stress wave starts to travel toward the right inside the bar at speed Cb (See figure 3-7). During the time t, the head of the wave travels Cbt. By assuming that the interval is evenly compressed, the compressive strain can be expressed as follows, since the left end of the bar has moved δ to the right during the time t.

$$\varepsilon = \frac{\delta}{Cbt}$$

The strain can also be expressed as follows by using dynamic impedance Z (See Appendix-C).

$$Z = \rho Cb$$

$$\delta = V\sqrt{E\rho} = V\rho Cb = VZ$$

Here, ρ is the density of the bar and E is the modulus of longitudinal elasticity.

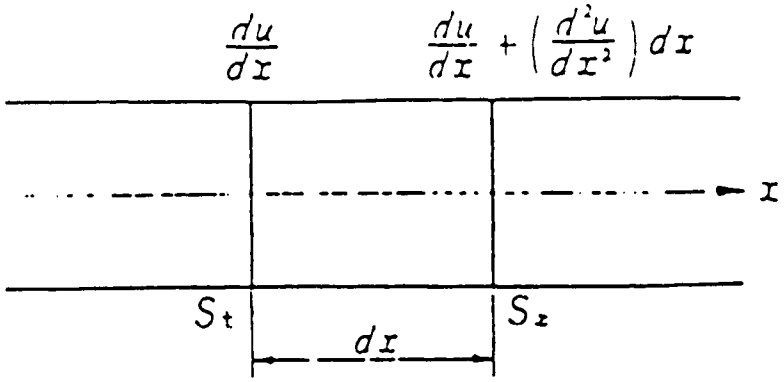
Problem Assumptions

1). The bar is made of a homogeneous, isotropic, and linearly elastic material.

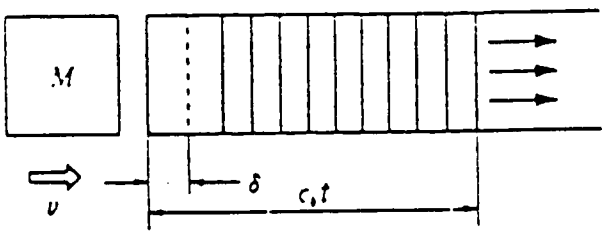
2). The striking object is rigid and undeformable.

3). The bar has a constant cross-sectional area.

4). The bar is infinitely long toward the right.



Transmission of the longitudinal wave



Axial impact at bar end

Figure 3-7.

Stress wave created by impact.

(Source: "Impact Fracture Mechanics published by Japan Mechanical Engineering Academy in 1990.)

c. Stress Wave Behavior at Boundary.

There are two cases of the boundary condition for the bar end opposite from the impact side. One is free, and the other is fixed (See figure 3-8). If the bar end is fixed on a hard wall, which is considered unmovable, the displacement at the fixed point must be zero even when the injected impact wave has reached to the end. In this case, the incoming stress wave is cancelled by the counter stress wave from the wall side. It is like "action" and the "reaction" in elementary physics. However, the resultant stress at the fixed end is twice as big of the injected stress wave due to the compression wave from both sides. This is very different from the stress distribution in static condition. (In static condition, the normal stress is the same on any cross section of the bar.)

If the bar end is free, there is no counter stress wave which must come from the other side of the bar end. However, there is a reflection wave at the bar end. The incoming wave bounces back at the end surface of the bar. In this case, the stress at the free end is zero due to the cancellation of the incoming wave by its own reflection.

Measuring the percent reflection and refraction rate at boundaries is very important since there is no perfectly linear-elastic material in the real world. Only some percentage of the stress is actually reflected back at boundaries.

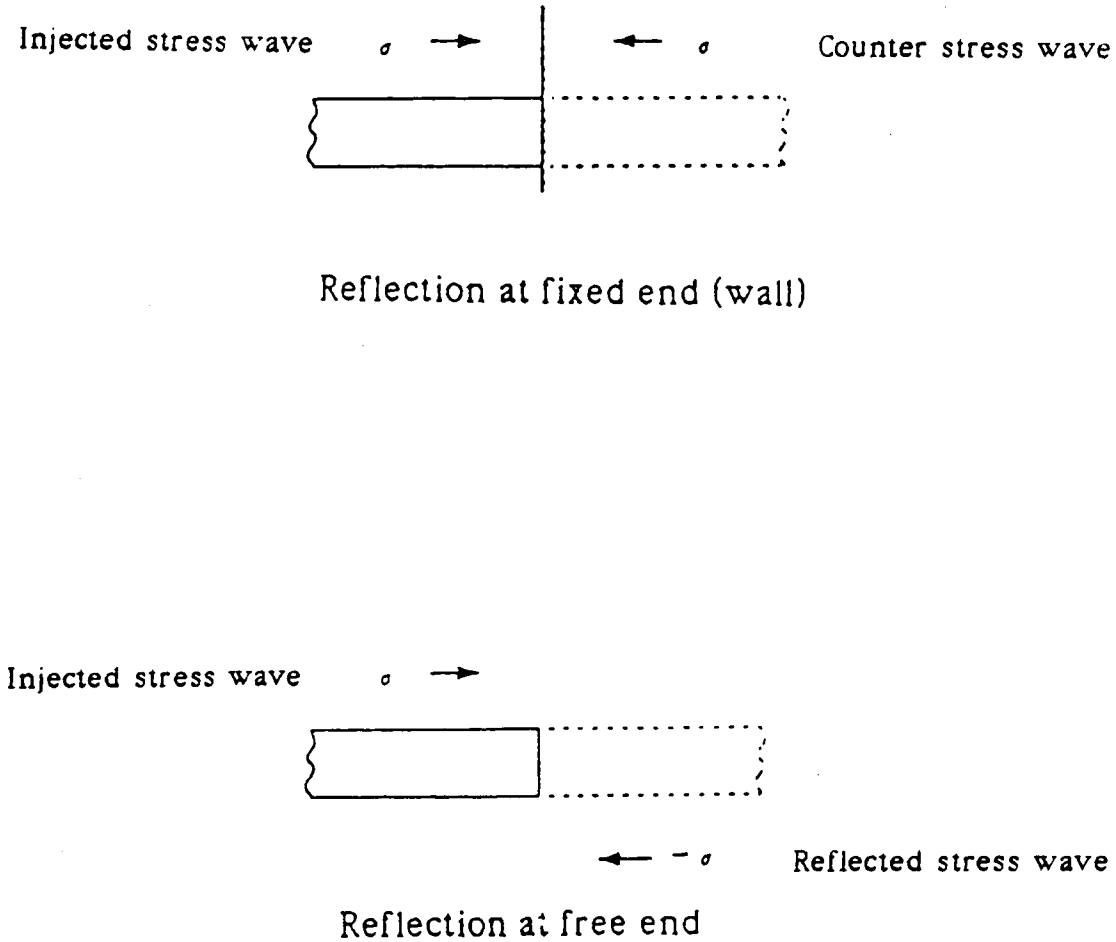


Figure 3-8.

Counter wave and reflection wave at boundary.

(Source: "Impact Fracture Mechanics published by Japan Mechanical Engineering Academy in 1990.)

d. Impact Collision Between Two Bars.

Consider the collision of two bars with the same diameter on the lines of their longitudinal axes (See figure 3-9). Let the dynamic impedance, length, and velocity of bars No.1 and No.2 be Z1, Z2, l1, l2, and v1, -v2, respectively. Velocity is positive to the right. At the time of impact, t=0. After the impact, both bars move together at speed -vc without losing contact with each other. For this case, the magnitude of the compressive stress σ generated by the impact is the same for both bars, since the cross sectional areas of the bars are the same. After impact, the stress wave starts to travel to both sides of the impact surface. The magnitude of σ in bar No.1 is expressed by the following equation:

$$\sigma 1 = Z1(v1 - (-vc)) = Z1(v1 + vc) \qquad \text{Eq 1}$$

For bar No.2:

$$\sigma 2 = Z2(v2 + vc) \qquad \text{Eq 2}$$

After the impact, the region where the stress wave has not yet reached is moving at the speed it was before the impact; that is, v1 for bar No.1 and v2 for bar No.2.

Assuming that $\sigma 1 = \sigma 2$, equate Eq 1 and Eq 2

$$\sigma 1 = Z1(v1 + vc) = Z2(v2 + vc) = \sigma 2$$

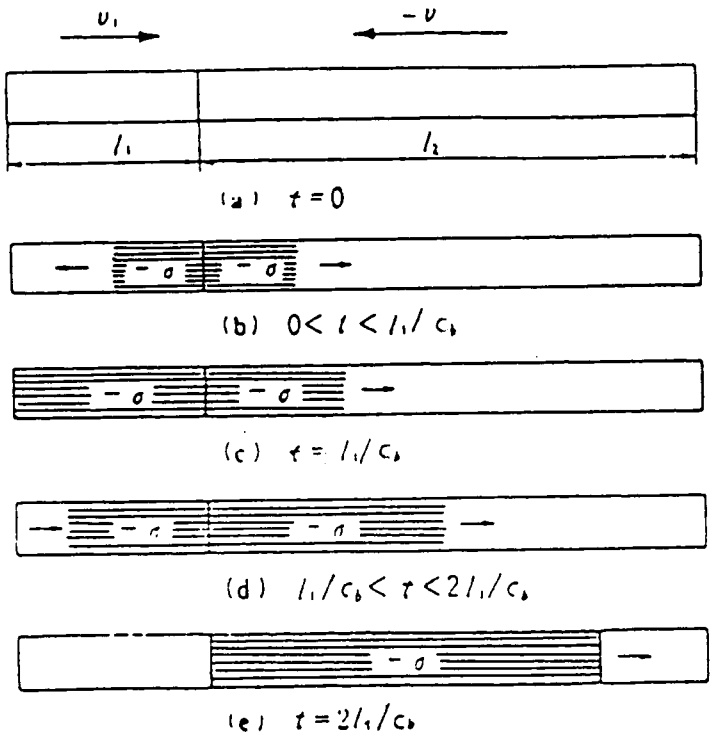


Figure 3-9.

Head to head collision of two bars.

(Source: "Impact Fracture Mechanics published by Japan Mechanical Engineering Academy in 1990.)

Solve above equation for vc

$$v_c = \frac{Z_2 v_2 - Z_1 v_1}{Z_1 + Z_2}$$

Substituting above equation back to Eq 1 or Eq 2, we get

$$\sigma_1 = \sigma_2 = \frac{Z_1 Z_2 (v_1 + v_2)}{Z_1 + Z_2}$$

The above equation indicates that the stress generated by the impact is proportional to the virtual impact speed (v1+v2) before the impact takes place. For the case of auto accidents, the momentum of pedestrians is almost negligible compared to the momentum of automobiles. Therefore, the impact stress is proportional to the speed of the automobile.

e. Collision of Bars with Different Cross Sections.

Consider the axial impact of two bars made of the same material but with different diameters (See figure 3-10). Bar No.1 and No.2 are traveling to the right at speeds v1 and v2, respectively. Let v1>v2 so that bar No.1 collides with bar No.2. The time t is zero at the contact. After impact, the stress wave begins to transmit into both bars from the impact surface. However, unlike the first case, the cross sectional areas are different (S1>S2). Therefore, the magnitude of the stress in bar No.1 and bar No.2 will be different.

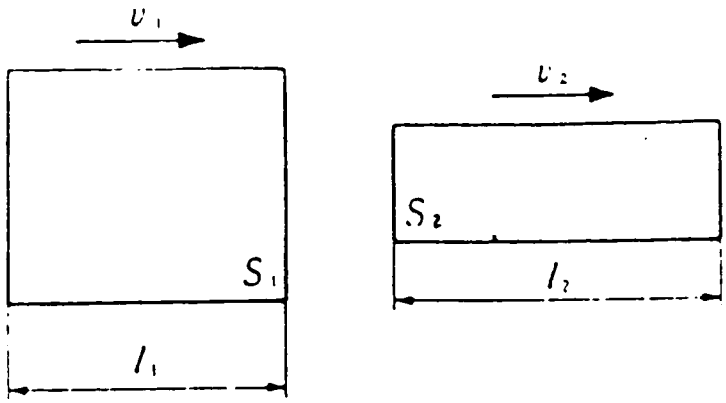


Figure 3-10.

Collision of two bars with different cross-sectional areas.

(Source: "Impact Fracture Mechanics published by Japan Mechanical Engineering Academy in 1990.)

Assuming force equilibrium at the impact surface, equate the transmitted impact force to the left hand side of the impact surface with the reflected impact force to the right hand side of the impact surface,

$$\sigma 1\ S1 = \sigma 2\ S2$$

If the length of bar No.1 is shorter than bar No.2, (l1 < l2), the stress wave travels inside bar No.1 until t= l1/Cb after the impact. When the stress wave reaches the free end of bar No.1, it reflects back toward the impact surface. While the reflection wave is coming back to the impact surface from the free end at the speed of v1, the impact surface travels to the right at speed vc without losing contact. The forces acting on the impact surface from both side are at equilibrium during the contact period.

$$S1\ Z\ (v1 - vc) = S2\ Z\ (vc - v2).$$

Solving for vc

$$vc = \frac{v1S1 + v2S2}{S1 + S2}$$

The stresses in bar No.1 and No.2 are as follows:

$$\sigma 1 = \frac{S2Z}{S1 + S2}(v1 - v2)$$

$$\sigma 2 = \frac{S1Z}{S1 + S2}(v1 - v2).$$

If bars No.1 and No.2 are not made of the same materials, the dynamic impedances are different. Let Z1 = the dynamic impedance for bar No.1 and Z2 that for bar No.2. The equations for impact stress will be modified as follows:

$$\sigma 1 = \frac{S2Z1Z2}{S1Z1 + S2Z2}(v1 - v2)$$

$$\sigma 2 = \frac{S1Z1Z2}{S1Z1 + S2Z2}(v1 - v2)$$

The above equation indicates that the magnitude of the impact stress is proportional to the area of the surface of the striking object and the relative impact velocity of two objects.

f. Stress in the Bar with Stepped Cross Sections.

Consider a bar with two parts. One part has cross section S1, and the other part has cross section S2 (See figure 3-11 (top)). When impact is applied at the left end of the bar, the stress wave starts traveling inside the bar toward the right. At the boundary B1-B2, where the diameter reduces, a portion of the stress wave transmits to S2, and the rest of the stress wave is reflected back to S1.

Let the injected wave, transmitted wave, and reflected wave be σi, σt, and σr, respectively.

Assuming force equilibrium at the boundary B1-B2,

$$S1(\sigma i + \sigma r) = S2\sigma t .$$

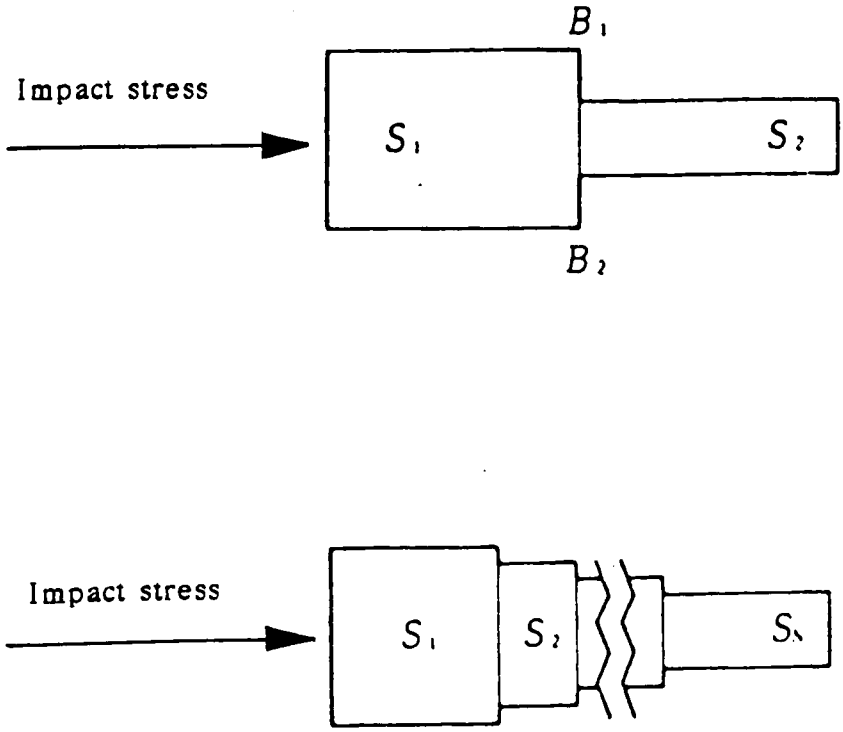


Figure 3-11.

Bar with stepped cross-sections.

(Source: "Impact Fracture Mechanics published by Japan Mechanical Engineering Academy in 1990.)

At the boundary, the displacement velocity of the S1 side is equal to the displacement velocity of the S2 side

$$Vi - Vr = Vt ,$$

which leads to the following stress relation

$$\sigma i = \sigma r + \sigma t .$$

Solving the above equations for σr and σt respectively,

$$\sigma t = \frac{2S1}{S1 + S2}\sigma i = \eta t \, \sigma i$$

and

$$\sigma r = \frac{S2 - S1}{S1 + S2}\sigma i = \eta r \, \sigma i .$$

Here, ηt and ηr are the coefficient of transmission and the coefficient of reflection at the boundary. If the cross sectional area changes smoothly from S1 to SN, as in figure 3-11 (bottom), the stress is expressed by the following formula.

$$\sigma t = \sum_{n=1}^{N-1} \frac{2Sn}{Sn + Sn+1}\sigma i$$

It is obvious that the smoother the cross sectional transition, the larger the coefficient of transmission: A bar with a smooth cross-sectional change transmits a greater portion of the injected wave to the other end.

Chapter IV

FUZZY LOGIC APPROACH

(A)

Introduction to Fuzzy Logic

1. General Information.

All computer programs require discrete numerical variables for input. Any ambiguous, non-numerical data must be converted into acceptable numerical form for use in a computer. Conventional computer logic uses binary logic, which is based on yes or no, true or false types of data transactions. Since the information to be input as data must be classified into one of two categories, such logic is not good for dealing with information that is on or close to the boundaries of the classification criteria.

Dr. L. A. Zadeh, a specialist in modern control logic at the University of California, had experienced the limitations and difficulties of detailed mathematical rules for factory control simulations and was looking for a new idea which would perform naturally and be easy to apply. His idea was to use fuzziness instead of pursuing mathematical precision and strictness. In 1966, Zadeh published the basic idea of fuzzy logic, which uniquely fills the gap between "yes" and "no" type of answers without complicating the entire program structure.

Unlike binary logic, fuzzy logic accepts the ambiguity of data for transactions. In binary logics, if the ordinary temperature is set between 36

and 37 C, any temperature above or below this temperature is classified as abnormal. This indicates that a slight difference of numerical input in the vicinity of the boundary makes a huge difference to its output. But, in fuzzy logic, a temperature of 37.0 C is classified as a little fever, and a temperature of 37.2 C is classified as a subtle fever, and so on. This type of answer is more natural for this case.

In fracture simulations, the yielding point is the limit at which the fracture start to occur. However, the yielding stress of a material is not a constant value. It always fluctuates in some range. If the estimated stress is in the ambiguous range of the yielding limit, the fracture occurrence cannot easily be distinguished by "yes" or "no". It is more natural to answer with the degree of possibility; for example, "A fracture almost certainly occurs", "A fracture most probably occurs" or "A fracture possibly occurs", and so on.

2. Merits of Fuzzy Logic.

Fuzzy logic offers six advantages over binary logic:

1. It can accept ambiguous data input.
2. It can convert fuzzy data into numerical values.
3. Need for strict math equations can be minimized.
4. It can perform fairly well based on limited data.
5. It can interpolate output from the given data.
6. It can handle a problem with many classified cases.

Ambiguous expressions, such as "slow," "fast," "long," "short," and so on can be used as input. Often factors that cannot be expressed as numerical expressions are ignored or are arbitrarily converted into mathematical expressions. However, fuzzy logic can easily overcome this dilemma.

The following example is adopted from Mitsuya's "*Fuzzy Logic Inference*" (1989). These fuzzy rules are for keeping a steady distance behind another car while driving. As you can see, fuzzy rules are based on common sense. There is no complicated description.

By using definitions, the following rules are written in shorthand.

Rule 1 IF X is A1 and Y is B1 THEN z is C1
Rule 2 IF X is A1 and Y is B2 THEN z is C2
Rule 3 IF X is A2 and Y is B1 THEN z is C3
Rule 4 IF X is A2 and Y is B2 THEN z is C1

A1:	narrow;	B1:	slow;	C1:	hold on
A2:	wide;	B2:	fast;	C2:	slow down
X:	distance between cars				
Y:	speed of the car				
Z:	speed control operation				

Fuzzy logic rules are very simple and straightforward. Anyone who has driving experience can come up with these rules. However, using only conventional strict mathematical logic without fuzzy control logic results in a mass of equations because such simply-worded rules are not accepted.

For example, to control a car with strict mathematical formulas, dynamic equations must first be constructed with all the related variables of concern, such as the position, direction, speed, acceleration, angle of the

steering wheel, degree of the gas pedal and brake pedal, size and weight of the car, and much more. By solving these equations, the control parameters can finally be determined. However, without solving these intricate mathematics, car drivers can adjust the steering, acceleration, and braking simply by their natural driving senses developed through the years of experience.

To reach the objective by the shortest path, the best method is structurally classifying the problem into several grouped cases instead of trying to describe the entire process with a single formula. If the strict mathematical formulation are applied, a battle against the large number of equations and associated variables and constants is inevitable, especially for non-linear problems.

3. Fields in which Fuzzy Logic is Applied.

Today, the application of fuzzy logic can be seen in various fields from engineering to economics. These are some examples of fuzzy logic application:

Medical diagnostic programs
Structure safety diagnostic programs
Stock market prediction programs
Auto focus control
Voice recognition programs
Photographic image identification programs
Automatic transmission control
Driving stability control
Space shuttle docking control
Subway speed control

(Mitsuya, 1990)

4. Expression of Fuzziness.

Fuzzy logic expresses parameter relationships by membership functions, a series of overlapped functions (usually triangle-shaped). By means of membership functions assigned for input and output, ambiguous input can be converted into a number, and fuzzy logic can make inferences humanly with some degree of fuzziness involved. The significance of membership functions is similar to that of probability functions in statistics. However, instead of expressing probability of occurrence, membership functions return the degree of trueness in each function which represents a fuzzy variable. The membership notations commonly used are PB (positive big), PM (positive medium), PS (positive small), Z (zero), NS (negative small), NM (negative medium), and NB (negative big).

(B)

The Basic Concept of Fuzzy Logic

Although the concept and the application of fuzzy logic is very simple and straightforward, the detailed explanation of the logic concept behind it tends to be quite lengthy. Since there is not enough space to do that here, only the basic logic concept is introduced. (Explanations and figures are adapted from the operator's manual of *FUZZLE1.8*, which is the program utilized to construct the fuzzy expert system to predict bone fracture possibility in this thesis.)

1. Fuzzy Variable.

Consider a continuous variable X as defined in calculus. Suppose that X can take any value between 1 and 10. There can be no more information attached to the variable X using this representation. For example, if X is denoting room temperature (F), then the information "x=3" simply means that the room temperature is 3 F. On the other hand, consider the heuristic approach, in which the range (universe) of X is divided into several regions, defined as the "low", "medium", and "high" regions of X, respectively. We can then redefine X as a fuzzy variable to take linguistic values of low, medium, and high. As one can infer from this discussion, the qualifications low, medium and large are approximate definitions. Figure 4-1 shows the universe of the variable X and its labelled regions.

The fuzzy representation entails more information about a variable than that of the standard representation in calculus. Using the example above, the information "X=low" means that the temperature is within 1-5 F range, and it is low with respect to some other values it can take. More importantly, the variable becomes susceptible to a range of numbers instead of a crisp number such as X=3. This representation is known to mimic human reasoning more accurately than using crisp variables.

The next section describes how to transform a numerical value to a linguistic value using membership functions.

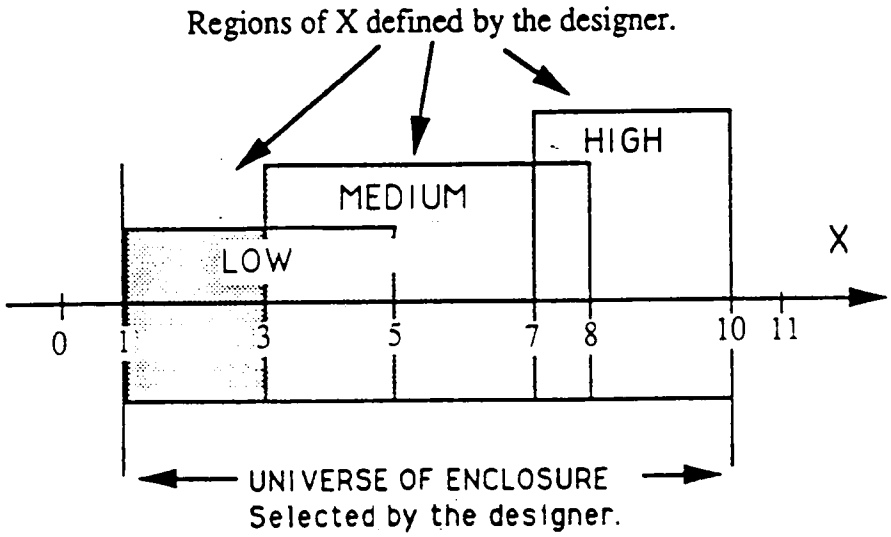


Figure 4-1.
Fuzzy variable.

(source: Fuzzle 1.8 manual, 1992)

2. Membership Function.

The fuzzy variable representation of X is defined by membership functions. For example, how is "low" defined in the interval of 1-5 ? The definition of "low" or any other term depends solely on the user and his/her judgement. In fuzzy logic, such a judgement is formulated by a possibility distribution function, which is called "membership function". For example, in the interval of 1-5, the membership function "low" must yield 1 (or whatever the maximum value may be) at a certain location on the universe which represents "low" the best. The figure 4-2 shows an example of the possibility (membership) distribution of X between 1 and 10.

The shape of the membership function can be in any form as it represents the relationship of interest. In the example above, the fuzzy variable X is designed to be completely low at X=2 (membership is equal to 1). In *FUZZLE*, the shape of the membership functions are piece-wise linear with 4 brake-points (coordinates) that include triangles and trapezoidals of any form. Also the maximum value of a membership function is always equal to 1 in *FUZZLE*.

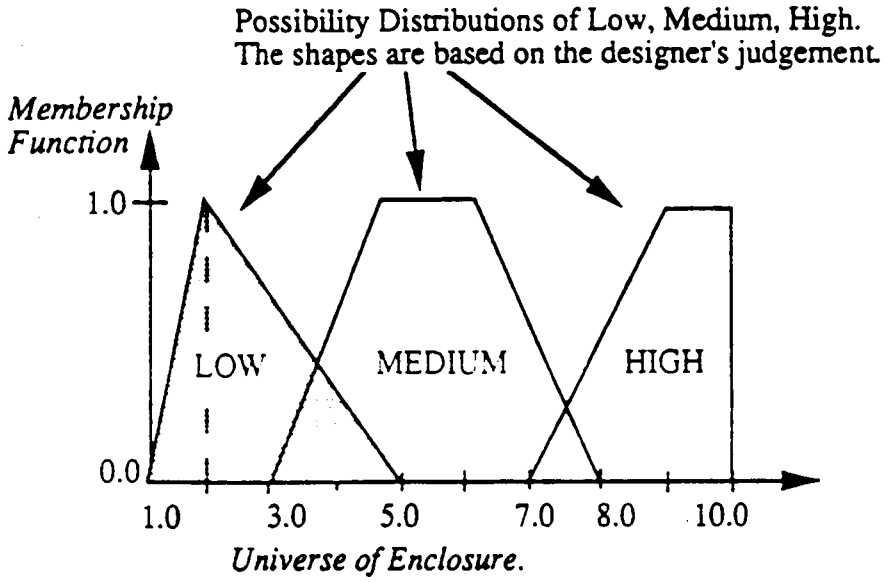


Figure 4-2.

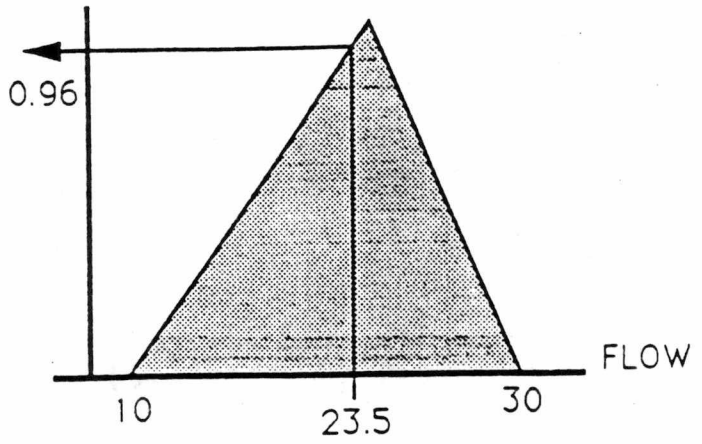
Membership function.

(source: Fuzzle 1.8 manual, 1992)

3. Membership Cuts.

Fuzzification and defuzzification are directly related to how the membership functions are cut by inputs and outputs. Once the inputs of an inference engine are projected onto the counters of membership functions, they may be considered as being mapped on a fuzzy space or fuzzy clusters (this is often called fuzzification). Figure 4-3 (top) shows a triangular membership function named "LOW" defined between 10. and 30. of a fuzzy variable called FLOW. If FLOW is 23.5 lbs/sec, then the value of the membership function will be evaluated as shown in the figure.

Similarly, if FLOW is an implication (RHS) variable, then the results of rule composition will be projected onto the counters of the membership function (say "LOW"). The cut is side-ways, leaving a shape underneath, often in the form of a trapezoidal (See figure 4-3 (bottom)). Another common method of cutting, which places a triangle inside the trapezoidal, is also shown below. If there are N rules, each will produce a shape like the one in the figure. The final decision will be made through the implication process that takes into account all of the resultant trapezoidals and computes the center of gravity.



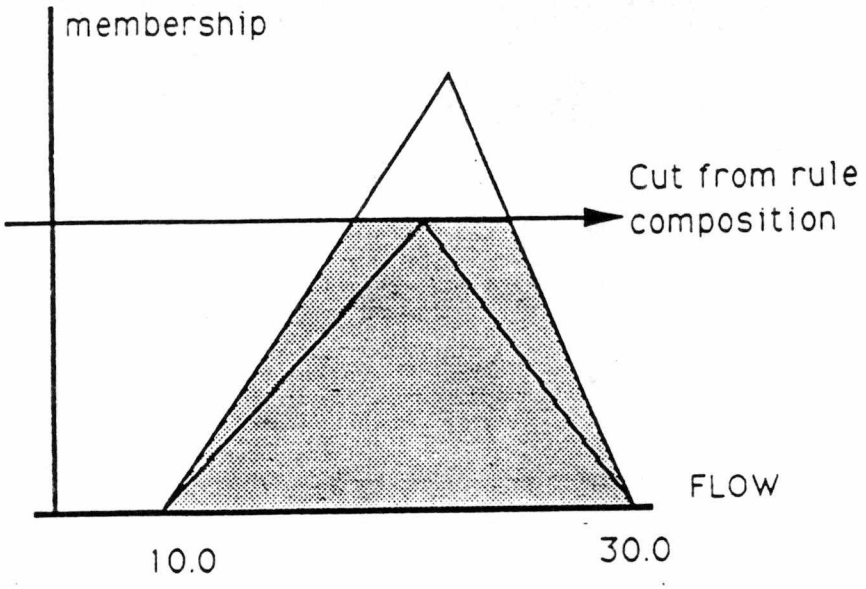


Figure 4-3.
Membership cuts.

(source: Fuzzle 1.8 manual, 1992)

4. Rule Composition.

Rule composition refers to the organization of left-hand-side (LHS) statements using logic operators such as (OR) and (AND). For example, consider the following fuzzy rule:

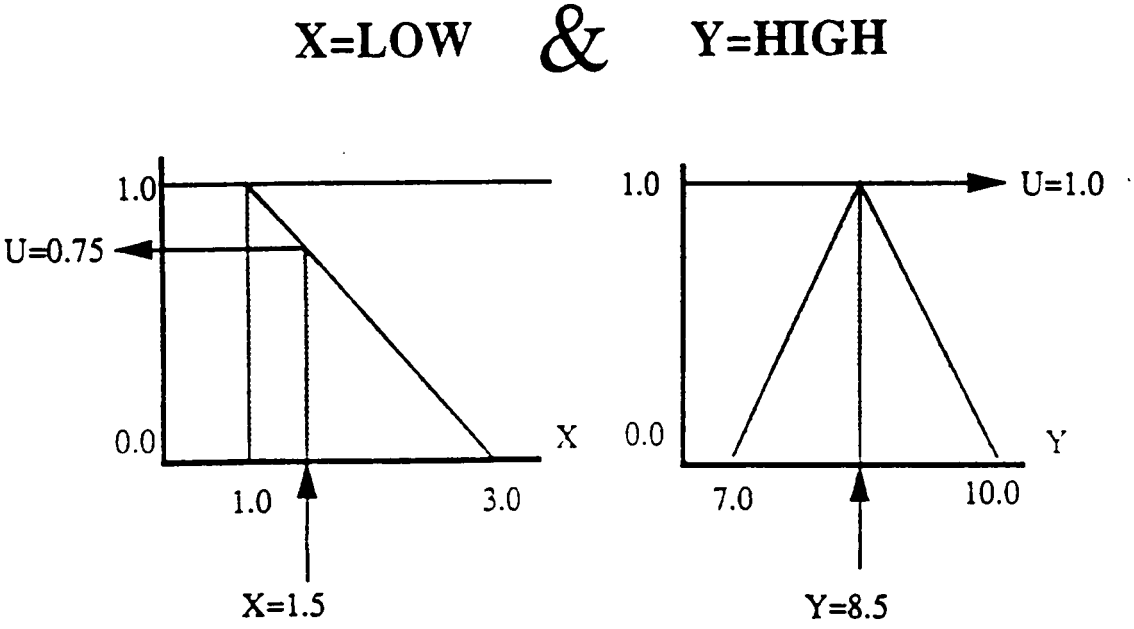
IF X = low AND Y = high THEN Z = medium

Here, the LHS statements (X=low, and Y=high) are composed by AND operator. Suppose that the membership functions for X=low and Y=high are designed as triangles as shown in figure 4-4. When there are instantaneous entries (inputs) of X=1.5 and Y=8.5, the corresponding values of the membership functions (U) are found as shown in the figures.

Then, AND operator uses the values of U_{xlow}=0.75 and U_{yhigh}=1.0 to compute the output of composition(AND finds the minimum = 0.75). This output will be used in the implication process by THEN operator.

5. Implication Principle.

One of the common approaches to interpreting the THEN operator is to calculate the center of gravity of the final shape obtained by cutting the right-hand-side (RHS) membership function with the results of the rule composition. For example, consider the fuzzy rule given above. The RHS statement (Z=medium) is shown in figure 4-5. The composition result was 0.75. Thus, the membership function (medium) is cut from 0.75 to yield the shaded trapezoidal area. The center of gravity of this area is the result. Very often,



The instantaneous value of X=1.5 yileds 75 % possibility for X being LOW.
The Instantaneous value of Y=8.5 yields 100 % possibility for Y being HIGH.

Figure 4-4.

Rule composition.

(source: Fuzzle 1.8 manual, 1992)

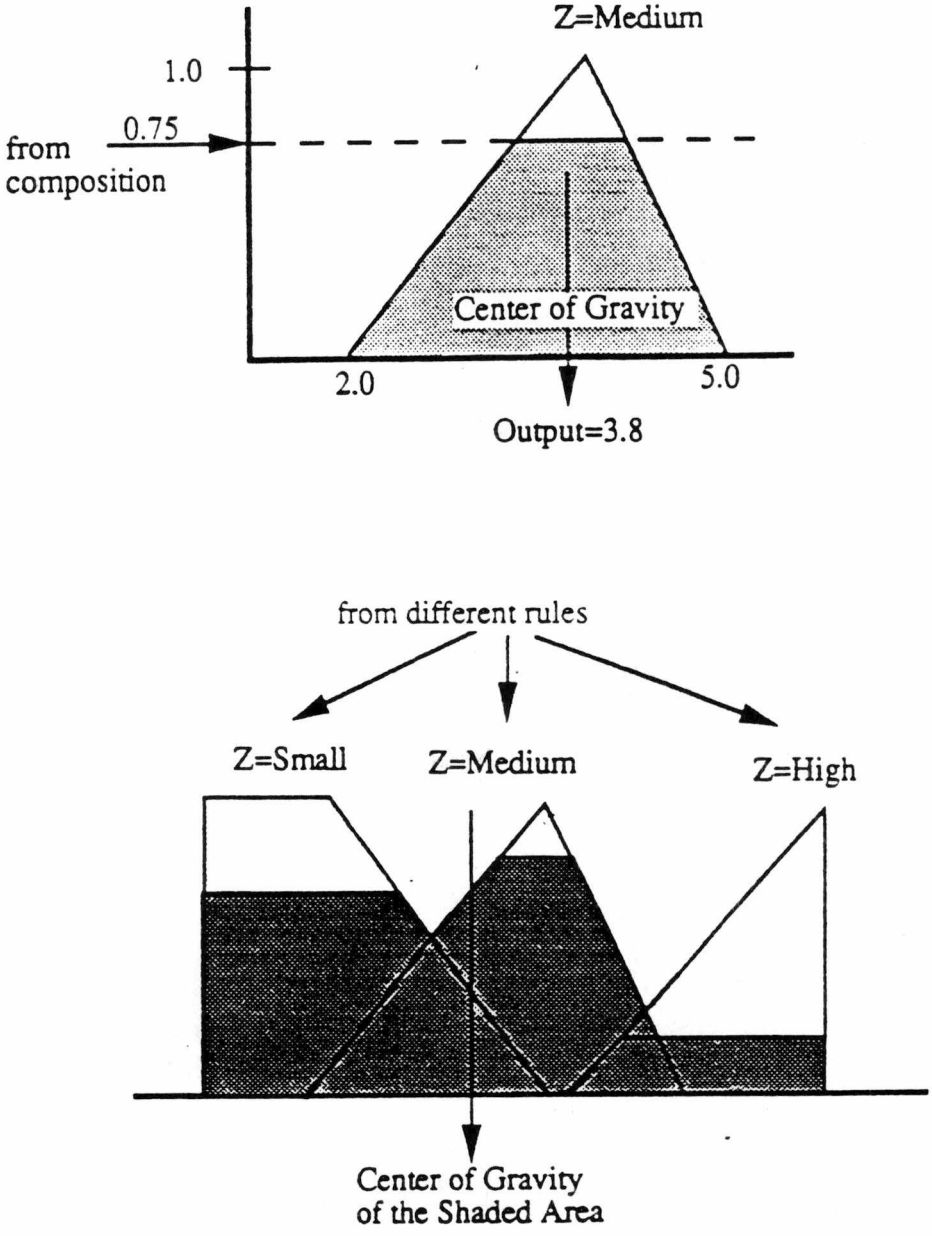


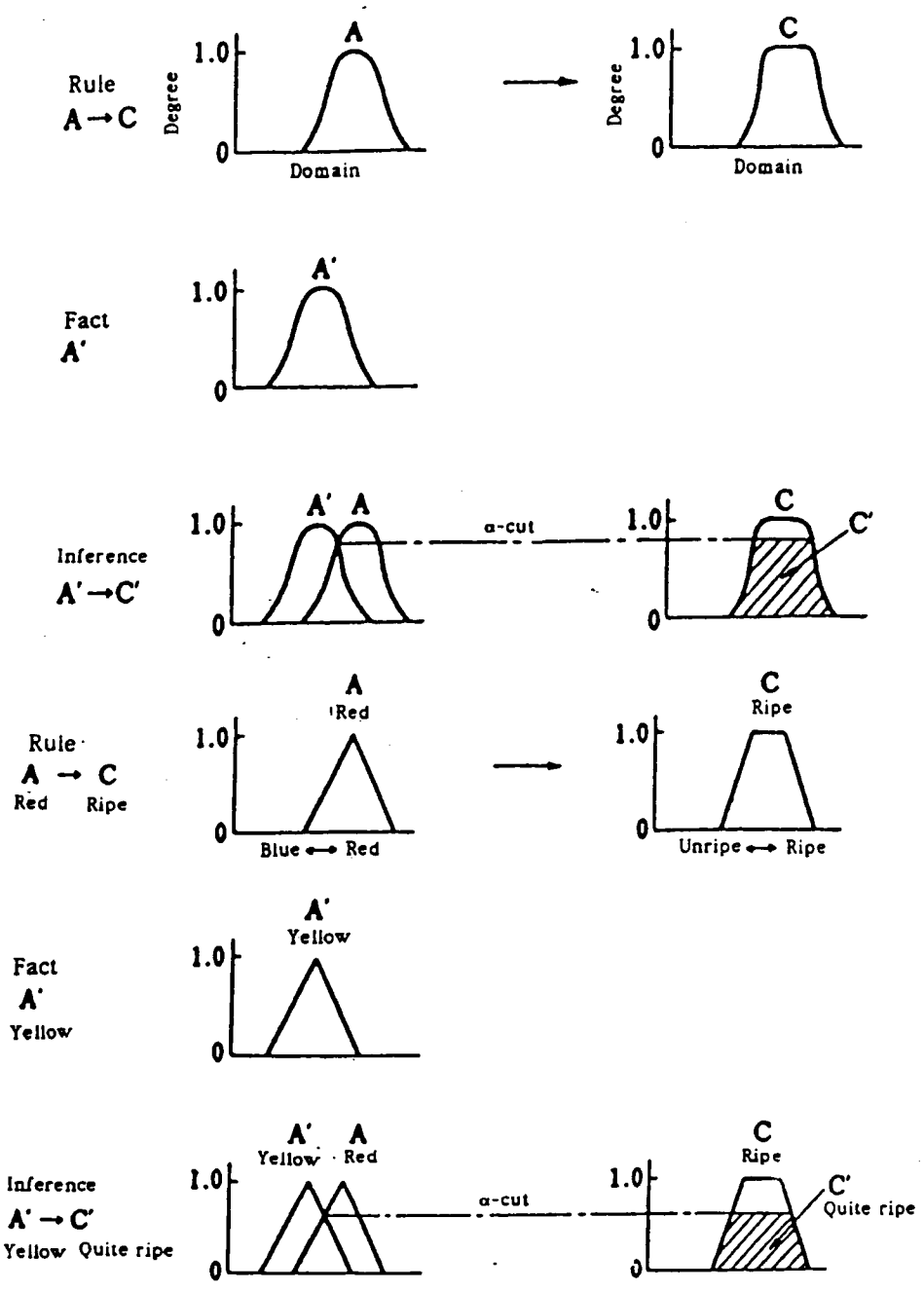
Figure 4-5.
Implication principle.

(source: Fuzzle 1.8 manual, 1992)

this process and the RHS variable are called "defuzzification" and "action variable," respectively.

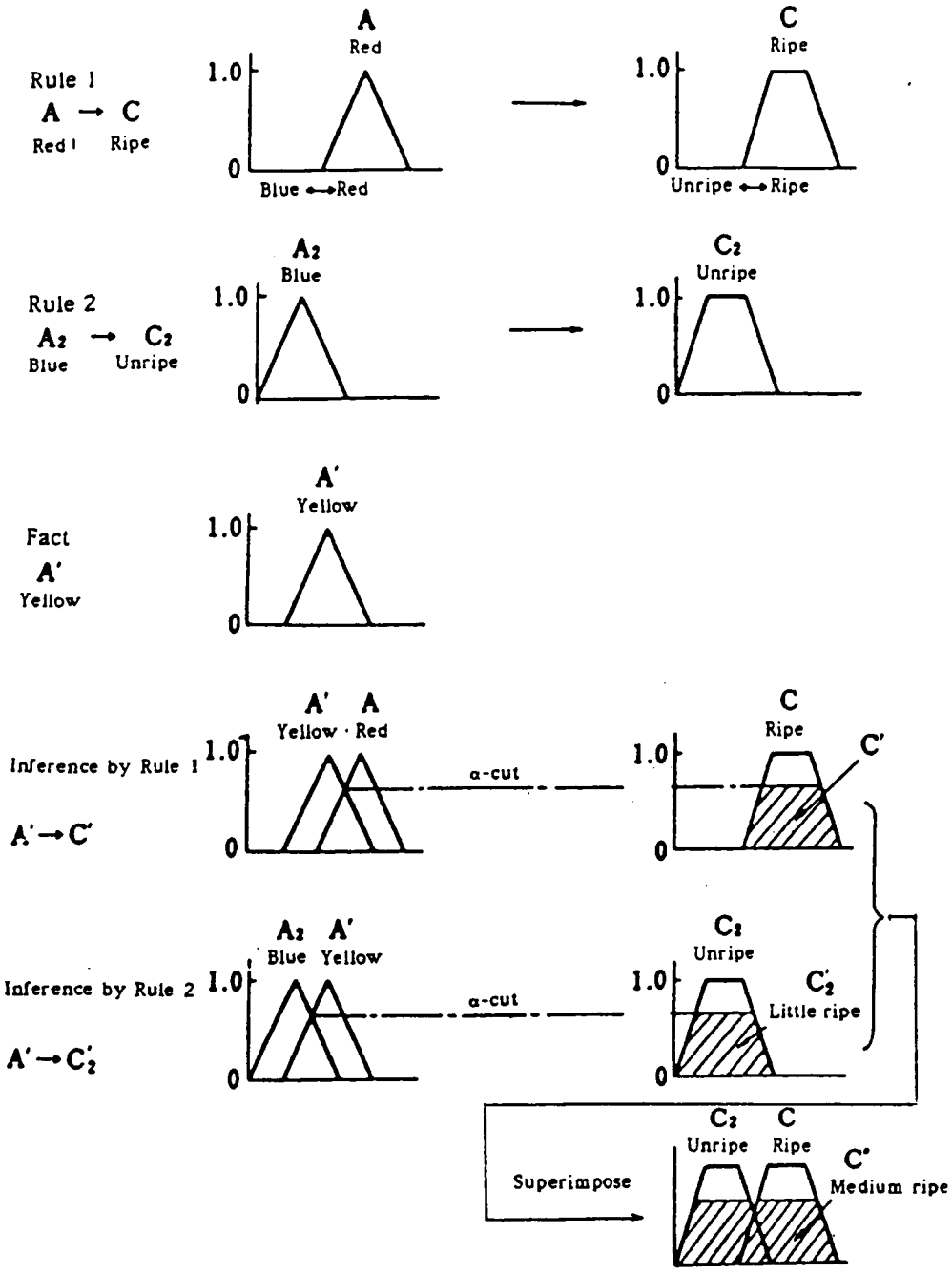
6. Graphical Concept of Fuzzy Logic.

The graphical process of fuzzy logic prediction of apple maturity level is very helpful in visualizing the basic concept of fuzzy inference step by step. Apple maturity level is inferred from its color and softness. Figure 4-6A shows the concept of α-cut. Figure 4-6B explains the concept of shape superimposition. Figure 4-6C shows the inference improvement potential by use of advanced rules. Compared to the simple rules in the form of "A then B," the advanced rules in the form "A and B then C" can make a better inference. Figure 4-6D shows that the center of gravity of the superimposed figure represents the numerical value of the inference result.



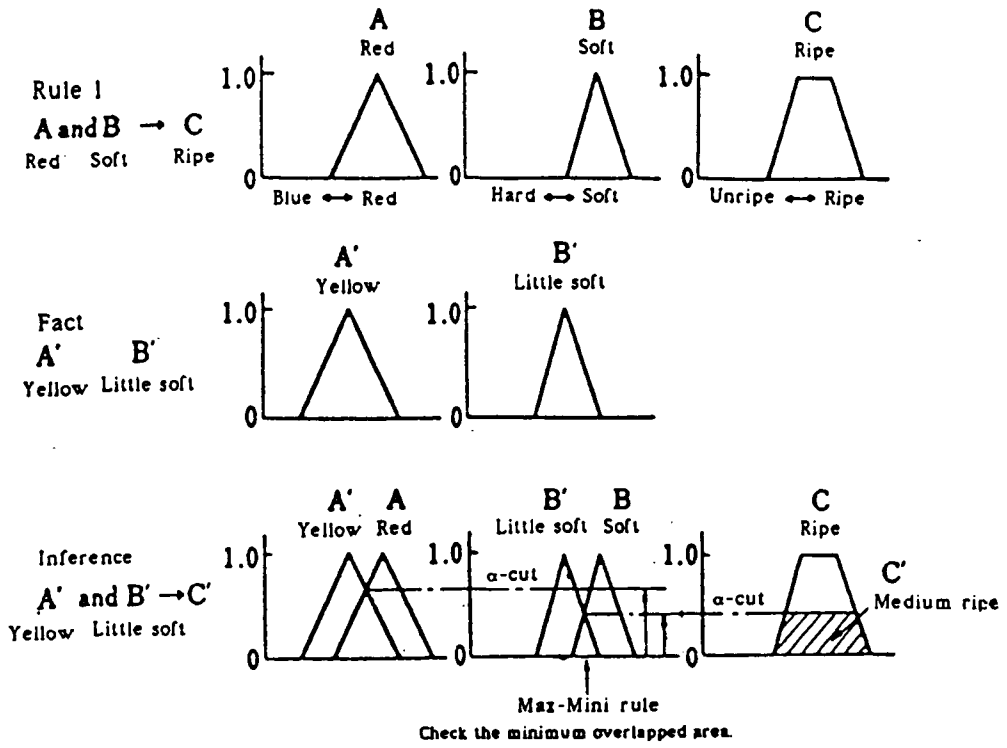
(A)

Figure 4-6.
Graphical explanation of fuzzy inference.



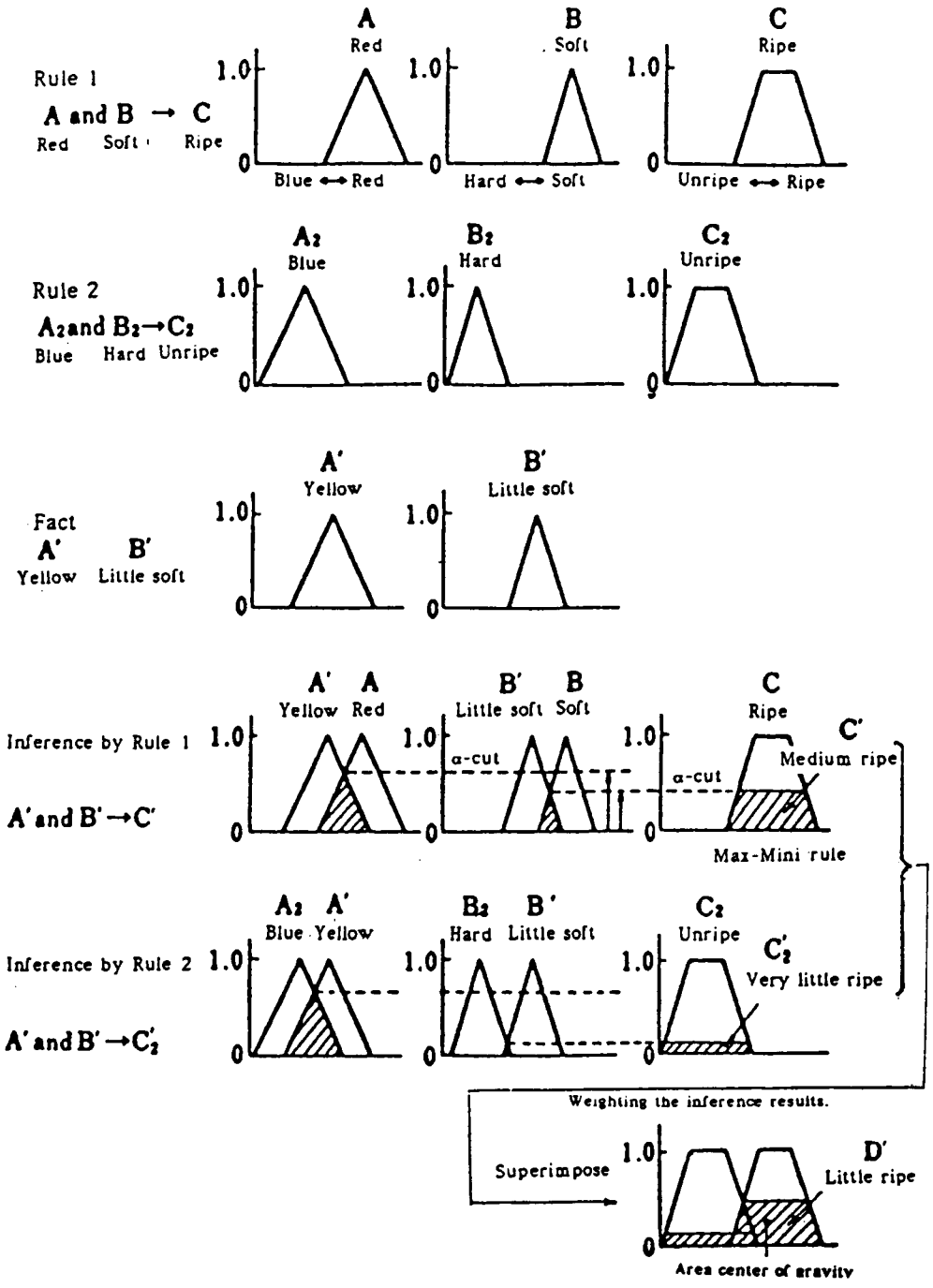
(B)

Figure 4-6. (continued)



(C)

Figure 4-6. (continued)



(D)

Figure 4-6. (continued)

(C)

Actual Examples of Fuzzy Logic Application

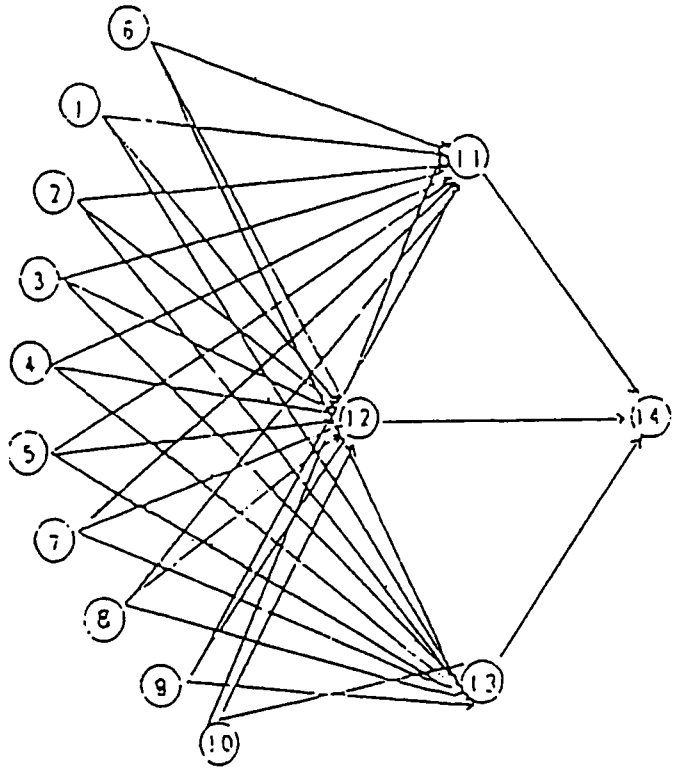
1. Application to Failure Analysis.

Since fuzzy logic does not relay on dynamic equations to express parameter correlations, some scientists are still reluctant to apply it to dynamic problems. However, there are many successful applications reported in the failure analysis field. The following example is a fuzzy logic application to structural damage assessment adopted from Yagawa's *Fuzzy Logic Inference* (1985). The variable relationship diagram is shown in figure 4-7A. Part of the rules and membership functions used in the fuzzy expert system are shown in figures 4-7B and 4-7C, respectively.

As shown in the figures, without using any complicated mathematical formula from material science or fracture mechanics, this fuzzy expert system can effectively induce reliable structural safety assessments from a series of visual inspection and local stress and strain analyses. For overall safety estimation, inspections results are combined and weighted by fuzzy logic.

For the analysis of structural weakening caused by material fatigue, rusting or decay, the finite element method approach is not suited at all because the first requirement of its application is the uniform properties of the model object. Micro cracks in a fatigued material and metal rust are hard to integrate into an FEM computer code. However, in fuzzy logic, there is no problem since it does not rely on dynamic equations. This is the reason that application of fuzzy logic has invaded the structural failure analysis field.

1. horizontal crack
2. inclined crack
3. concrete peel off
4. steel beam deformation
5. steel beam fracture
6. deformation, sinking, shifting
7. crack in concrete
8. corrosion of steel beams
9. arrangement of steel beams
10. stress and strain
11. damage due to deformations
12. damage due to displacements
13. damage due to cracks
14. decision



(A)

Figure 4-7.
Evaluation diagram for structure safety assessment (A),
Actual example of rules used (partial) (B), and
Actual examples of designed membership functions (C).
(Yagawa, 1991, p. 182)

Rule1 IF (Horizontal crack = Very small)
THEN (Damage due to deformation = Very small)

Rule2 IF (Horizontal crack = Small)
THEN (Damage due to deformation = Very small)

Rule3 IF (Horizontal crack = Medium)
THEN (Damage due to deformation = Very small)

Rule4 IF (Horizontal crack = Large)
THEN (Damage due to deformation = Small)

Rule5 IF (Horizontal crack = Large)
THEN (Damage due to deformation = Small)

Rule6 IF (Diagonal crack = Very large)
THEN (Damage due to deformation = Very small)

Rule7 IF (Diagonal crack = Small)
THEN (Damage due to deformation = Very small)

Rule8 IF (Diagonal crack = Medium)
THEN (Damage due to deformation = Very small)

Rule9 IF (Diagonal crack = Large)
THEN (Damage due to deformation = Medium)

Rule10 IF (Diagonal crack = Very large)
THEN (Damage due to deformation = Medium)

:
:
:
:

Rule46 IF (Stress and strain = Very small)
THEN (Damage due to deformation = Very small)

Rule47 IF (Stress and strain = Small)
THEN (Damage due to deformation = Small)

Rule48 IF (Stress and strain = Medium)
THEN (Damage due to deformation = Medium)

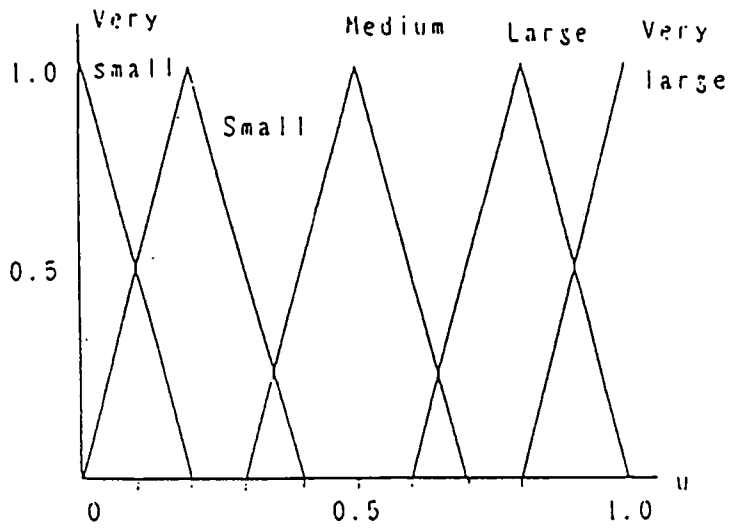
Rule49 IF (Stress and strain = Large)
THEN (Damage due to deformation = Large)

Rule50 IF (Stress and strain = Very large)
THEN (Damage due to deformation = Very large)

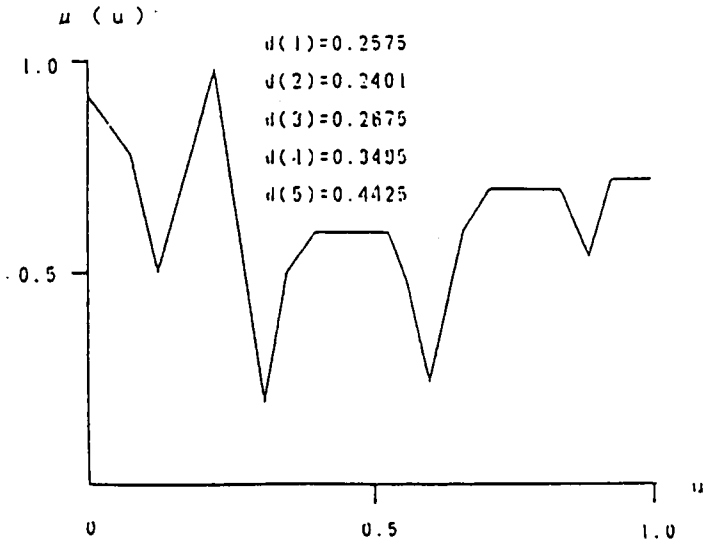
:
:
:
:

(B)

Figure 4-7. (continued)



Membership Functions for Damage Degree Expression



Membership Functions for Allowable Displacement

(C)

Figure 4-7. (continued)

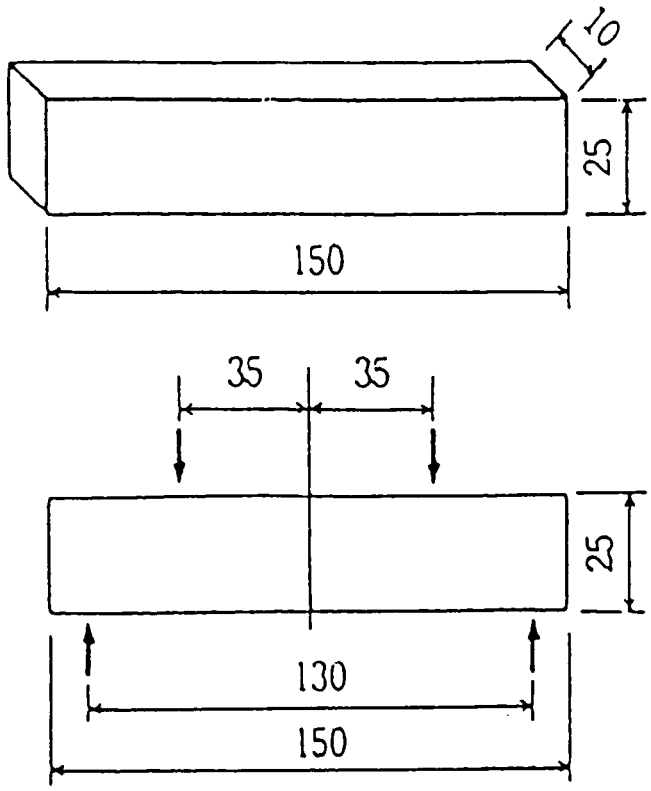
2. Application to Dynamic Failure Analysis.

After an actual fracture test, the test material is no longer usable; therefore it is important to find a way to estimate the strength and quality of materials without destroying the materials. In industry, it is also important to inspect the strength and quality of a material in a fast and inexpensive way. For carbon materials, it is known that there is a strong correlation between finished surface coarseness and bending fracture strength. This quality has been used as one inspection standard to judge bending fracture toughness.

The following example is done by Yagawa to relate bending fracture strength and surface coarseness of carbon bar specimens by fuzzy logic.

Carbon bar specimens with various surface coarseness are prepared. The specimen dimension is as in figure 4-8A. Before performing actual bending strength tests, the bending fracture strength of each specimen is inferred by an expert based on visual inspections and subjective judgement of surface coarseness. The expected strength of each specimen is then classified into one of the three categories: (S) strong, (M) medium, and (W) weak. After the classification of all specimens is made, the coarseness of each specimen is measured in μm. The specimens are then sent to the actual bending strength test (four points loading is used as shown in figure 4-8A).

Design of membership functions is based on the visual boundary image appearing on the graph (see figure 4-8B, top). The bottom figure of 4-8B shows the corresponding membership functions designed and evaluated by an expert.

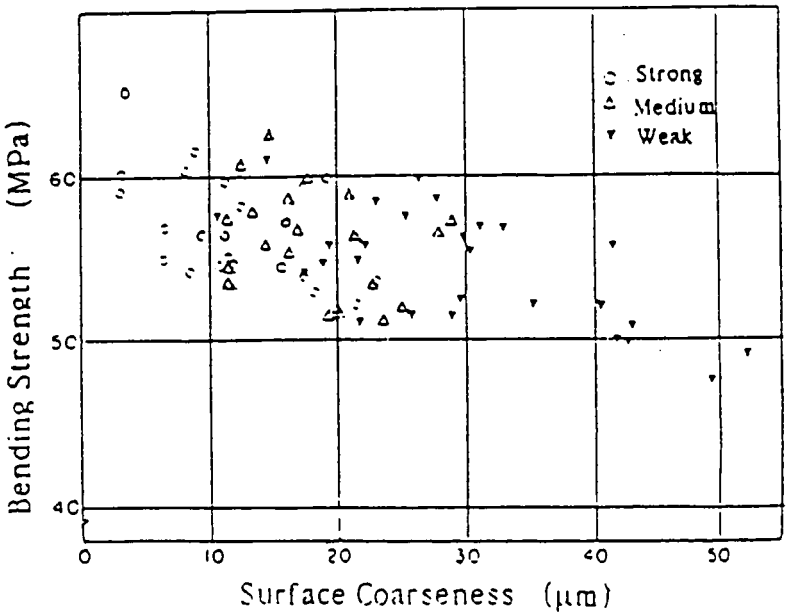


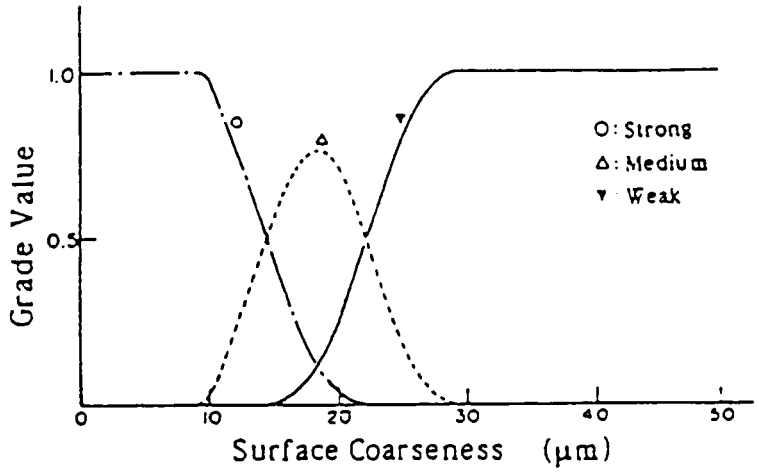
Number of specimens	= 70
Mean value of surface coarseness	= 20.69
Standard deviation of surface coarseness	= 10.87
Mean value of bending strength	= 55.63
Standard deviation of bending strength	= 3.154

(A)

Figure 4-8.
Specimen data and four points loading (A) and Bending strength vs. surface coarseness (B).

(Yagawa, 1991)





(B)

Figure 4-8. (continued)

3. Fuzzy Data Analysis Concept.

Analysis frequently encounters resultant graphs of experimental data which look like scattered dots. The cloud of data points may seem to have some kind of linear correlation. However, since the data points are scattered in some range, their relationship is fuzzy. Strictly speaking, linear regressions can only be applicable for the data points which are packed in the narrow strip range. In other words, one-to-one correspondence in data must exist. Sometimes the data correspondence is more like the shape of a two-dimensional figure (one-to-multi point correspondence). In most cases, the parameter relationships of experimental data are forcibly converted into a linear correlation to be usable for strict math formulations. Since the data scattering is unavoidable if the variance among the data specimens is significant, it is very important to establish parameter relationships through fuzzy logic to deal with this kind of fuzziness.

Examples of successful applications of fuzzy logic in the material failure analysis field ensure the possibility of fuzzy logic application to bone fracture simulations and fracture diagnosis. Scientists generally avoid uncertainty, lack of clarity, and fuzziness as much as possible. However, engineers know very well that uncertainty and fuzziness are inevitable. Therefore, engineers also rely on experience, intuition, and statistical judgments based on engineering knowledge.

Chapter V

FUZZY EXPERT SYSTEM DEVELOPMENT FOR BONE FRACTURE PREDICTION

(A)

Bone Fracture Simulation Construction Steps

1). Select effective parameters which reflect the output.

2). Connect and group related parameters to construct a flow chart.

3). Accumulate knowledge and data for parameter correlations.

4). Construct IF-THEN rules for parameter relationships.

5). Design membership functions for IF part rule statements.

6). Design membership functions for THEN part rule statements.

7). Do test runs and evaluate the results based on available data.

8). Modify membership functions.

9). Repeat steps 7 and 8 until the results become satisfactory.

10). If results are not satisfactory, add, eliminate, or alternate rules.

11). Go back to step 7.

12). If results are still not satisfactory, go back to step 1.

In step 1, the parameters that are technically difficult to measure by experiment should be avoided because they generate impractical complexity in the logic flow. In fuzzy logic, it is very important to choose parameters whose effects and relationships are conspicuous.

In step 2, relating parameters are connected, and the relationships of the affecting parameters and the affected parameters are defined. The resultant diagram becomes a skeletal structure of inference rules.

In step 3, all the experimental data and information is gathered to define the relationships among parameters. Some of the relationships between two parameters can be deduced from impact fracture mechanics, but most of the relationships have to rely on experimental data and human intuition. In many cases, multiple factors affect a single element. Because of this, evaluation of the degree of effect from each factor tends to be a series of trial and error processes, since all the factors are involved simultaneously.

In step 8, by supplying a quantity of experimental data to the prototype model, the effects of each factor are evaluated. In any fuzzy expert system, the validity range of input and output parameters is limited within the data variance ranges of parameters. Statistical assurance will not be established until enough data is collected.

In step 7, the membership functions and grade functions are modified according to the test run evaluation. If the modification steps are not successful, it means that there are problems with the rules. Addition, elimination, and alteration of rules needs to be done. If that does not work either, original parameter selections must be changed.

(B)

Experimental Approach

1. Test Set-up.

To research lower leg impact injuries and identify specific counter measures experimentally, a laboratory apparatus was designed and constructed in the biomedical laboratory at the University of Tennessee in 1986. The basic apparatus was originally designed by Kress for his master's thesis, *Mechanical Behavior of Lower Limbs in Response to Impact Loading* (1989).

2. Experimental Testing Devices.

The major components of the system are a 300-pound impact cart and its thrusting device, which utilizes an air-compressed piston cylinder system. By releasing compressed air from a chamber (inside diameter of 0.311 m, 1.829 m in length) to the piston, the piston pushes the rear end of the cart. Receiving the initial pushing force, the impact cart runs down along the guide rails. Assuming the friction between rails and wheels is negligible for the short run, the speed of the cart is considered steady while running because there is no external force acting on the cart. The speed of the impact cart is controlled by changing the amount of air pressure. However, due to the capacity of the installed air compressor (maximum limit of 120 psi), the maximum speed of the impact cart is limited to under 26 mph.

To measure the impact force, a force transducer is placed in between the bumper plate and the rigid cart body frame. The force transducer provides force vs. time data during the impact. The cart speed is calculated from a electrical timing device which is located beside the guide rail. The timer system utilizes a photo sensitive sensor to turn the timer switch on and off by cutting off the spot light emitted on the sensor. Two blades separated by a calibrated distance are fixed on the cart. One is fixed on the front, with another fixed behind it. As the cart runs along the rail, the first blade turns the timer on, and the second blade turns the timer off. Since the distance between the two blades and the travel time are known, the speed of the cart can be computed from them.

3. Impactor Cart Bumper Design.

A number of experiments have been done previously using the impact simulation system described above. However, most of the previous impact tests were done with a narrow steel plate or a pipe which have no shock absorption capability. If auto bumpers were more shock absorbant, some of the bone fracture accidents occurring at slow impact speeds could be avoided. Obviously, the shock absorption capacity of bumpers is one of the major factors which affects the impact force concentration. If a bumper system possesses good shock absorption characteristics, there should be a notable difference in the speed at which bone fractures start to occur. To test the effect of bumper shock absorption capability, a new bumper system was designed. To obtain an excellent impact shock reduction capability, air springs were used instead of

conventional coiled metal springs. The air springs (Code No. 324663-01 made by Firestone) used for the new bumper system were originally designed and used for the driver seats of large trucks to reduce the discomfort from seat vibration.

An air spring consists of a rubber cylinder tube and thick plastic disk ends as shown in figure 5-1. The diameter is 8 cm and the length is 17.5 cm. At the center of the top plastic disk, there is an air intake hole. In normal use for the truck seats, an air tube is connected to the hole from an air compressor to control inside air pressure. The higher the inside air pressure, the stiffer the air spring gets. However, for the use of the bumper system, the air intake hole was left open to release energy as the air springs get compressed. Unlike a conventional coiled spring, which stores the kinetic energy in deformation, an air spring with the hole open does not store energy as its deforms. By leaving the air spring ends open, the impact shock is dispersed much more effectively. A schematic drawing of the air spring bumper system is shown in figures 5-2A and 5-2B.

Air springs are sandwiched between the front slide plate and the back support beam, which is bolted to the cart. The slide plate can slide smoothly along the long guiding bolts as the air springs compress. To measure the impact force on the bumper system, the force transducer must be mounted on the front side of the slide plate. A cover plate (impact plate) is placed over the slide plate to cover the top surface of the force transducer on the sliding plate. To transmit the impact shock directory to the transducer, the impact plate can slide smoothly along the bushings.

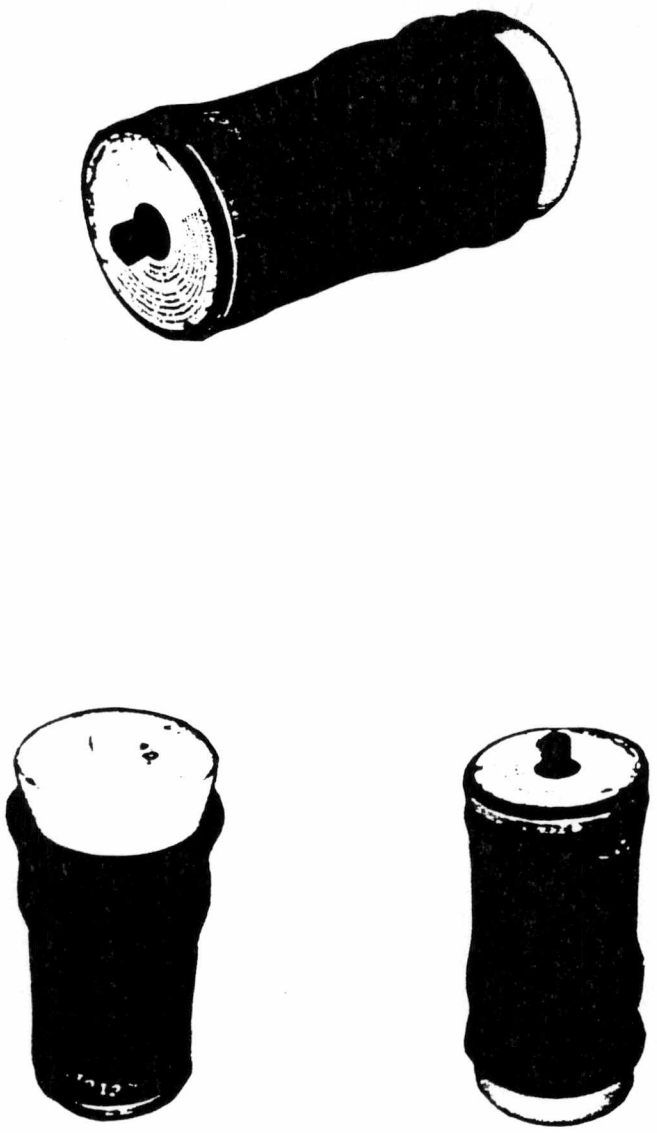
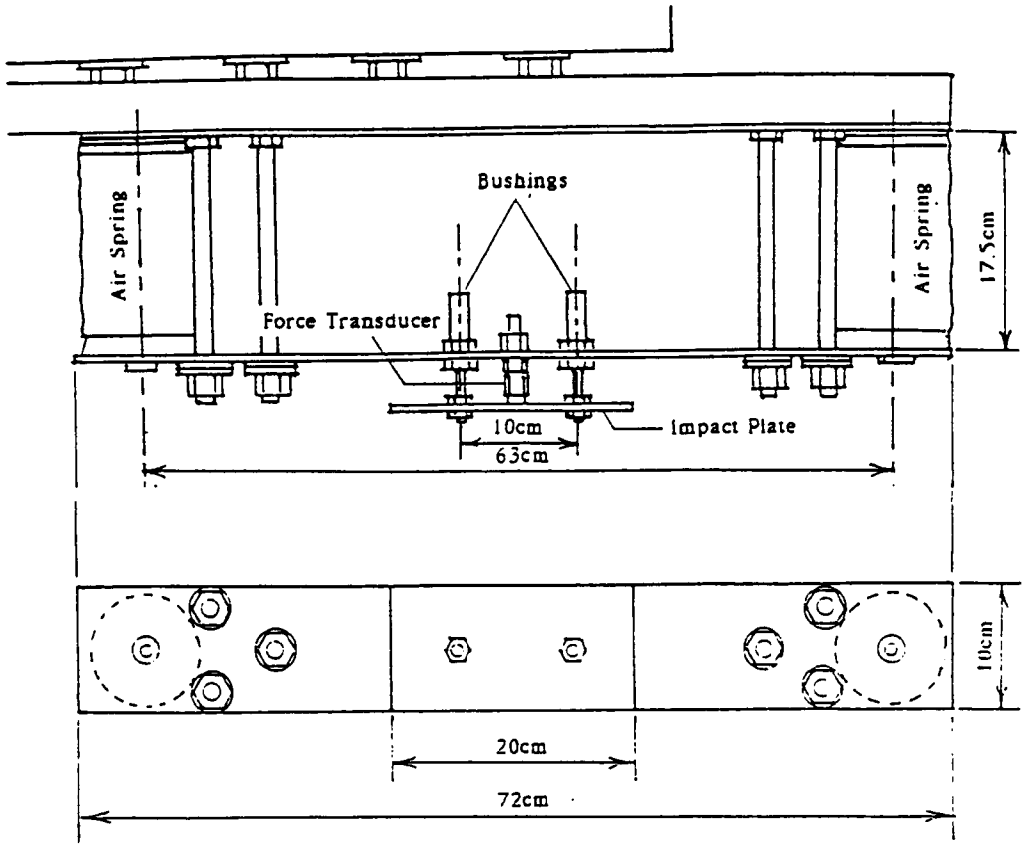
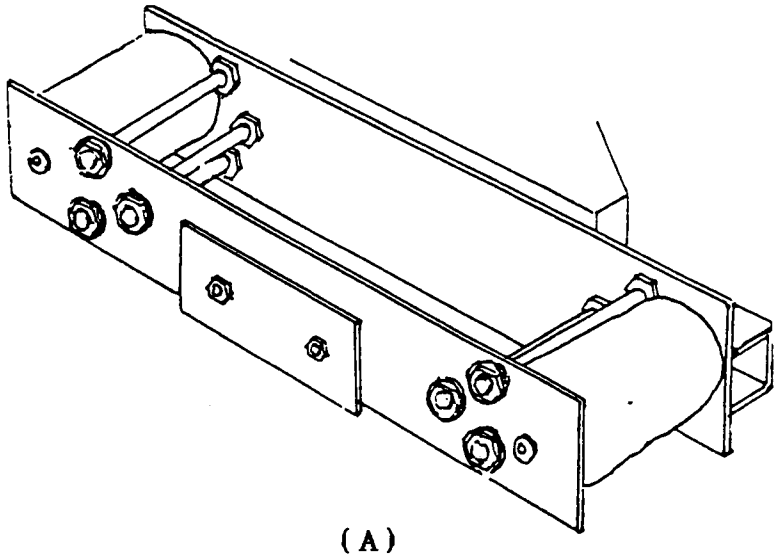


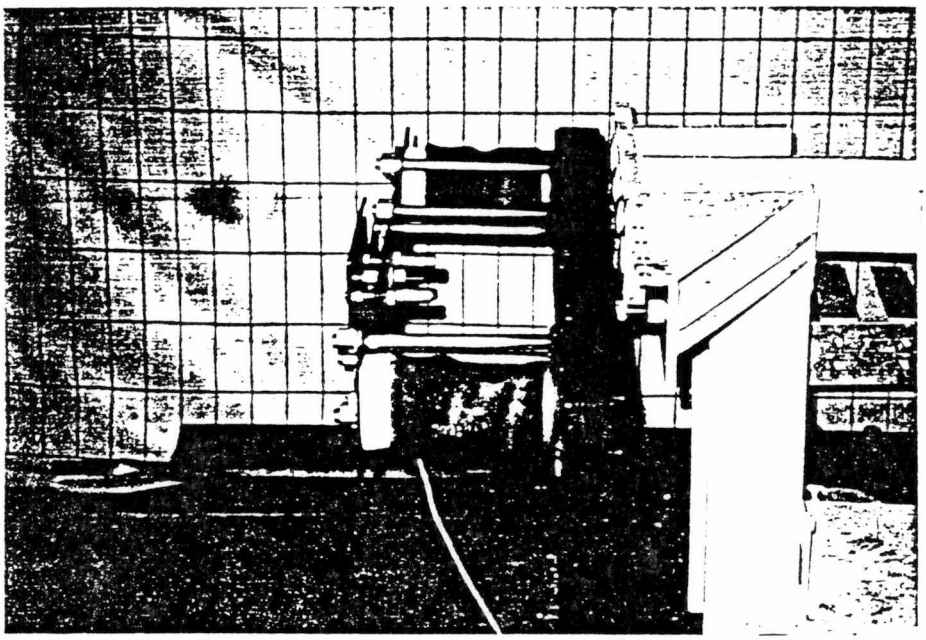
Figure 5-1.
Firestone air-springs used for the new bumper system.
(Item code - Airide 324663-01)



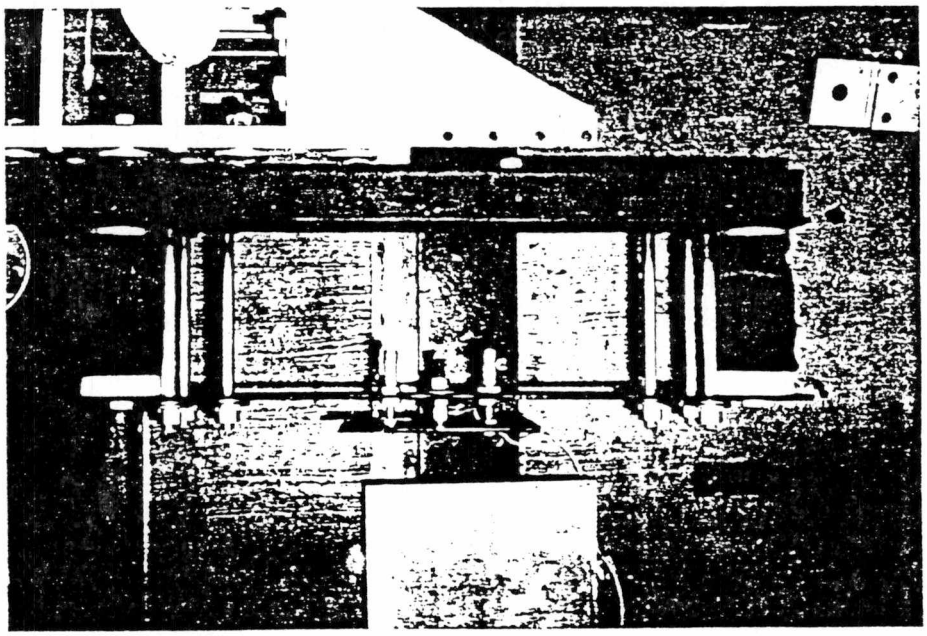


(A)

Figure 5-2.
Schematic design of the air-spring bumper system (A) and Photographs of the air-spring bumper system (B).



Side view of the air-spring bumper system



Top view of the air-spring bumper system

(B)

Figure 5-2. (continued)

4. Impactor Attachments.

Several steel impact panels with different widths (4 cm and 10 cm) were prepared to test the effect of the size of the contact surface area. As an attachment of the impact plate surface, sponge blocks were prepared to see whether they would make a notable difference in the injury condition and the fracture impact speed.

5. The Leg Holding Device.

For visibility purposes, the majority of bone fracture experiments done by other researchers in Japan and United States. were performed on extracted bones with no surrounding muscles and skin tissues. Bone ends are usually fastened by steady structures for basic loading tests. In such cases, test specimens always break at any speed as the impacting object pushed through the fixed points since the bone ends are both pinned. In this manner, the vicinity impact speed at which fractures start to occur can never be found. Therefore, to research the minimum impact speed required for bone fracture, a new leg holding device was designed by making the bone boundary condition as realistic as possible to the real auto injury situation. In my experiments, entire human intact legs were used with the new movable holding device instead of using extracted bones with the fixed holding device. Leg specimens used were preserved in embalming fluid at room temperature. No skin and muscle tissues were removed from leg specimens during the impact tests. However, to check the fracture generation visually on the bone

for each impact test, a square window was cut open on the skin at the impact location.

To recreate the foot friction condition of a human standing on both legs, half of the upper body weight, about 20kg, was loaded on top of the specimen leg, and a shoe was put on the foot. To simulate a person standing on a concrete road, concrete plates were placed underneath the foot.

The leg holding device consists of a pair of brackets which are joined by a steel rod on which dumbbell weights were placed. The schematic drawing is shown in figures 5-3A and 5-3B. Assuming that a human body will rotate at the weight center of the body when the impact is applied at the lower leg, the weight height was fixed at the height of the body weight center, which is located slightly above the navel. The weights can move freely up and down, but back and forth motions are restrained since they act as the mass center. To prevent the impact shock of the weights against the slot end of the bracket when weights fall down, several elastic cords were loosely put around the weights to arrest the weight bar when it drops.

A total of eight intact legs were used for series of experiments. Three of them were full length legs which were amputated at the hip. The full length legs were used to simulate the situation of a standing pedestrian. They were pinned at the point close to the top femur end. However, two matched pair legs used for the front and rear impact experiment were amputated at slightly lower locations than the other three legs, so that they were shorter and lighter. Due to the length, these short legs were pinned at a location closer to the knee. That situation can be compared to the boundary condition of a motorcyclist's leg at riding position since the knee does not move much.

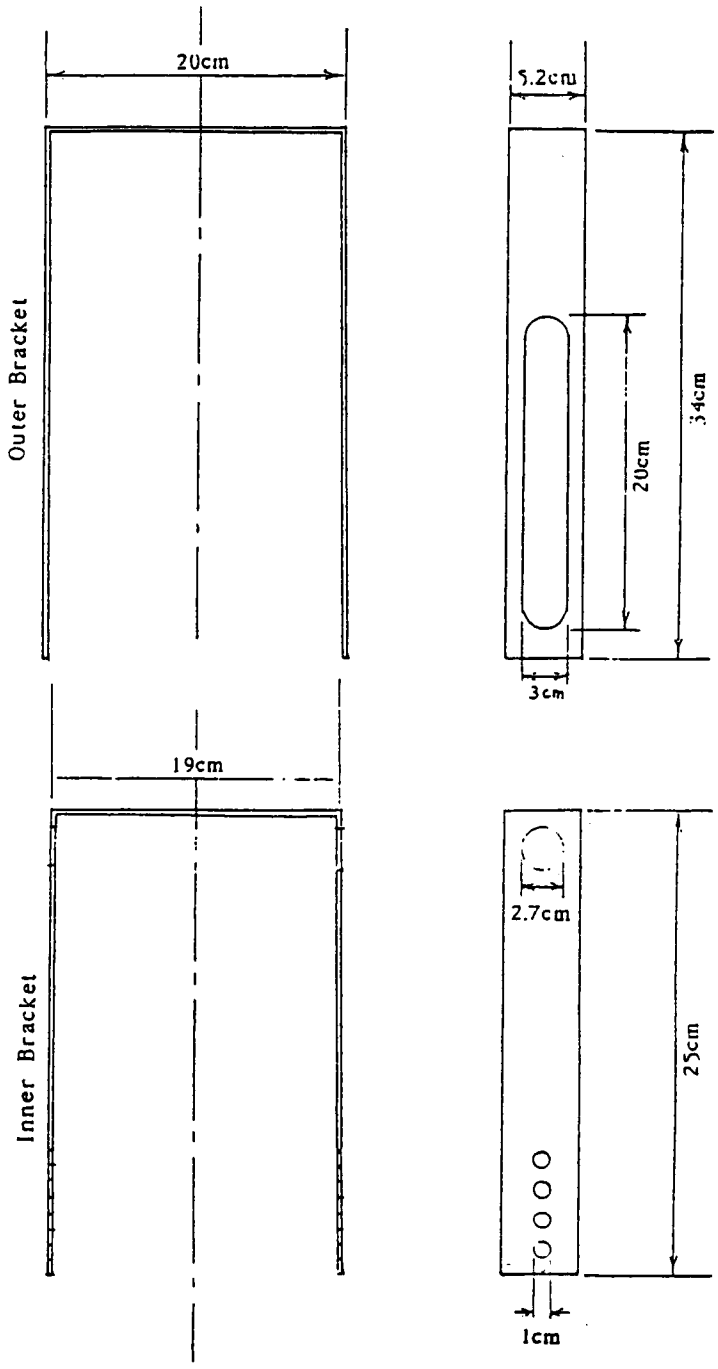
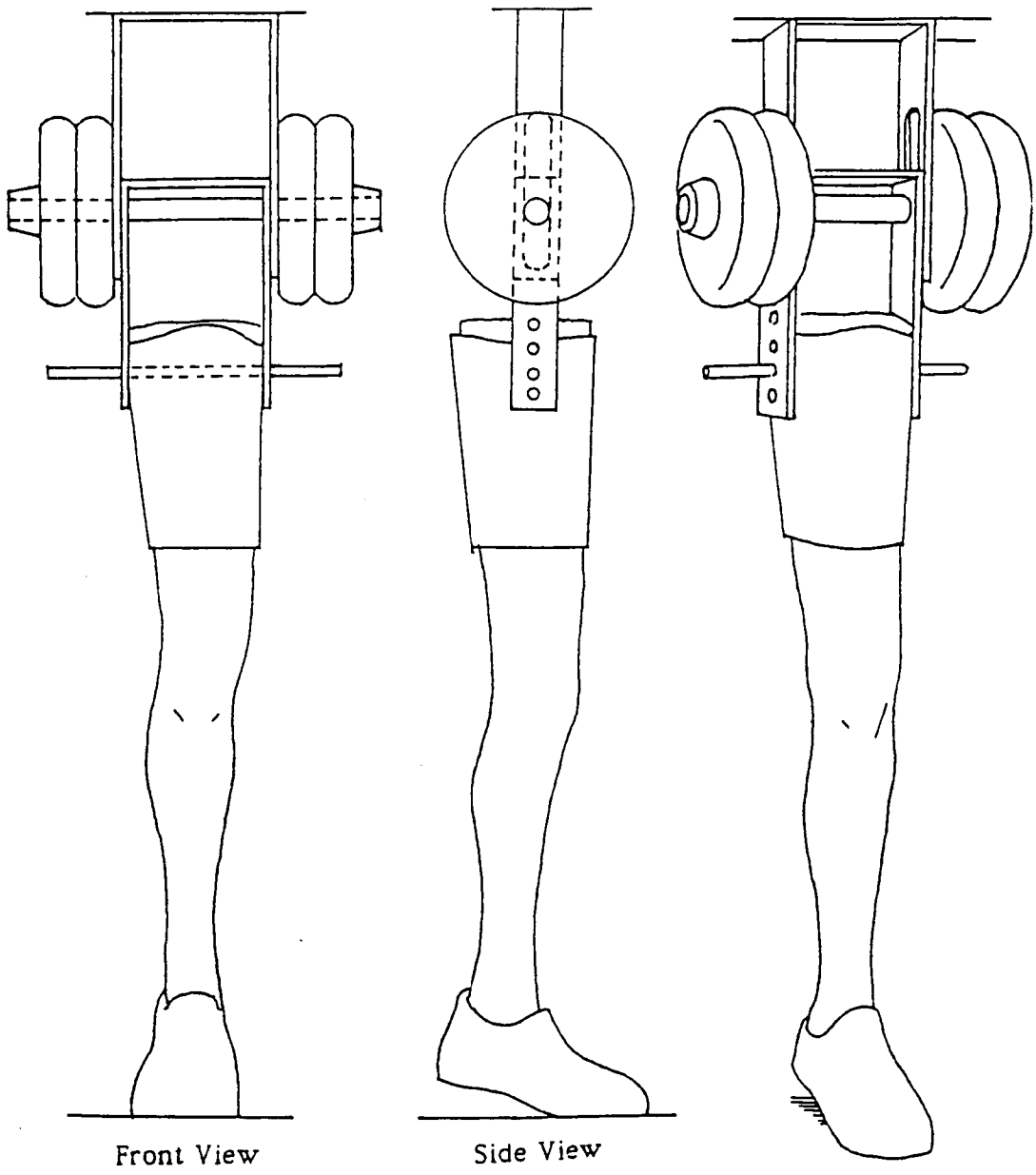


Figure 5-3.

Schematic design of the leg holding cramp couple (A) and A leg specimen mounted on the leg holding device (B).



(B)

Figure 5-3. (continued)

6. Test Parameters.

In each of the impact tests, the impact cart velocity just before the impact and the peak impact force were measured and recorded. The skin damage state and the fracture generation were checked visually at each time. The detailed bone fracture condition and the cortex thickness at the fracture point were recorded after dissection. Age, sex, race and the specimen reference number were recorded as bone data. The width of the impactor plate and the existence of the surface attachment (sponge block) were recorded as the impactor data. The high-speed camera video filmed by Kodak EKTAPRO (up to 11,000 frames/second) was used for some impact tests. All the experimental footages were recorded by conventional video cameras. Original tapes were available in both 8mm and VHS format.

7. Specimen Preparation.

Since an entire leg must be mounted on the holding device, several preparation steps were taken. For some legs, the amputated end needed to be trimmed off so that it could fit inside the holding clamp. Next, a medical plastic thigh cast was put around the thigh, and straps on the cast were tightened to have a firm contact. After the cast was stabilized, a hole was drilled through the cast aiming at the femur end. The drilled hole completely penetrated the thigh through the plastic cast. After a hole was drilled, a steel rod was put through the hole for the leg installation. The plastic cast was helpful in

guiding a drill tip to penetrate a femur end in straight line and was also helpful to stabilize the inserted shaft.

8. Specimen Mounting.

First, the steel rod ends penetrating the thigh were put through the holes on the holding clamp. Then a shoe was put on the foot. The shoe string was put around the ankle and tightened to prevent the shoe from flying off at high speed during the test. Dumbbell weights (20 kg) were put on the steel rod which was hinging the holding brackets. Concrete plates were placed underneath the foot, and the leg was balanced to keep the weight on top so that a full weight force would transmit to the foot. After finding a good balanced location, the foot location was marked on the concrete plate. Since the hip joint simulated by the steel rod was not fixed at a steady fixture and was free to move back and forth, balancing a leg required careful positioning of the foot.

The knee and ankle of each leg specimen were stiffened at slightly different angles. Since the knees and ankles of the specimen could no longer bend flexibly, full surface contact between a shoe and the concrete plate was not easy to obtain. As a result, most of the legs were slightly tip-toed at balanced position. However, a factor of surface contact should not be the matter for the friction force since the formula is $F = \mu N$ (contact area is not a parameter). In normal standing position, the body weight is supported by the toe region, not by the heel region. Since the impact fracture generates within 1/1000 sec at the moment of impact, there is virtually no time for the knee or ankle to bend.

The bumper impact height was adjusted to the location slightly above the mid point of a tibia shaft by adjusting the height of the top beam on which the holding device is fixed. The fixed height of the impact plate installed on the cart is 42.5 cm above the top surface of the concrete plate. Small height adjustments can be made by changing the holes for the insertion rod.along the bottom bracket.

(C)

Test Objectives

1. Main Objective.

The main objective of my tests is to find the minimum velocity at which fracture starts to occur in realistic conditions with the effects of bumper springs taken into consideration. To find the bone fracture velocity, each leg specimen was subjected to a series of impact tests staring from slow impact speeds to higher speeds with gradual increment increases. Another objective of the test was to provide a sample data base for the fuzzy expert system program which predicts bone fracture possibility. As additional interest, the effects of the newly designed air spring bumper to the impact force-speed relation, the width of the impact plate, and the direction of the impact are considered.

2. Test Focal Points.

The following lists were the interest points of the tests.

1) Direction of the Impact

Forward Impact (Anterior-Posterior Direction Impact)

Rear Impact (Posterior-Anterior Direction Impact)

2) Friction Condition

Pinned - frictional

Pinned - free

3) Pinned Point Location

Pinned at the location close to the hip

Pinned at the location close the knee

4) Impact Radius

Distance between the pinned point and the impact point

5) Shock absorption Capacity of the Bumper

With the air spring bumper

Without the air spring bumper

6) Bumper Surface Material

With a foam block on the bumper surface

Without a foam block on the bumper surface

7) Bone Specimen Variance

Age, sex and the mean cortex thickness

(D)

Experimental Result and Disection Notes

The experimental results are shown in Tables 5-1 through 5-8, and the and the disection notes are shown in Table 5-9 and 5-10.

(E)

Plots of Experimental Result

The experimental results are shown in plot form in Figure 5-4 through 5-12.

(F)

Rules and Variables Behaviors of the TEST program (Fuzzy Logic Bone Fracture Prediction Program)

Rules and variable behaviors of the TEST program are shown in Table 5-11 through 5-18.

(G)

Designed Membership Functions for the TEST Program

Designed membership functions for the TEST program are shown in Figure 5-13 and 5-14.

Table 5-1(A).

Consecutive impact force vs. speed data from specimen, TL009L

(10cm width impact plate with air springs)

55 year-old white male
Specimen Number 009L (left leg)
10cm width impact plate with air springs attached
no foam on the plate
friction on foot
Anterior-Posterior Impact

Impact No.	Impact Speed		Peak Force	Fracture
TL009L1.	17.80km/h	(4.94m/s)	2413.5 newton	
	11.06mi/h	(16.22ft/s)	524.6 lbforce	No
TL009L2.	21.53km/h	(5.89m/s)	2943.2 newton	
	17.18mi/h	(19.33ft/s)	661.6 lbforce	No
TL009L3.	24.96km/h	(6.93m/s)	3671.8 newton	
	15.51mi/h	(22.751ft/s)	825.4 lbforce	No
TL009L4.	27.94km/h	(7.76m/s)	lost data	
	17.36mi/h	(25.46ft/s)		No
TL009L5.	29.56km/h	(8.21m/s)	3568.9 newton	
	18.37mi/h	(26.94ft/s)	802.3 lbforce	No
TL009L6.	31.13km/h	(8.65m/s)	4164.4 newton	
	19.34mi/h	(28.371ft/s)	936.2 lbforce	No
TL009L7.	32.86km/h	(9.13m/s)	3894.7 newton	
	20.19mi/h	(29.95ft/s)	875.5 lbforce	No
TL009L8.	34.26km/h	(9.52m/s)	4466.4 newton	
	21.29mi/h	(31.22ft/s)	1004.0 lbforce	No
TL009L9.	35.97km/h	(9.99m/s)	4399.6 newton	
	22.21mi/h	(32.57ft/s)	989.0 lbforce	No
TL009L10.	38.92km/h	(10.81m/s)	4649.9 newton	
	24.19mi/h	(35.47ft/s)	1045.3 lbforce	No

Table 5-1(B).

Consecutive impact force vs. speed data from specimen, TL009L

(4cm width impact plate with air springs)

55 year-old white male
Specimen Number 009L (left leg)
4cm width impact plate with air springs attached
no foam on the plate
friction on foot

* Since the bone (009L) did not break at the maximum impact speed that the air compressor can produce, the 10cm width impact plate was replaced by the 4cm width impact plate.
Anterior-Posterior Impact

Impact No.	Impact Speed		Peak Force	Fracture
TL009L11	21.70km/h	(6.03m/s)	2565.7newton	
	13.49mi/h	(19.78ft/s)	576.8 lbforce	No
TL009L12.	26.10km/h	(7.25m/s)	3499.8 newton	
	16.28mi/h	(23.79ft/s)	786.8 lbforce	No
TL009L13.	26.10km/h	(8.82m/s)	3805.4 newton	
	19.72mi/h	(28.931ft/s)	855.5 lbforce	No
TL009L14.	34.55km/h	(9.60m/s)	4974.5newton	
	21.47mi/h	(31.49ft/s)	1118.3 lbforce	No
TL009L15.	36.37km/h	(10.101m/s)	5161.8 newton	
	22.60mi/h	(33.15ft/s)	1160.1 lbforce	No
TL009L16.	40.90km/h	(11.36m/s)	6257.9 newton	
	25.42mi/h	(37.281ft/s)	1406.8 lbforce	No
TL009L17.	41.63km/h	(11.56m/s)	7081.6 newton	
	25.87mi/h	(37.94ft/s)	1591.9 lbforce	No

Table 5-1(C).

Consecutive impact force vs. speed data from specimen, TL009L

(4cm width impact plate without air springs)

55 year-old white male
specimen number 009L (left leg)
4cm width impact plate without air springs
no foam on the plate
friction on foot

* Due to the fact that the speed reached the maximum limit that the air compressor can produce, air springs were removed from the bumper at this point. Then the experiment started over from a slower speed.

Impact No.	Impact Speed		Peak Force	Fracture
TL009L18.	27.55km/h	(7.65m/s)	3123.2 newton	
	17.12mi/h	(25.11ft/s)	702.1 lbforce	No
TL009L19.	28.92km/h	(8.03m/s)	6242.0 newton	
	17.98mi/h	(26.36ft/s)	1403.2 lbforce	Yes

* distal fracture, no comminuted fracture

Table 5-2.

Consecutive impact force vs. speed data from specimen, TL961R

80 year-old White female
Specimen Number TL961R (right leg)
10cm width impact plate with air springs attached
no foam on the plate
friction on foot
Posterior-Anterior Impact

Impact No.	Impact Speed		Peak Force	Fracture
TL961R1.	13.48km/h	(5.13m/s)	1339.7 newton	
	11.49mi/h	(16.851ft/s)	301.2 lbforce	Yes

* A tensile wedge fracture opened toward the posterior side from the anterior side.
* Instantaneous foot twist was observed on the high speed video.

Table 5-3.

Consecutive impact force vs. speed data from specimen, TL755L

56 year-old white female
Specimen Number 755L (left leg)
10cm width impact plate with air springs attached
8.5cm thick foam on the plate
friction on foot
Anterior-Posterior Impact

Impact No.	Impact Speed		Peak Force	Fracture
TL755L1.	7.68km/h	(2.13m/s)	635.3 newton	
	4.82mi/h	(7.07ft/s)	142.8 lbforce	No
TL755L2.	8.86km/h	(2.46m/s)	628.3 newton	
	5.40mi/h	(8.07ft/s)	141.2 lbforce	No
TL755L3.	9.77km/h	(2.71m/s)	795.8 newton	
	6.07mi/h	(8.90ft/s)	178.9 lbforce	No
TL755L4.	10.9km/h	(2.46m/s)	842.6 newton	
	6.75mi/h	(9.90ft/s)	189.4 lbforce	No
TL755L5.	16.0km/h	(4.43m/s)	1210.5 newton	
	9.90mi/h	(14.55ft/s)	272.1 lbforce	No
TL755L6.	17.2 km/h	(4.79m/s)	1378.6 newton	
	5.50mi/h	(15.71ft/s)	310.0 lbforce	No
TL755L7.	20.46km/h	(5.68m/s)	1604.1 newton	
	12.7mi/h	(18.65ft/s)	360.6 lbforce	No
TL755L8.	22.7km/h	(6.29m/s)	1489.0 newton	
	14.0mi/h	(20.65ft/s)	334.7 lbforce	Yes

* comminuted and complete fracture
* no localized soft tissue damage evident

Table 5-4.

Consecutive impact force vs. speed data from specimen, TL991L

92 year-old white female
Specimen Number TL991L (left leg)
10cm width impact plate with air springs attached
no foam on the plate
friction on foot
Anterior-Posterior Impact

Impact No.	Impact Speed		Peak Force	Fracture
TL991L1.	12.32km/h	(3.42m/s)	1286.6 newton	
	7.66mi/h	(11.23ft/s)	289.2 lbforce	No
TL991L2.	17.51km/h	(4.86m/s)	1898.9 newton	
	5.40mi/h	(8.07ft/s)	426.9 lbforce	No
TL991L3.	19.32km/h	(5.37m/s)	2192.5 newton	
	12.00mi/h	(17.611ft/s)	492.9 lbforce	No
TL991L4.	20.73km/h	(5.76m/s)	2671.8 newton	
	12.88mi/h	(18.89ft/s)	600.6 lbforce	No
TL991L5.	23.80km/h	(6.61m/s)	2763.3 newton	
	14.79mi/h	(21.69ft/s)	621.2 lbforce	No
TL991L6.	25.13km/h	(6.98m/s)	3068.4 newton	
	15.61mi/h	(22.90ft/s)	689.8 lbforce	No
TL991L7.	255.61km/h	(7.11m/s)	3224.9 newton	
	15.92mi/h	(23.34ft/s)	725.0 lbforce	No
TL991L8.	27.84km/h	(7.73m/s)	3773.1 newton	
	17.30mi/h	(25.37ft/s)	848.2 lbforce	No
TL991L9.	28.29km/h	(7.86m/s)	3290.8 newton	
	17.87mi/h	(25.78ft/s)	739.8 lbforce	Yes

* comminued fracture, thick cortex

Table 5-5.

Consecutive impact force vs. speed data from specimen, TL070L

81 year-old white female
Specimen Number TL070L (left leg)
10cm width impact plate without air springs
no friction on foot (no contact with the ground)
Anterior-Posterior Impact

Impact No.	Impact Speed		Peak Force	Fracture
TL070L1.	9.43km/h	(2.61m/s)	1001.9 newton	
	5.86mi/h	(8.59ft/s)	225.2 lbforce	No
TL070L2.	12.33km/h	(3.42m/s)	1391.4 newton	
	7.66mi/h	(11.24ft/s)	312.8 lbforce	No
TL070L3.	18.81km/h	(5.22m/s)	1140.7 newton	
	11.69mi/h	(17.14ft/s)	256.4 lbforce	Yes

* comminuted fracture, thin cortex

Table 5-6.

Consecutive impact force vs. speed data from specimen, TL070R

Specimen Number TL070R (right leg)
10cm width impact plate without air springs
no friction on foot
Posterior-Anterior Impact

Impact No.	Impact Speed		Peak Force	Fracture
TL070R1.	9.97km/h	(2.77m/s)	566.8 newton	
	6.19mi/h	(9.08ft/s)	127.4 lbforce	No
TL070R2.	13.66km/h	(3.79m/s)	803.8 newton	
	8.49mi/h	(12.45ft/s)	180.7 lbforce	No
TL070R3.	17.96km/h	(4.99m/s)	1136.3 newton	
	11.16mi/h	(16.37ft/s)	255.4 lbforce	Yes

* comminuted fracture

Table 5-7.

Consecutive impact force vs. speed data from specimen, TL949L

84 year-old white female
Specimen Number TL949L (left leg)
10cm width impact plate without air springs
friction on foot
Anterior-Posterior Impact

Impact No.	Impact Speed		Peak Force	Fracture
TL949L1.	13.65km/h	(3.79m/s)	1962.6 newton	
	8.48mi/h	(12.44ft/s)	441.1 lbforce	No
TL949L2.	17.62km/h	(4.89m/s)	1674.3 newton	
	10.95mi/h	(16.06ft/s)	376.4 lbforce	Yes

* comminuted fracture

Table 5-8.

Consecutive impact force vs. speed data from specimen, TL949R

Specimen Number TL949R (right leg)
10cm width impact plate without air springs
friction on foot
Posterior-Anterior Impact

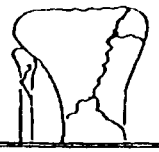
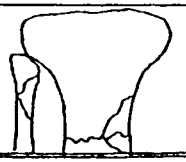
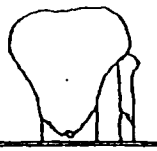
Impact No.	Impact Speed		Peak Force	Fracture
TL949R1.	13.6km/h	(3.78m/s)	1202.1 newton	
	2.57mi/h	(12.41ft/s)	270.2 lbforce	No
TL949R2.	16.4km/h	(4.55m/s)	1532.9 newton	
	3.10mi/h	(14.93ft/s)	344.5 lbforce	No
TL949R3.	18.41km/h	(5.11m/s)	1792.4 newton	
	3.48mi/h	(16.78ft/s)	402.9 lbforce	No
TL949R4.	19.72km/h	(5.48m/s)	1961.3 newton	
	3.73mi/h	(17.97ft/s)	440.9 lbforce	No
TL949R5.	22.57km/h	(6.27m/s)	2057.7 newton	
	4.27mi/h	(20.57ft/s)	462.6 lbforce	Yes

* comminuted fracture

Table 5-9. Pre-disection notes for leg impacts

CAD #	755L	991L	009L		961R
Impact	A-P (Tai)	A-P (Tai)	A-P (Tai)		P-A (Tai)
Negatives #	0693A	0693B	0693C		0693C
Weight (lbs.)	12	12	12¼		10
Top - Heel (cm)	85	77	82		79
Top -Laceration (cm)	55	49.5	52		No Laceration
Lac - Patella (cm)	8	12	14		na
Laceration site	Anterior	Anterior	Anterior		na
Lac description	Multiple 1-2 cm	7 cm vertical	8 cm vertical		na
Heel - Toe (cm)	22.5	24	24		22
Top Circ (cm)	45	48.5	48		39
Supra-pat Circ (cm)	27.5	32.5	28.5		25.5
Patellar Circ (cm)	29.5	34.5	32.5		34
Sub-pat Circ (cm)	25.5	26.5	25		27.5
Circ @ Impact (cm)	23	22	20.5		22
Midleg/Midthigh Circ	23/29	22/35	20.5/31		22/29
Circ @ Ankle (cm)	14.5	17	17		17.5
Pre/Post X-rays	✓/✓	✓/✓	✓/✓		✓/✓
Etc.		Patellar Tendon Cut			

Table 5-10. Disection notes for leg impacts

CAD #	755L	991L	009L		961R
Tibia/Femur Width (mm)	24.23/23.36	23.71/27.51	26.26/28.24		20.37/19.71
Tibia/Femur Depth	30.28/25.47	31.56/29.34	35.18/35.07		19.60/24.28
Tibia/Femur-1 (mm)	10.52/5.01	13.42/4.78	11.09/6.46		4.23/5.65
Tibia/Femur-2	3.37/4.98	4.68/6.81	3.22/8.87		3.50/6.22
Tibia/Femur-3	3.51/4.71	6.01/5.12	6.02/6.63		2.56/6.52
Tibia/Femur-4	6.32/7.76	7.88/7.48	5.94/15.53		2.12/4.59
Tibia/Femur5	3.84/5.22	4.79/6.06	6.61/6.48		3.24/4.55
Tibia/Femur-6	3.55/5.51	4.21/6.20	3.63/7.01		6.75/5.83
Tibia/Femur Circ (cm)	9.4/7.8	9.0/9.4	9.9/10.2		6.1/7.8
Fibula Width (mm)	10.17	10.39	9.49		13.18
Fibula Depth (mm)	7.35	14.66	10.43		13.16
Fibula-1 (mm)	2.65	4.31	3.48		5.43
Fibula-2	2.49	2.81	4.21		2.77
Fibula-3	1.74	3.15	3.41		3.10
Fibula Circ (cm)	3.3	4.0	3.5		3.7
Fracture L (cm)	9	15	16		6
Fracture Pattern ETC.					Tension wedges in both t/f. @ bottom of plate?

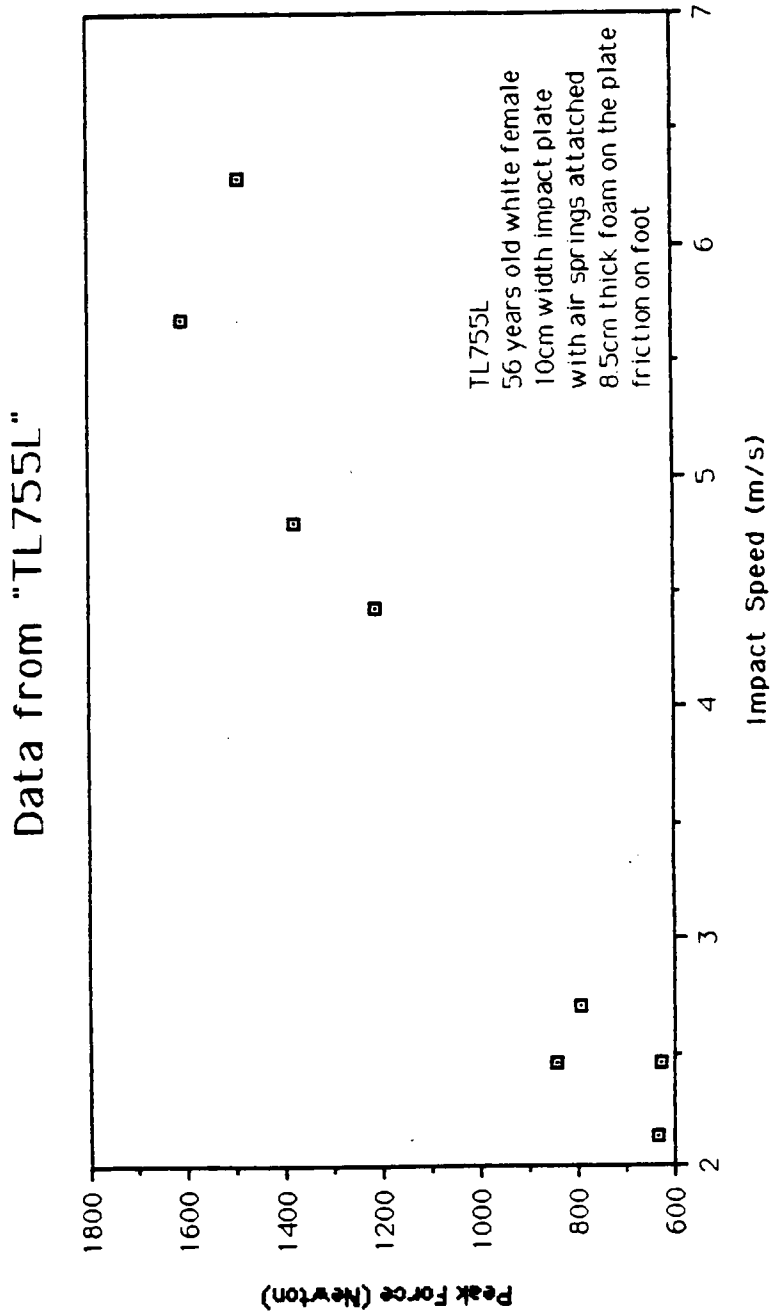


Figure 5-4.

Plot of impact data from the tibia specimen, TL755L.

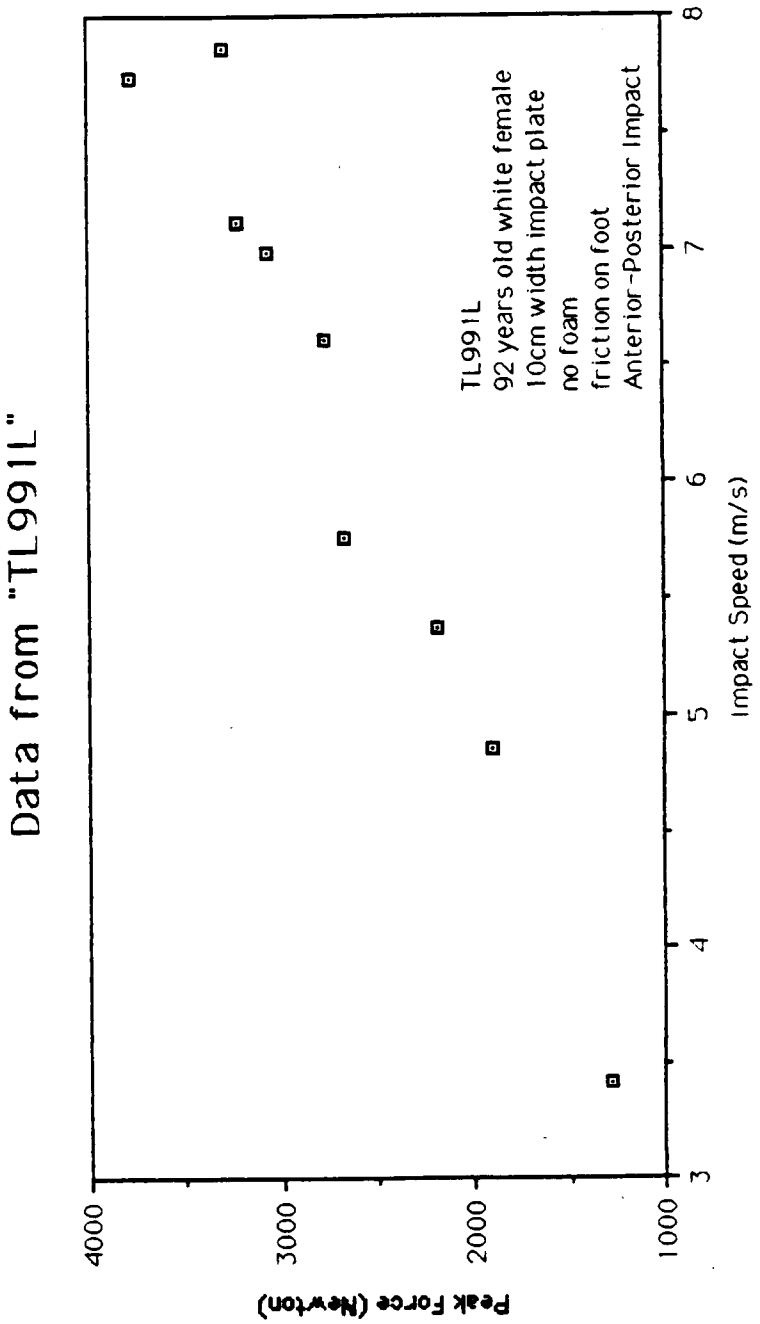


Figure 5-5.

Plot of impact data from the tibia specimen, TL991L.

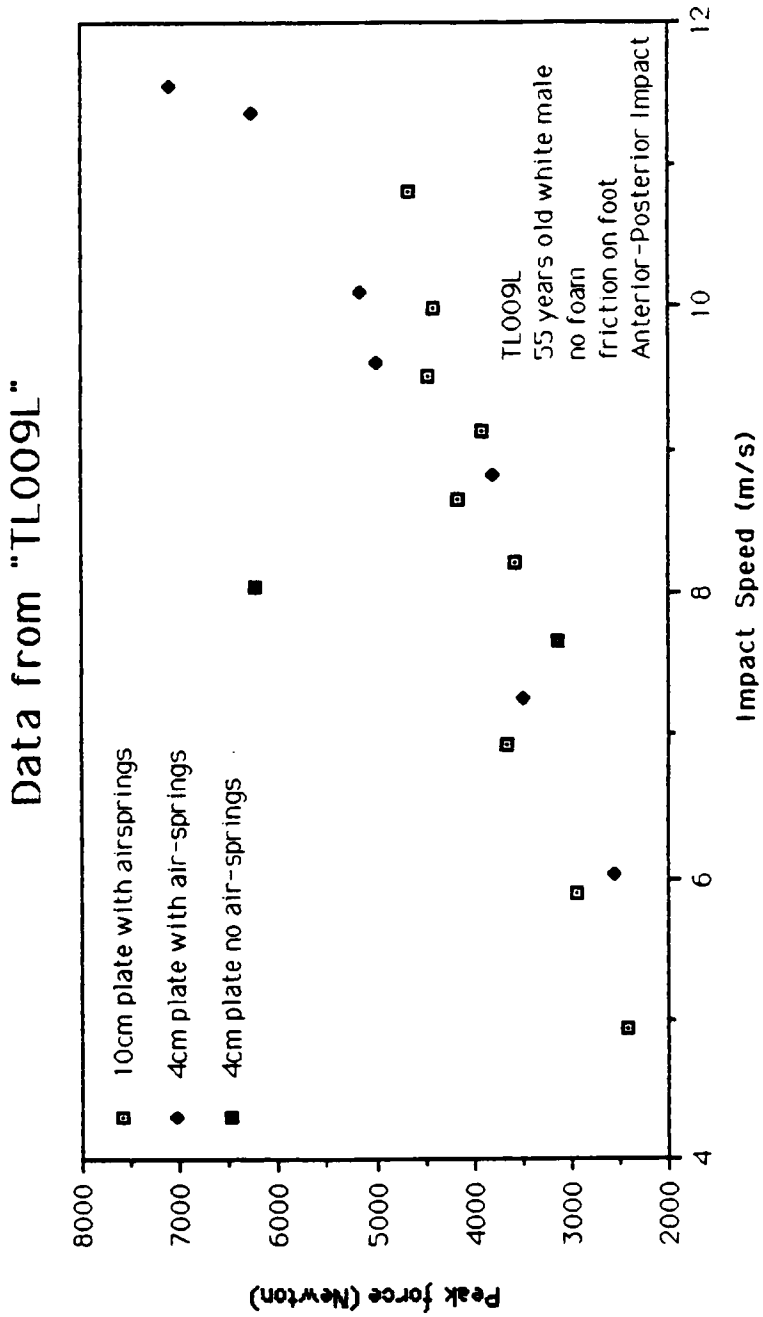


Figure 5-6.

Plot of impact data from the tibia specimen, TL009L.

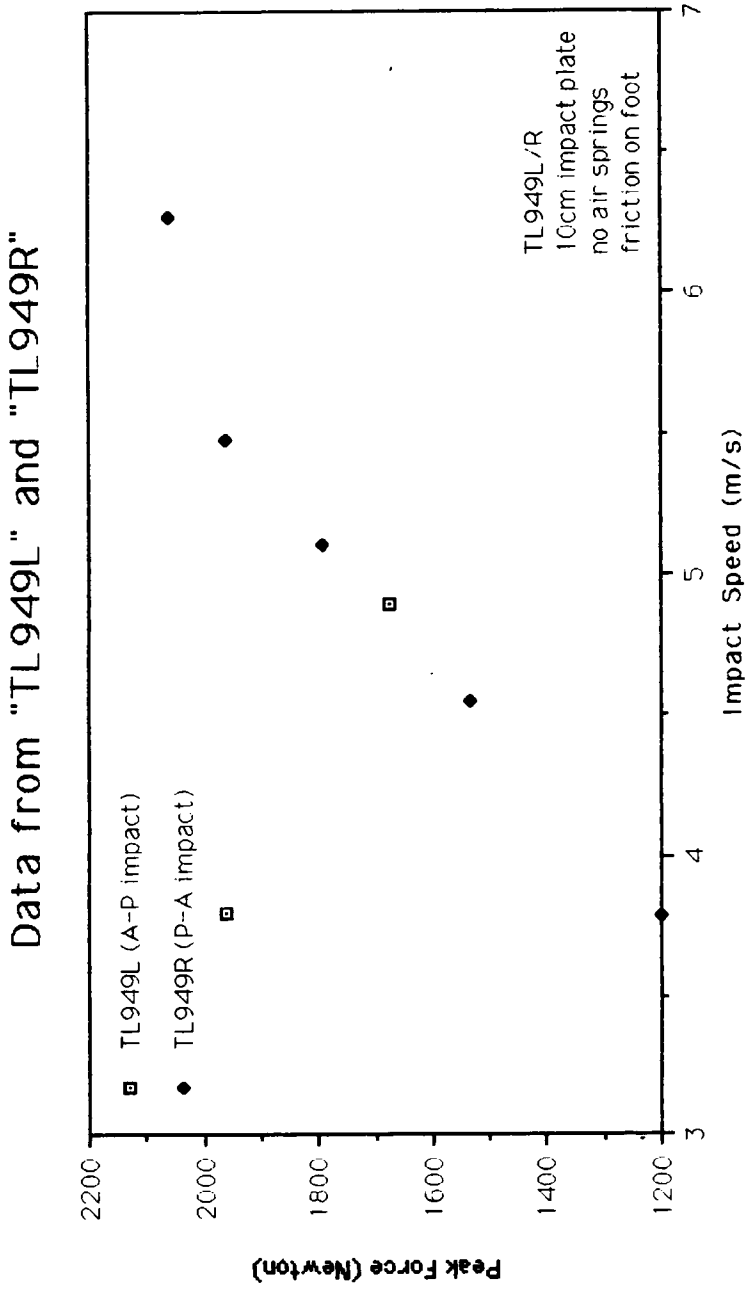


Figure 5-7.

Plot of impact data from tibia specimens, TL949L and TL949R.

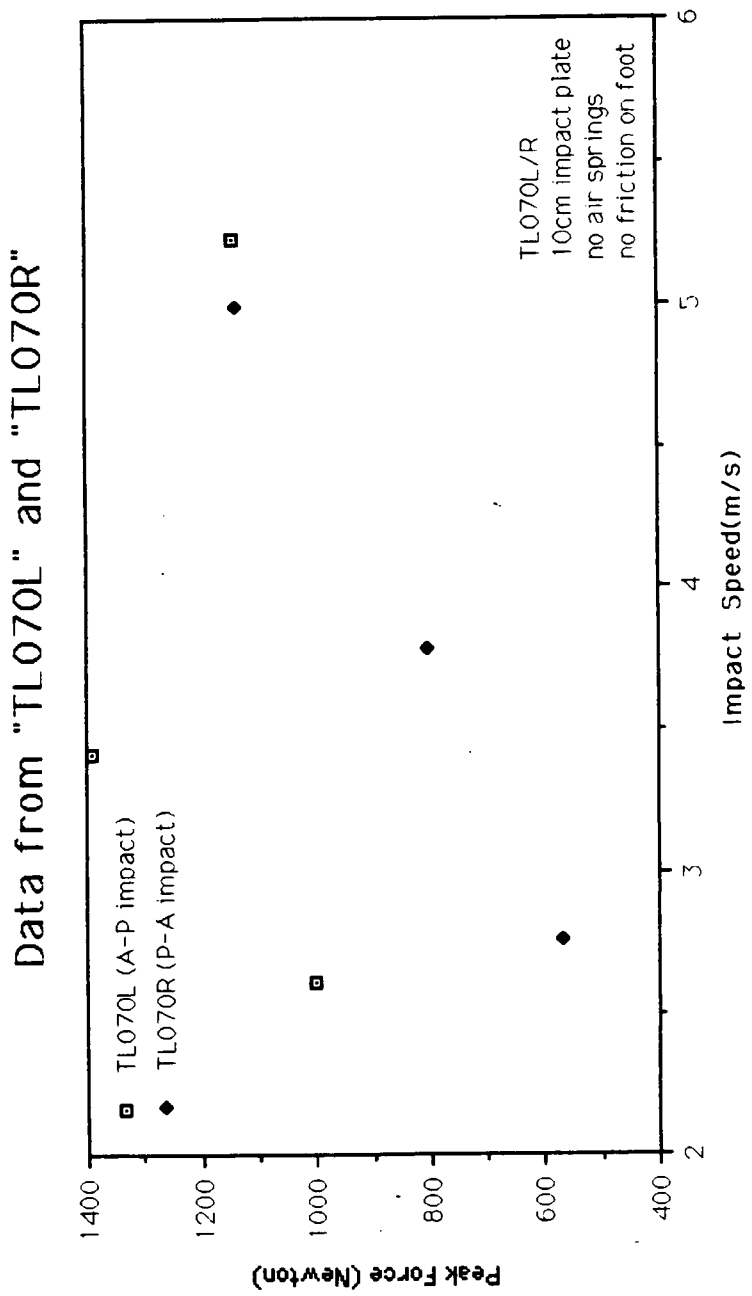


Figure 5-8.

Plot of impact data from tibia specimens, TL070L.and TL070R.

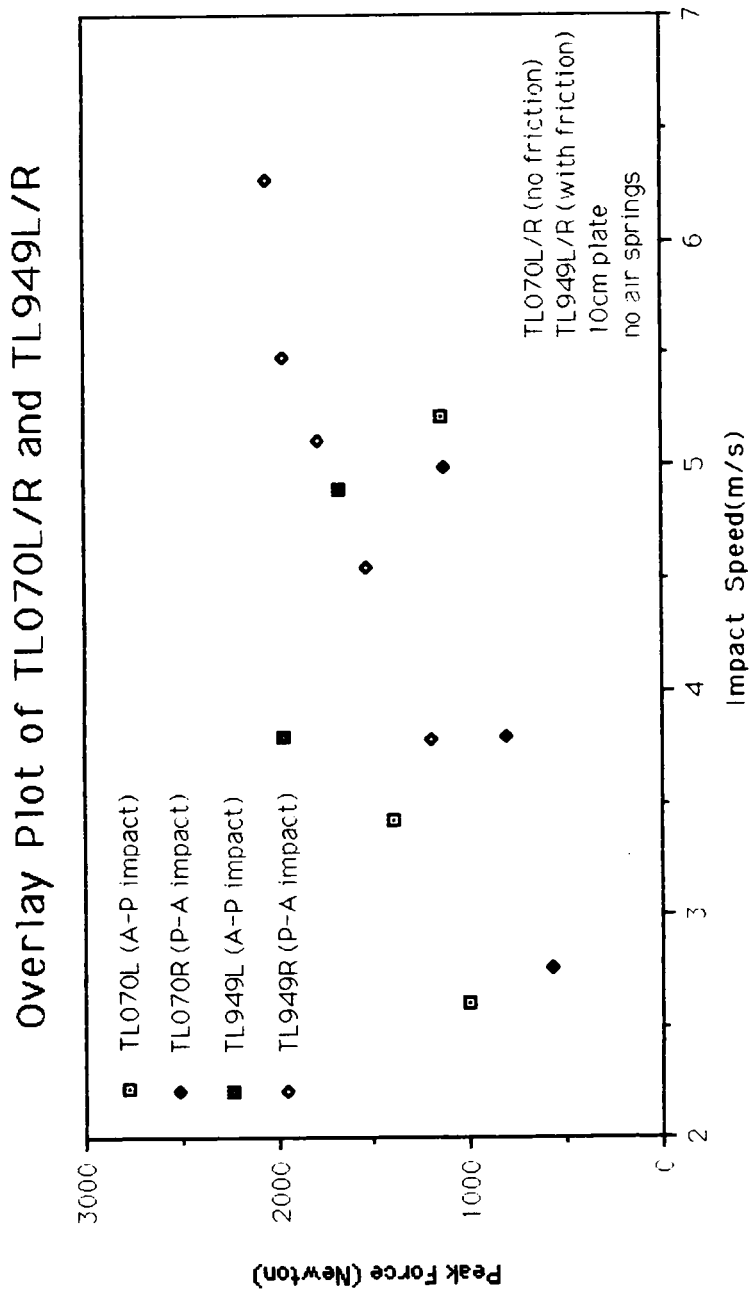


Figure 5-9.

Overlay plot of impact data from TL070L/R and TL949L/R.

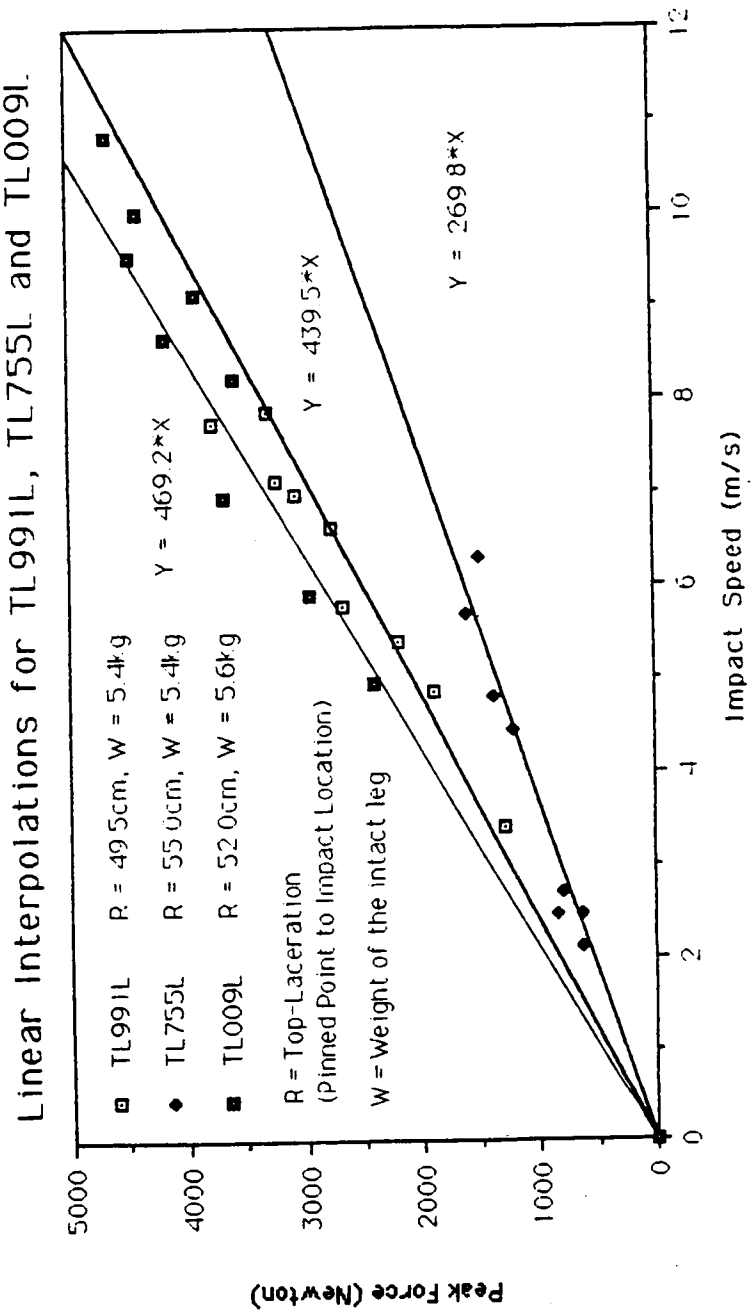


Figure 5-10.

Linear interpolations (slopes) for TL991L, TL755L, and TL009L.

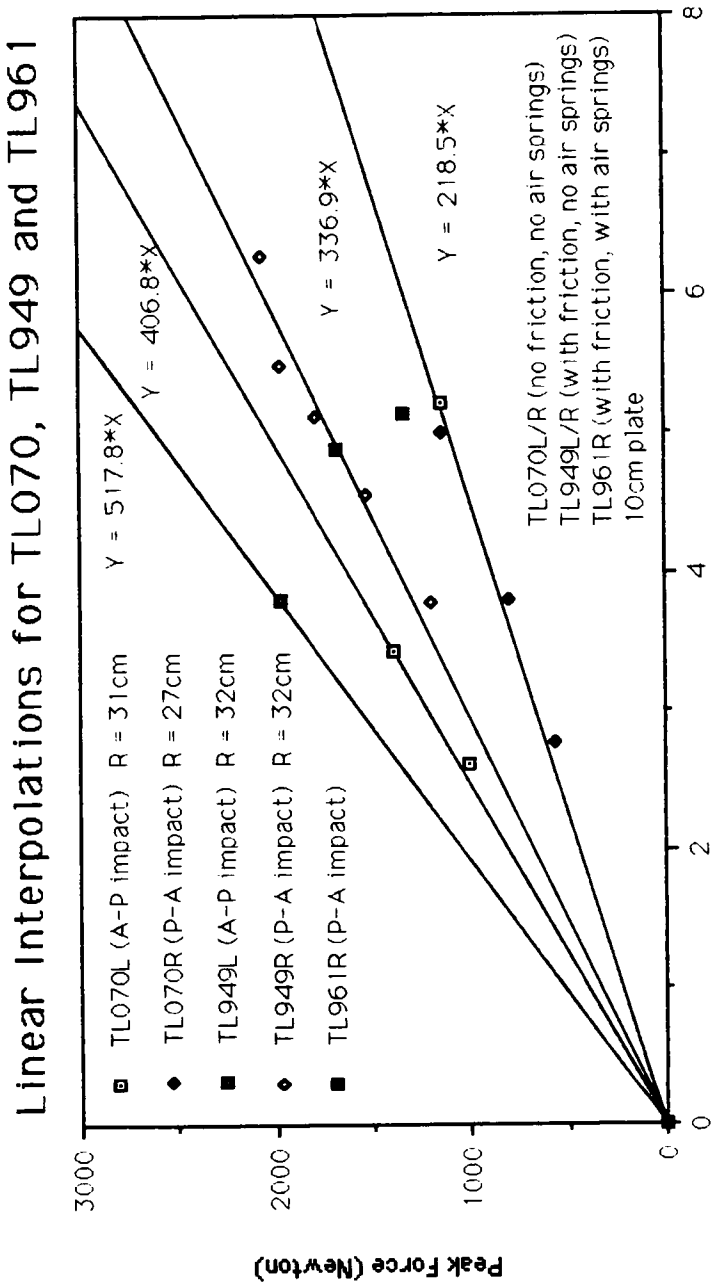
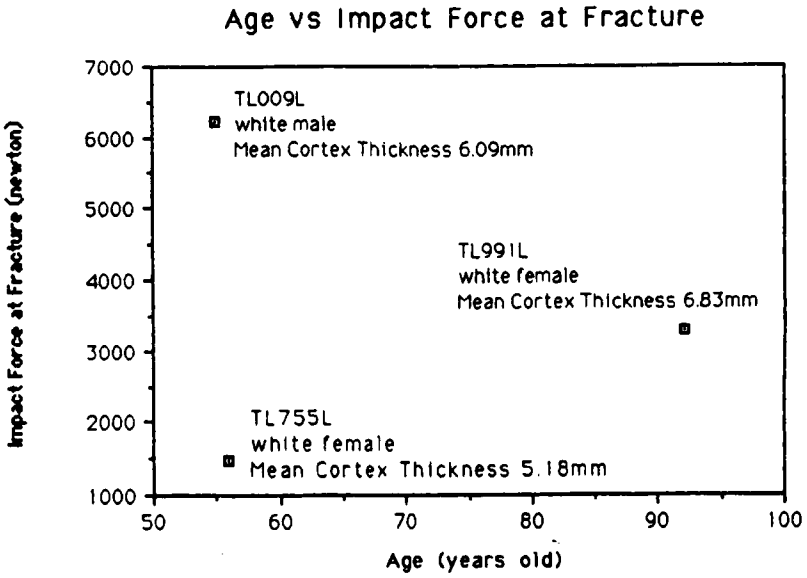


Figure 5-11.
Linear interpolations (slopes) for TL070, TL949, and TL961.



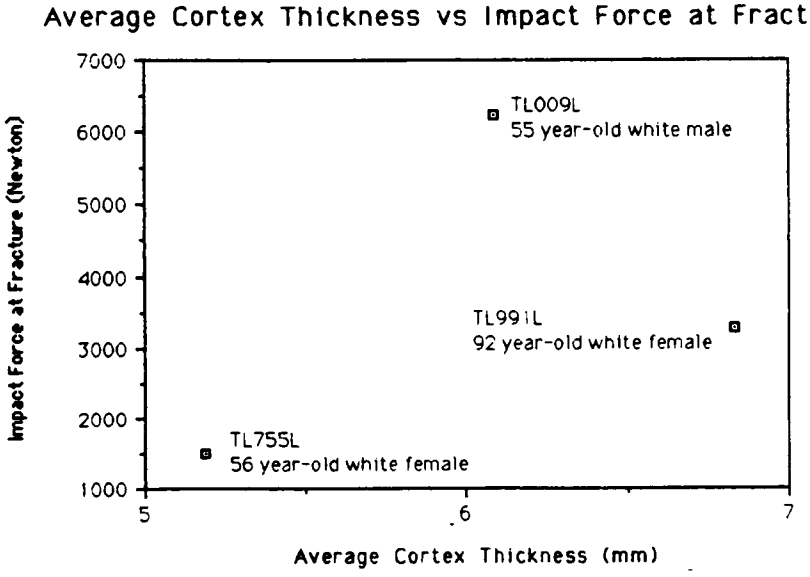


Figure 5-12.

Plots of age vs. impact force at fracture and average cortex thickness vs. impact force at fracture.

TEST program

The fuzzy expert system program named TEST.EXE developed for demonstration has four subroutine programs named TEST1, TEST2, TEST3 and TEST4. Each subroutine performs an assigned fuzzy operation. The details of rules and variables in each subroutine are as follows.

Abbreviations

pb = positive big
pm = positive medium
zz = zero
nm = negative medium
nb = negative big

Subroutine Name: TEST1

Input Variable:

radius:

The distance between the pinned point and the impact point

Universe of Discourse: (49.0 to 55.5 cm)

Number of Membership Functions: 5 (nb, nm, zz, pm, pb)

Output Variable:

slope:

The slope of the linear relationship between the impact speed and the impact force

Universe of Discourse: (240 to 480 Newton sec /m)

Number of Membership Functions: 5 (nb, nm, zz, pm, pb)

* Universe of Discourse is a term used in fuzzy logic theory to denote a fuzzy variable range covered by its membership functions.

* Since *Fuzzle1.8* cannot accept variable names with more than 6 characters in the program, long variable names must be abbreviated within 6 characters.

The rules in Table 5-11 appear to describe a simple linear correlation. However, by manipulating weighting factors and membership functions, they can actually describe a non-linear relationship between the radius and the slope. Usually, a high order polynomial function or an exponential function must be used to interpolate a non-linear relationship between two variables. But, this is not necessary for a fuzzy expert system.

Table 5-11.

Rules and Weighting factors for TEST1

Condition	Operation	Weighting factor
IF radius = nb	THEN slope = pb	Weight =10
IF radius = nm	THEN slope = pm	Weight = 5
IF radius = zz	THEN slope = zz	Weight = 1
IF radius = pm	THEN slope = nm	Weight = 5
IF radius = nb	THEN slope = nb	Weight =10

Description of TEST1:

This part of the expert system is based on the series of impact tests performed on the intact leg specimens, TL991L, TL755L, and TL009L. The plots of impact speed vs. impact force show clear linear relationships. The plots of TL991L and TL009L are close together. However, the plot of TL755L is lower than the other two due to its longer radius.

Experimental Conditions of TEST1:

* All specimens are impacted from A-P direction only.
* All specimens are tested with friction (20 kg weight).
* TL991 and TL755 are tested with air springs only.
* TL009L is tested both with and without air springs.
* Legs are pinned at the location near the hip joint to simulate the leg boundary condition of a person standing normally.
* The weight variation among specimens is very small (5.4 to 5.6 kg).
* Since there is not enough variance in weight among specimens, the leg weight is omitted from the input variables.
* No pair specimens are used due to the lack of availability.
* The radius variation is 49.5 to 55.0 cm.
* The high speed camera is used for the test of TL009L without air springs.
* The bumper impact height is adjusted at the location slightly above the mid shaft of tibia.

Table 5-12.

TEST1 Variable Behavior.

Specimen	Input radius	Output/Target value Slope
TL991L	49.5	450.0 (469.2)
	51.5	449.8
TL009L	52.0	434.7 (439.5)
	53.0	351.1
	54.0	276.9
TL755L	55.0	270.0 (269.8)

In Table 5-12, the values inside parentheses are the target values for the corresponding input values based on the experimental data. It is possible to match the output values to the target values by fine tuning the membership functions. However, since this program is made strictly for demonstration based on the experimental results of only eight legs, pursuing the exact matching of the output by fine tuning membership functions does not carry significant importance.

Subroutine Name: TEST2

Input Variables:

radius:

The distance between the pinned point and the impact point

Universe of Discourse: (10.0 to 33.0 cm)

Number of Membership Functions: 5 (nb, nm, zz, pm, pb)

direct:

The impact direction (1.0 = A-P direction, -1.0 = P-A direction)

Universe of Discourse: (-2.0 to 2.0)

Number of Membership Functions: 2 (nb, pb)

frictn:

The friction condition between the foot and the concrete load

(1.0 = with friction, -1.0 = without friction)

Universe of Discourse: (-2.0 to 2.0)

Number of Membership Functions: 2 (nb, pb)

Output Variable:

slope:

The slope of the linear relationship between the impact speed and the impact force

Universe of Discourse: (150 to 630 Newton sec /m)

Number of Membership Functions: 5 (nb, nm, zz, pm, pb)

Table 5-13.

Rules and Weighting Factors for TEST2

Condition	Operation	Weighting factor
IF radius = nb	THEN slope = pb	Weight = 1
IF radius = nm	THEN slope = pm	Weight = 1
IF radius = zz	THEN slope = zz	Weight = 1
IF radius = pm	THEN slope = nm	Weight = 1
IF radius = pb	THEN slope = nb	Weight = 1
IF direct = pb & friction = pb	THEN slope = pb	Weight = 6
IF direct = nb & friction = pb	THEN slope = zz	Weight = 6
IF direct = pb & friction = pb	THEN slope = pm	Weight = 6
IF direct = nb & friction = pb	THEN slope = nb	Weight = 6

TEST2 Variable Behavior.

Values between -1.0 and 1.0 are acceptable for "direct" and "frict." For example, direct = 0.0 can be related to the side impact, and frict = 0.0 can be related to medium friction force (mid point of between no friction and maximum friction) if the membership functions and rules are fine tuned based on the expanded data.in the future.

Table 5-14.

TEST2 Variable Behavior

Specimen	Input			Output/Target value	
	radius	direct	frict	Slope	
TL949L	31.0	1.0	1.0	516.3	(517.8)
TL949R	32.0	-1.0	1.0	333.9	(336.9)
TL070L	31.0	1.0	-1.0	406.2	(406.8)
TL070R	27.0	-1.0	-1.0	218.1	(218.5)
	29.0	1.0	1.0	516.5	
	28.0	1.0	1.0	520.0	
	27.0	1.0	1.0	526.0	
	29.0	-1.0	1.0	334.6	
	28.0	-1.0	1.0	339.8	
	27.0	-1.0	1.0	346.2	
	29.0	1.0	-1.0	406.8	
	28.0	1.0	-1.0	411.9	
	27.0	1.0	-1.0	419.8	
	28.0	1.0	1.0	520.0	
	28.0	0.0	1.0	445.1	
	28.0	-1.0	1.0	339.8	
	28.0	1.0	-1.0	411.9	
	28.0	0.0	-1.0	314.4	
	28.0	-1.0	-1.0	216.1	
	28.0	1.0	1.0	520.0	
	28.0	1.0	0.0	476.6	
	28.0	1.0	-1.0	441.9	
	28.0	-1.0	1.0	339.8	
	28.0	-1.0	0.0	277.6	
	28.0	-1.0	-1.0	216.1	

Description of TEST2:

This part of the expert system is based on the series of impact tests performed on the intact leg specimens, TL070L, TL070R, TL949L, TL949R and TL961R. Matched pairs are used to study the effects of the impact direction and the friction condition on the impact force. Since the variance among paired specimens is negligible, the test results can be compared more reliably. Again, the plots show a clear linear relationship between impact speed and impact force. The angle of the slope for the P-A impact is lower than P-A impact since the thick calf muscle acts as a shock absorber in the P-A direction. However, there is almost no difference in the impact force at which bone fracture occurs for A-P and P-A directions. Compared to the impact tests done without friction, the tests done with friction show about 35 to 45 % increase in the impact force.

Slope Angle and Boundary Conditions.

1).	A-P impact with friction	Approximate Slope = 517 Newton sec/m (from TL949L)
2).	A-P impact without friction	Approximate Slope = 406 Newton sec/m (from TL070L)
3).	P-A impact with friction	Approximate Slope = 337 Newton sec/m (from TL961R)
4).	P-A impact without friction	Approximate Slope = 218 Newton sec/m (from TL070R)

Experimental Conditions of TEST2:

* TL070L is impacted from A-P direction without friction.
* TL070R is impacted from P-A direction without friction.
* TL949L is impacted from A-P direction with friction.
* TL949R is impacted from P-A direction with friction.
* TL961R is impacted from P-A direction with friction
* Legs are pinned closer to the knee due to the short amputated length compared to the specimens used in TEST1.
* All specimens are tested without air springs except TL961R.
* The high speed camera is used for the test of TL961.

Because legs were pinned at the location closer to the knee, this experimental condition can be comparative to the lower leg injuries of motorcycle riders. At riding position, both knees are bent, and heels are on the foot rests. Because knees are used to secure the rider's body to the motorcycle, the movement of knees is restricted in a very small range.

Subroutine Name: TEST3

Input Variables:

age:

The age of the specimen (person)

Universe of Discourse: (30 to 95 years old)

Number of Membership Functions: 5 (nb, nm, zz, pm, pb)

cortex:

The mean thickness of the bone at the fracture point

(Bone thickness were measured at six different locations)

Universe of Discourse: (4.5 to 7.5 mm)

Number of Membership Functions: 5 (nb, nm, zz, pm, pb)

sex:

The gender of the specimen (1.0 = male, -1.0 = female)

Universe of Discourse: (-1.0 to 1.0)

Number of Membership Functions: 2 (nb, pb)

Output Variables:

strng:

The estimated maximum endurable impact force by the bone

Universe of Discourse: (0 to 9000 Newton)

Number of Membership Functions: 5 (nb, nm, zz, pm, pb)

Table F-15

Rules and Weighting factors for TEST3

Condition	Operation	Weighting factor
IF cortex = nb	THEN strength = nb	Weight = 4
IF cortex = nm	THEN strength = nm	Weight = 3
IF cortex = zz	THEN strength = zz	Weight = 3
IF cortex = pb	THEN strength = pb	Weight = 3
IF age = nb & sex = pb	THEN strength = pb	Weight = 2
IF age = nb & sex = nb	THEN strength = pm	Weight = 1
IF age = nm & sex = pb	THEN strength = pb	Weight = 2
IF age = nm & sex = nb	THEN strength = zz	Weight = 1
IF age = zz & sex = pb	THEN strength = pm	Weight = 1
IF age = zz & sex = nb	THEN strength = nm	Weight = 1
IF age = pm & sex = pb	THEN strength = nm	Weight = 1
IF age = pm & sex = nb	THEN strength = nb	Weight = 1
IF age = pb	THEN strength = nb	Weight = 5

Table 5-16

TEST3 Variable Behavior

Specimen	Input			Output/Target value	
	age	cortex	sex	strng	
TL775L	56.0	5.2	-1.0	1664.4	(1489.0)
TL009L	55.0	6.1	1.0	6004.0	(6242.0)
TL991L	92.0	6.8	-1.0	3656.3	(3290.8)
	60.0	6.0	1.0	5352.2	
	70.0	6.0	1.0	4369.7	
	80.0	6.0	1.0	2488.9	
	60.0	6.0	-1.0	4173.9	
	70.0	6.0	-1.0	3532.7	
	80.0	6.0	-1.0	2364.7	
	60.0	5.0	1.0	2434.5	
	60.0	6.0	1.0	5352.2	
	60.0	7.0	1.0	7554.2	
	60.0	5.0	-1.0	1553.7	
	60.0	6.0	-1.0	4173.9	
	60.0	7.0	-1.0	6851.4	

Description of TEST3:

In this part of the program, the maximum endurable impact force of a bone is estimated from the bone data: age, sex and mean cortex thickness. The estimation of the test program utilizes dissection data and impact force data at fracture of the specimens used in the tests. The development of fuzzy rules for this section is based Motoshima's work (1959).

Subroutine Name: TEST4

Input Variables:

diffrn:

The difference between the expected impact force and the maximum possible force that can be sustained by a bone without fracturing

Universe of Discourse: (-7500 to 7500 Newton)

Number of Membership Functions: 5 (nb, nm, zz, pm, pb)

Output Variables:

possib:

The possibility of fracture

Universe of Discourse: (-16.666 to 116.666 percent)

Number of Membership Functions: 5 (nb, nm, zz, pm, pb)

Table 5-17

Rules and Weighting Factors for TEST4

Condition	Operation	Weighting factor
IF difference = nb	THEN possibility = nb	Weight = 1
IF difference = nm	THEN possibility = nm	Weight = 1
IF difference = zz	THEN possibility = zz	Weight = 1
IF difference = pm	THEN possibility = pm	Weight = 1
IF difference = pb	THEN possibility = pb	Weight = 1

Table 5-18

TEST4 Variable Behavior

Input diffrn	Output possib
-4000.0	0.0
-3500.0	8.4
-3000.0	14.3
-1500.0	34.8
0.0	42.9
500.0	57.1
1500.0	65.2
3000.0	85.7
3500.0	91.6
4000.0	100.0

Description of TEST4:

In this section of the program, the maximum endurable impact force of a bone, which is estimated from the bone data, is compared to the expected impact force, which is estimated from the force vs. speed slope at a given speed. Since there are variances among bone specimens, it is unsafe to conclude that bones are going to break 100% if the estimated impact force exceeds the estimated max endurable force. Therefore, the program translates the fracture occurrence in terms of a percent possibility by checking the difference between the expected impact force and the maximum endurable force. The percent possibility ranges in the test program are my initial guesses, and they must be fine tuned by accumulating more data.

1. Functions of TEST Program.

1). Estimating the slope of the linear relationship between the impact speed force and the impact force from the distance between the pinned point and the impact point, direction of the impact, and friction condition. The slope estimation can be done for two different pinned cases. The first case is that a leg is pinned at the hip (managed by **TEST1**), and the second case is that a leg is pinned at the knee (managed by **TEST2**).

2). Computing the expected impact force from the impact speed and the slope. Within the linear range, **Impact force = slope * impact speed.**

3). Estimating the approximate maximum tolerable impact fracture force for a bone from age, sex and the mean cortex thickness (managed by **TEST3**).

4). Estimating % fracture possibility from the difference between the maximum tolerable impact force and the estimated impact force (managed by **TEST4**).

* A series of impact experiments revealed the clear linear relationship between the impact force and the impact speed, which is very useful to predict impact forces from impact speeds. The slope angle is characterized by the boundary condition and the impact location.

* Rules and membership functions are fine tuned so that the input and the output match with the actual experimental data, which were used as way points and templets. The transition between the way points are interpolated smoothly by fuzzy logic calculation.

2. Questions and Input Variables at Program Run.

* Is the leg pinned at the hip or the knee ?
  1 = **CASE1**: pinned at the hip, 2 = **CASE2**: pinned at the knee

  Read ***case***

* Does the bumper has **air springs** ? 1 = yes : 0 = no

  Read ***spring***

* Is there **friction** on the foot ?
  1.0 = friction (by body weight) : -1.0 = No friction

  Read ***frictn***

* **Age** of the person ? (years old)
  The value must be a real number between 30.1 and 94.9.

  Read ***age***

* What is the **gender** of the leg ? 1.0 = male : -1.0 = female

  Read ***sex***

* What is the **mean cortex thickness** at the point of impact ? (mm)
  The value must be a real number between 4.6 and 7.4.

  Read ***cortex***

* **Direction** of impact ? 1.0 = A-P impact : -1.0 = P-A impact
  P-A option is only available for CASE2.

  Read ***direct***

* What is the **distance** between the pinned point and the impact point ? (cm) The value must be a real number between 49.1 and 55.4 for CASE1 and between 10.1 and 32.9 for CASE2.

  Read ***radius***

* What is the **speed of impact** ? (m/s) A real number between 0.0 to 10.0.

  Read ***speed***

3. Subroutine Calls and Output.

if (case .eq. 1) then

call **test1(radius, slope)**.....estimate the slope for Case1.

else if (case .eq. 2) then

call **test2 (radius, direct, frictn, slope)**.....estimate the slope for Case2.

end if

call **test3 (age, cortex, sex, strng)**.....estimate the bone strength.

force = slope*speed.....estimate the impact force.

diffrn = force-strng.....obtain the difference in estimated forces.

call **test4 (diffrn, possib)**.....estimate the % fracture possibility.

pinned point to impact point (cm) = ***radius***

slope (Newton*sec/m) = ***slope***

impact speed (m/s) = ***speed***

age (years old) = ***age***

sex (1=male: -1=female) = ***sex***

mean cortex thickness (mm) = ***cortex***

maximum tolerable impact force (Newton) = ***strng***

if (spring .eq. 0 .and. speed .gt. 7.7) then.....no air springs, speed over 7.7m/s

estimated impact force (Newton) = over 6500

possib = 100.0

else if (speed .le. 7.7 .or. spring .eq. 1) then

estimated impact force (Newton) = ***force***

difference in force (Newton) = ***diffrn***

end if

fracture possibility (%) = ***possib***

end

4. Sample Output.

Case 1 (pinned at hip), with air springs, A-P impact, with friction

pinned point to impact point (cm) =	50.0
slope (Newton*sec/m) =	450.0
impact speed (m/s) =	9.0
age (years Old) =	39.0
sex (1=male: -1=female) =	-1.0
mean cortex thickness (mm) =	4.8
maximum tolerable impact force (Newton) =	3075.0
estimated impact force (newton) =	4050.0
difference in force (Newton) =	975.0
fracture possibility =	60.9

Case 1 (pinned at hip), no air springs, A-P impact, with friction

pinned point to impact point (cm) =	52.0
slope (Newton*sec/m) =	428.2
impact speed (m/s) =	8.2
age (years Old) =	44.0
sex (1=male: -1=female) =	-1.0
mean cortex thickness (mm) =	5.5
maximum tolerable impact force (Newton) =	3649.2
estimated impact force (newton) =	over 6500.0
fracture possibility =	100.0

Case 2 (pinned at knee), with air springs, A-P impact, with friction

pinned point to impact point (cm) =	15.0
slope (Newton*sec/m) =	547.6
impact speed (m/s) =	9.5
age (years Old) =	55.0
sex (1=male: -1=female) =	-1.0
mean cortex thickness (mm) =	6.0
maximum tolerable impact force (Newton) =	4178.0
estimated impact force (newton) =	5201.0
difference in force (Newton) =	1023.8
fracture possibility =	61.3

Case 2 (pinned at knee), with air springs, P-A impact, no friction

pinned point to impact point (cm) =	31.0
slope (Newton*sec/m) =	212.5
impact speed (m/s) =	6.5
age (years Old) =	45.0
sex (1=male: -1=female) =	1.0
mean cortex thickness (mm) =	7.2
maximum tolerable impact force (Newton) =	7779.0
estimated impact force (newton) =	1381.3
difference in force (Newton) =	-6397.8
fracture possibility =	4.76E-06

Case 1 (pinned at hip), with air springs, A-P impact, with friction

pinned point to impact point (cm) =	55.0
slope (Newton*sec/m) =	270.0
impact speed (m/s) =	5.5
age (years Old) =	95.0
sex (1=male: -1=female) =	-1.0
mean cortex thickness (mm) =	4.7
maximum tolerable impact force (Newton) =	1125.0
estimated impact force (newton) =	1485.0
difference in force (Newton) =	360.0
fracture possibility =	55.6

Case 1 (pinned at hip), with air springs, A-P impact, with friction

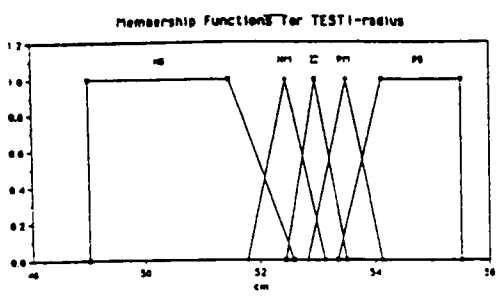
pinned point to impact point (cm) =	50.0
slope (Newton*sec/m) =	450.0
impact speed (m/s) =	7.5
age (years Old) =	38.0
sex (1=male: -1=female) =	1.0
mean cortex thickness (mm) =	6.2
maximum tolerable impact force (Newton) =	6689.2
estimated impact force (newton) =	3375.0
difference in force (Newton) =	-3314.2
fracture possibility =	10.7

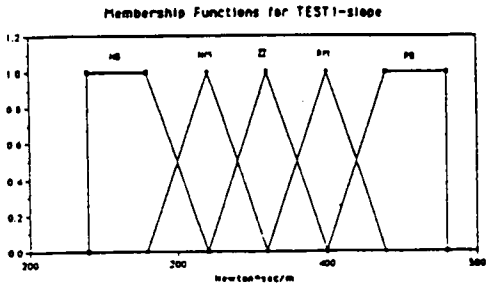
Case 2 (pinned at knee), with air springs, A-P impact, no friction

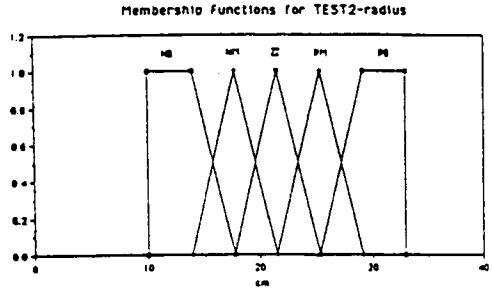
pinned point to impact point (cm) =	14.0
slope (Newton*sec/m) =	523.3
impact speed (m/s) =	12.0
age (years Old) =	88.0
sex (1=male: -1=female) =	-1.0
mean cortex thickness (mm) =	4.8
maximum tolerable impact force (Newton) =	1125.0
estimated impact force (newton) =	6279.2
difference in force (Newton) =	5154.2
fracture possibility =	100.0

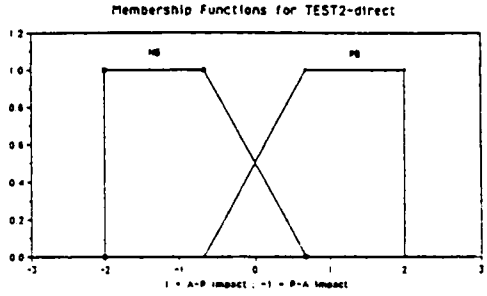
Case 2 (pinned at knee), with air springs, P-A impact, with friction

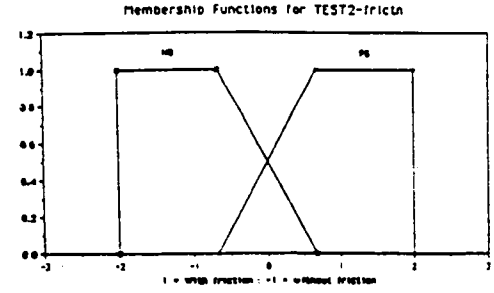
pinned point to impact point (cm) =	28.0
slope (Newton*sec/m) =	285.4
impact speed (m/s) =	11.0
age (years Old) =	35.0
sex (1=male: -1=female) =	1.0
mean cortex thickness (mm) =	6.1
maximum tolerable impact force (Newton) =	6513.8
estimated impact force (newton) =	3139.3
difference in force (Newton) =	-3374.6
fracture possibility =	9.9











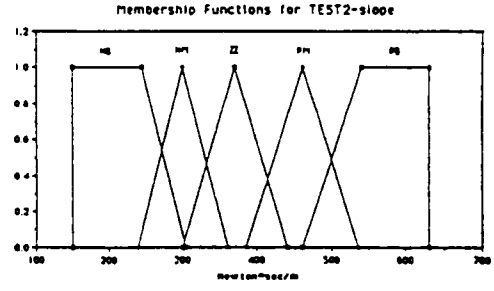


Figure 5-13.
Membership functions for TEST1 (radius and slope) and for TEST2 (radius, frict, direct and slope).

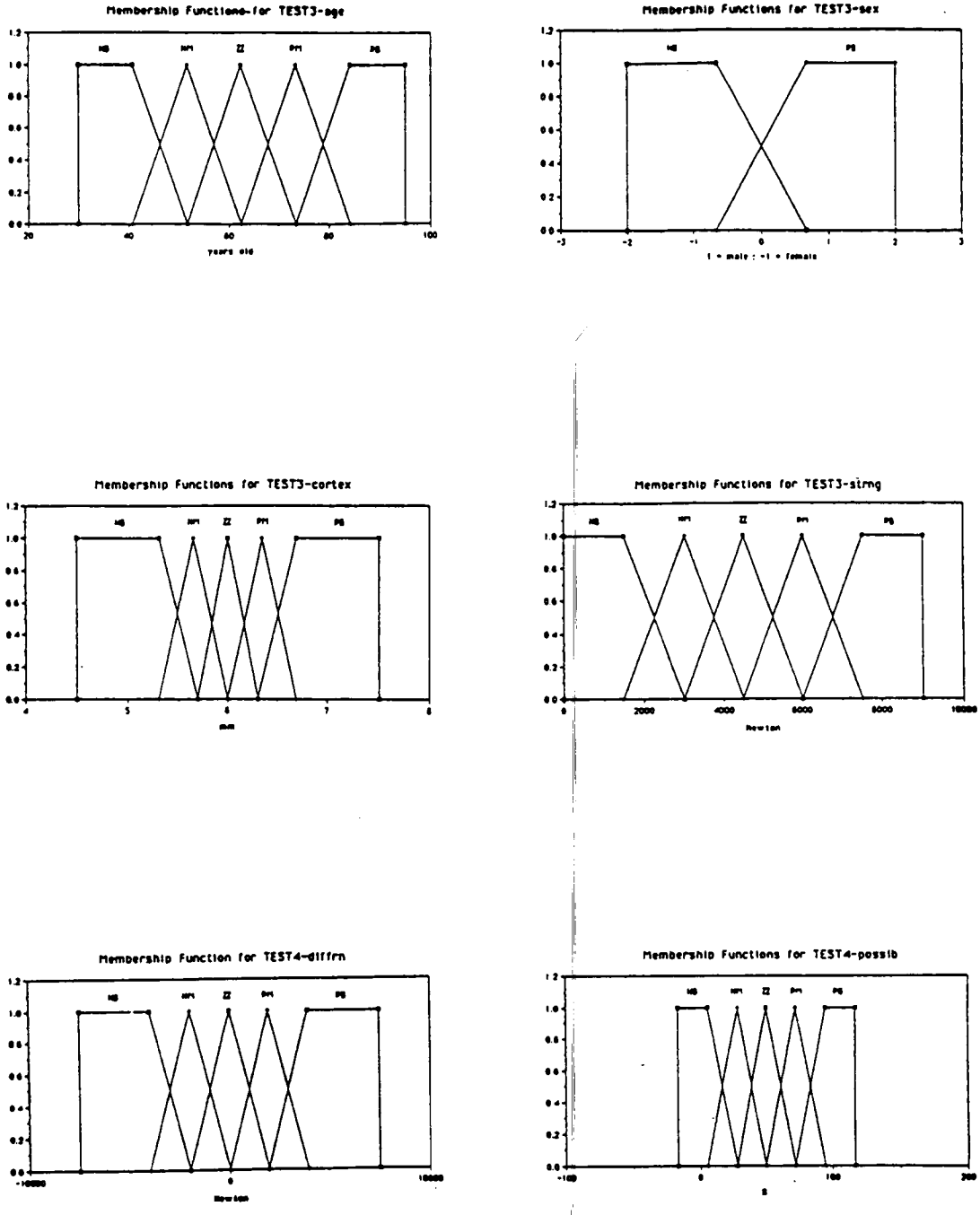


Figure 5-14.
Membership functions for TEST3 (age, sex, cortex and strng) and for TEST4 (diffrn and possib).

(H)

Briefing of FUZZLE 1.8

(The Fuzzy Expert System Construction Shell)

and Developed Program

The source code of the fuzzy bone fracture prediction program is written in FORTRAN language. Fuzzy computation subroutines in the program are generated by *FUZZLE 1.8* software. *FUZZLE 1.8* is a fuzzy logic inference system construction program developed by MODiCO Inc. in Knoxville, TN. Dr. R. C. Berkan, the developer of *FUZZLE* software, obtained a Ph.D degree from the Nuclear Engineering Department of the University of Tennessee in 1991. One of the purposes of the program development is to make an inexpensive introductory program of fuzzy logic for college education since the selection of commercially available fuzzy software is limited and very expensive. Although *FUZZLE* is not as elegant as *TILShell* developed by Togai Fuzzy InfraLogic Inc. in terms of the ease of operation and available options, Berkan's *FUZZLE* securely covers all the basics of fuzzy logic computation.

Due to the very small data base size, the test program is written only to demonstrate the ease of application and modification of the fuzzy logic expert system with regard to bone fracture predictions. The rules and membership functions used for the test program are designed based on the experimental results of eight intact legs. The designed membership functions and rules shall give reasonable output within the specified input parameter ranges at the input based on the current data base. It should be noted that although these membership functions and rules work fine as they are intended, this is not the

final and only form. Many other variations of rules and membership functions can be considered, and they should also work fine based on the judgements of individuals. Due to the limited number of experiments, statistical assurance is not yet proven. To improve the estimation of the ultimate failure force from age, sex and bone thickness, much more data is required. However, the estimation of the impact force at a given speed should be fairly accurate since the impact speed-force relationship has shown very good linear correlations in the experiments over all.

Chapter VI

CONCLUSIONS and RECOMMENDATIONS

(A)

Age, Sex and Mean Cortex Thickness

Age and sex of a bone are the notable factors which affect bone strength. After age 40, bone strength gets weaker linearly as aging occurs. For the same age range, male leg bones are about 15% stronger than female bone (Motoshima 1960). Another factor of bone strength is cortex thickness, since weakening in strength is caused by cortex thinning. Generally, male bones are thicker than female bones for the same age range. These common sense rules also hold in my experiment, and fuzzy rules for the test program are written based on them. Generally, the cortex thickness shows more direct correlation to the bone strength than age and sex. However, at ages over 80, bones are weak regardless of the cortex thickness. In the test, TL991L (92 year-old white female, cortical thickness of 6.8mm, the thickest among used specimens) broke at a lower impact force than TL009L (55 year-old white male, cortical thickness of 6.1mm). This means that the age is a more important factor than cortex thickness at higher ages. This correction is done by giving a higher weight factor to the rule "If age = positive big then strength = negative big" than the age and sex condition rules.

(B)

Leg Mass Variation

For the pinned-free and the pinned-friction boundary condition, the mass of the leg should be an affecting factor since a pinned leg maintains its position by inertia during the fracture. Generally speaking, the heavier the mass, the higher the impact force. However, since there should not be enough weight variance among adult leg specimens to cause notable difference in impact force, it is safe to say that the weight variation among adult legs is not a strong factor with regard to the fracture force. It is especially true for the knee-pinned legs.

(C)

Impact Location

To swing a hanging bar by a minimum force, the force should be applied at the bottom end of the bar. If a point closer to the pinned point is pushed on the bar, the required force to move is larger. Generally, the longer the distance between the pinned point and the pushing point, the smaller the pushing force is. Similarly, the longer the distance between the pinned point and the impact point (in the program, it is called "radius"), the smaller the impact force is. This means that a long-legged person will experience lesser peak impact force than a short legged person for the same impact height because the radius is longer. The effect of the distance to the impact force becomes clearer between hip pinned legs and knee pinned legs. Knee pinned

legs experience a higher peak force than hip pinned legs since the distance is shorter. Compared to the mean slope (impact speed vs. impact force) of hip pinned legs, TL991L, TL755L and TL009 (A-P impact with friction) the slope of a knee pinned leg, TL949L (A-P impact with friction) is approximately 30 % higher.

(D)

Friction Condition

Two leg boundary cases are considered for a pedestrian. The first case is a leg standing up on the ground so that the friction force is generated as the foot moves during the impact. The second case is a leg completely lifted from the ground; therefore there is no friction force. Compared to the lifted foot condition, the standing condition results in about 20% higher impact force for the same impact speed due to the resistance force generated by friction on the foot. In the experiments, the friction situation is limited to the condition of a tennis shoe with 20 kg normal weight on a concrete plate. The friction condition varies according to the type of shoes, the road conditions, and the weight on a leg. The normal weight can go up as high as 40 to 50 kg depending on the person's weight and the weight allocation to each leg. The effects of these variations are left for future study.

(E)

Impact Direction

The peak force recorded by the force transducer varies according to the thickness of the skin, fat, and muscle surrounding the tibia bones. The thickness is a variable of the impact direction and the height. On the front side of the tibia, there are no muscles. However, on the back side of the tibia, there is a lump of calf muscles. Matching pairs are used in the experiment to compare the directional effects between the front impacts and the rear impacts. If there is no friction on the foot, the rear side impact force can be 50% smaller than the front side impact force at the same impact speed. If there is friction on the foot, the directional effect to the impact force gets a little smaller (up to 35% decrease). In rear-direction impacts, the region of calf muscles has proven to be an excellent shock absorber by avoiding the force concentration.

One front side impact test (TL755L) and one rear side impact test (TL961R) were filmed by the Kodak EKTAPRO high speed video camera. For the front side impact, the video shows no sign of leg twisting. In slow motion, the leg is simply pushed way by the bumper as it proceeds. The swing motion for the front side impact looks very stable because the impact point is located ahead of the toe region so that there is no chance of the foot twisting. However, for rear side impact, the situation is different because the toe region is located behind the impact point. This makes the swing motion somewhat unstable at high speed impact. The video tape of TL961R shows a twisting motion of the foot around the toe during the impact. The rear side impact lifts

the heel instantaneously before breaking the toe contact. This motion seems to pin down the toe region as a pivoting point. As the impactor proceeds, the foot rotates around the toe, and the tibia is twisted.

(F)

Impact Speed vs. Impact Force

The experimental data shows that there is a strong linear correlation between the impact speed and the peak impact force. The formulas from impact fracture mechanics in section III-B shows a direct linear relationship between the impact speed and the impact stress. Since the change of contact surface area during the impact could not be measured in the experiment due to technical difficulties, only the impact force was recorded. Without the information of contact surface area, the stress localization during the impact in the vicinity of the impact point cannot be obtained experimentally. Strictly speaking, therefore, the impact fracture conditions cannot be discussed in terms of the impact stress from the experimental data.

However, the impact force shows a very clear linear relationship with the impact speed even though it is not the impact stress. This can mean that the area of contact during the impact is almost constant within the linear range. Beyond the linear range, the impact force sharply rises. This indicates that the impact force starts to concentrate in a very small area after the linear range.

(G)

Effect of the Bumper Springs

Obviously, the spring constant of the bumper support spring is the major factor that affects impact force. The softer the bumper springs, the longer the linear relationship range of impact speed vs. peak impact force. Without springs, the linear relationship quickly ends at the speed at which the peak force is about 3000 N around 7 m/s. Beyond that speed, the impact force shoots up very sharply. At 8 m/s, the bumper without springs exerts about 6000 N peak impact force, which is twice as high as the impact force at 7 m/s. With air springs, the between impact speed and force relationship is still in the linear range at speed 8 m/s, and the peak impact force is about 3500 N. The extended linear range depends on the shock absorption capability of bumper springs. Therefore, the linear range must be found experimentally for each new bumper design. Once it is found, the impact force can be predicted easily from the impact speed.

(H)

Impact Surface

In the experiment, two impact plates with different widths are used. One is 10 cm wide and the other is 4 cm wide. The result shows that when the air springs are attached to the bumper, the difference in the peak impact force between a 10 cm plate and 4 cm plate is minimal. On the plot, the relationships between the impact speed and the peak force with a 4 cm plate and a 10 cm

plate are almost overlapping until up to 9 m/s. However, above 9 m/s, the impact force of the 4 cm plate starts to deviate from that of the 10 cm plate. After 9m/s, the impact force seems to increase exponentially, and the difference in between the impact force between a 4 cm plate and a 10 cm plate gets wider as the speed increases (See Figure 5-6).

(I)

Bumper Surface Covering Material

A 10 cm thick sponge block is used as an impact plate surface covering material. Although it provides good protection against skin damage, it does not have much effect on the impact force. This is mainly due to the fact that the 10cm sponge block used for the test is too soft and too thin to prevent the total collapsing during the impact.

(J)

Comments on Fuzzy Expert System Development

Before designing fuzzy membership functions, the fuzzy logic rules which declare the relationship between parameters must be made. The conspicuous experimental data correlations should first be converted to rules, and then rules that provide extra details should be added. To establish the relationship between two parameters, the theory of impact fracture mechanics, experimental data, and the intuition of experts must all be used.

It looks like that the inference gets better and better as the number of rules and parameters increases. However, in reality, increasing the number of

rules may not always be helpful. At worst, it may harm the logic flow if added rules are not appropriate. Therefore, increasing the number of rules and variables must be carefully managed in the modification process.

One of the best benefits of fuzzy logic is that the necessity for deriving complicated equations and interpolation to relate parameters can be minimized. However, if fuzzy logic is used carelessly, there is a potential risk to relate parameters which do not actually relate to each other. Therefore, it is necessary to verify the parameter relationships not only by experimental data correlations but also by engineering theories and observations.

Since the data size was small, only two to five membership functions were used for some parameters in the TEST program to describe parameter variations. However, if sufficient amount of data is collected, the number of membership functions for a parameter can be increased up to seven to nine for more detailed description. The primary parameter candidates for increase of membership functions are "impact direction" and "foot friction" since only two membership functions were assigned for each in the TEST program.

Combined IF-conditions of IF-THEN rules (ex. IF A and B then C) are quite effective for a couple of strongly related parameters (for example, age and sex to the bone strength). Tuning the membership functions of combined IF-condition is easier than tuning the two separate single condition rules (ex. IF A then C / IF B then C). However, using the combination of single condition rules is more responsive to the membership function tuning. If three or more conditions are expected to be superimposed, the combination of single rules is recommended. Since *Fuzzle 1.8* does not have the option to design each membership function shape, membership function tuning can only be done

by either sifting a membership function or changing the base length of a triangle function. However, as a compensation for the membership design limitations, *fuzzle* includes the weighting factor setting option. It is a very useful and powerful tool to navigate the output to the desired target value.

(K)

Recommendations

Due to the small number of specimens (total of eight intact legs), experimental data for age, sex, cortex thickness, impact directions and locations were limited. Therefore, inevitably valid ranges of input variables in the TEST program are restricted. However, as more data become available, boundaries of input variables can be removed totally, and the impact force can be predicted at any height of any direction with variations of muscle and bone thickness taken into consideration. In the experiment, impact fracture tests were limited to tibia bones. But, if sufficient amount of experimental data become available for femurs, radius, humerus, and skulls, the injury prediction of an entire human body (fracture locations, types, and severities) becomes possible as well as the impact speed and location prediction from the injury conditions. By utilizing the Muller's classification code (See Section 2-(C)) combined with the fuzzy logic prediction of the basic body motion in various conditions, the prediction and assessment program of bone fractures for entire human skeletal system can be developed in a short time.

BIBLIOGRAPHY

BIBLIOGRAPHY

Achenbach, J. D., "Wave Propagation in Elastic Solids." North-Holland, 1973.

Albin, M., "Fuzzy Sets and Their Application to Medical Diagnosis and Pattern Recognition." Ph.D. Thesis, University of California, Berkeley, 1975.

Amis, A. "Biomechanics of ligaments. Ligament injuries and their treatment." D. H. R. Jenkins Chapman and Hall Medical, P3-28, 1985.

Akaishi, T., Asada, K., Shimazu, A. et al, "Orthopaedics from Biomechanical View Points." Kanehara LTD., P133-147, 1988.

Asai, K., Tanaka, H., & Okuda, T. "Decision-making and its goal in a fuzzy environment." Academic Press, New York, 1975.

Berkan, R. C., "GUIDE TO FUZZLE OPERATIONS (FUZZLE 1.8 Operation manual)." MODiCO Inc, Knoxville, TN, 1992.

Buckwalter, J. A., Cooper, R. R. "Bone Structure and Function." A.A.O.S. Instructional Course Lectures, Vol. 36: P27-48, 1987.

Cook, R. D., Malkus, D. S. & Plesha, M. E., "Concepts and Applications of Finite Element Analysis." John Wiley & Sons, New York, 1989.

Dubois, J. & Parade, H. "Fuzzy Sets and Systems." Academic Press, Inc., California, 1980.

Evans, F. G., Pedersen, H. E. and Lissner, H. R., "The Role of Tensile Stress in the Mechanism of Fractures." J. Bone & Joint Surg., P485-501, 1951

Frankel, V. H. and Burstein, A. V. "Orthopedic Biomechanics. Lea & Febiger." 1970.

Frankel, V. H., Nordin, M. "Basic Biomechanics of the Skeletal System." 15-16, Lea & Febiger, Philadelphia, 1980.

Fung, Y. C. "Foundations of Solid Mechanics." Prentice-Hall, 1965.

Goldsmith, W. "Impact-Theory and Physical Behavior of Colliding Solids." Edward Arnold Publishing Co., 1960.

Gray, T. G. F. "Fracture Mechanics in Engineering Practice." Applied Science Publishers LTD., London, 1977.

Hayashi, Sano, Asai "Impact Buckling of a Beam." Japan Mechanical Engineering Academy Thesis Collections Vol 38, 1972.

Hutchunson, J. W., "Singular behavior at the end of a tensile crack in a hardening material." Journal of the Mechanics and Physics of Solids, 1968.

Johnson, W. "Impact Strength of Materials." Crane, Rusak & Company, Inc., New York, P5-12, 281-288, 1972.

Kitagawa, K. et al, "Role of Fracture Mechanics in Modern Technology." 1987.

Kress, Tyler a. "Mechanical Behavior of Lower Limbs in Response to Impact Loading." Master of Science Thesis in Engineering Science, The University of Tennessee, Knoxville, 1989.

Lanz, J., Wachsmuth, W. "Praktische anatomy." Springer-Verlag, Berlin: Heidelberg: New York: 1972.

McRae, R. "Practical Fracture Treatment." Longman group Limited, harlow, 1981

Miklowitz, J. "Theory of Elastic Waves and Waveguids." North-Holland, 1984.

Morita, Y., and Iida, H. "Measurement, information and human subjectivity described by an order relationship." Working Group Fuzzy Syst., Tokyo, 1975.

Motoshima, T. "Studies on the Strength for Bending of Human Long Extremity Bones." The 64th Japan Anatomy Conference, Kyoto, Japan: The Kyoto prefectural University of Medicine, 1959.

Mitsuya, N. & Tanaka, K. "Practical Fuzzy in C language." Russel Inc., 1990.

Muller, M. E. "The comprehensive Classification of Fractures of Long Bones." Springer-Verlag Berlin Heidelberg, 1990.

Murakami, Y., et al. "Stress Intensity Factors Handbook." Pergamon Press, 1987.

Okuda, T., Tanaka, H., & Asai, K., "A formulation of fuzzy decision problems with fuzzy information." using probability measures of fuzzy events. Inf. Control, 1978.

Okuda, T., Tanaka, H., & Asai, K., "Decision-making and information in fuzzy events." University Osaka.

Paris, P. C., et al. "Elastic-Plastic Fracture." ASTM STP, 1979.

Paris, P. C. and Sih, G. C., "Fracture Toughness Testing and its Applications." ASTM STP, 1965.

Pauwels, F. "Biomechanics of the Normal and Diseased Hip Theoretical Foundation; Technique and Results of Treatment." Springer-Verlag: Berlin: Heidelberg: New York: 1976.

Rice, J. R. and Rosengren, G. F. "Plastic strain deformation near a crack tip in a power-low hardening material." Journal of the Mechanics and Physics of Solids, 1968.

Saha, S. and Hayes, W. C. "Instrumented Tensile-impact Tests of Bone." Paper presented at Third SESA International Congress on Experimental Mechanics held in LA, CA on May 13-18, 1973.

Tamura, S., Higuchi, S., & Tanaka, K. "Pattern classification based on fuzzy relations." IEEE Trans. Syst., Man Cybern, 1971.

Timoshenko, S. P. & Gere, J. M. "Mechanics of Materials." Wadsworth, Inc., California

Timoshenko, S. P. & Goodiner, J. N. "Theory of Elasticity." 3rd Ed., McGraw-Hill, 1970.

Togai, Masaki & Ota, Masahiro "Fuzzy Logic for a Million People." Nikkankogyoshinbun, 1990.

Tsukamoto, Y. & Terano, T., "Failure diagnosis by using fuzzy logic." Proc. IEEE conf. Decision Control, New Orleans, 1977.

Tucker, Guy V. "The Mechanical Behavior of the Human Femur Subjected to Impact Loading." Master of Science Thesis in Engineering Science, The University of Tennessee, Knoxville, 1991.

Weibull, W., A. "Statistical Theory of the Strength of Materials." Ingeniors Vetenskaps Akademiens Handlingar Nr, 1939.

Wolff, J. "The low of Bone Remodeling." translated by P. Macquet and R. Furlong. Springer-Verlag, Berlin, Heidelberg, New York: London: Paris: Tokyo:, 1986.

Yagawa, G., Takahashi, Y & Ueda, H. "Three-dimensional fully plastic solutions for plates and cylinders with through-wall cracks." Transactions of the ASME, Journal of Applied Mechanics, 1985.

Yagawa, M. "Fuzzy Inference." Baifukan Inc., Tokyo:, 1991

Yagawa, M. "Fracture Mechanics." Baifukan Inc., Tokyo:, 1990

Yamada, H. In F. G. Evans (ed.) "Strength of Biological materials." Robert, Baltimore: Williams & Wilkins, 1970.

Zadeh, L. A., "Fuzzy sets as a basis for a theory of possibility." Int. J. Fuzzy Sets Syst., 1978.

Zadeh, L. A., "The concept of linguistic variable and its application to approximate reasoning." Inf. Sci., 1975.

APPENDIX

(A)

Photographs from impact test lab

Lab photographs are shown in Figure APN-1 through APN-4.

(B)

Force vs. time plots of each impact test series

Force vs. time plots of each impact test are shown in Figure APN-5.

(C)

Additional data resource

Additional data resource are shown in Figure APN-6 through APN-8 and Table APN-1.

(D)

TEST program Fortran source code

The Fortran source code of the TEST program is attached at the end.

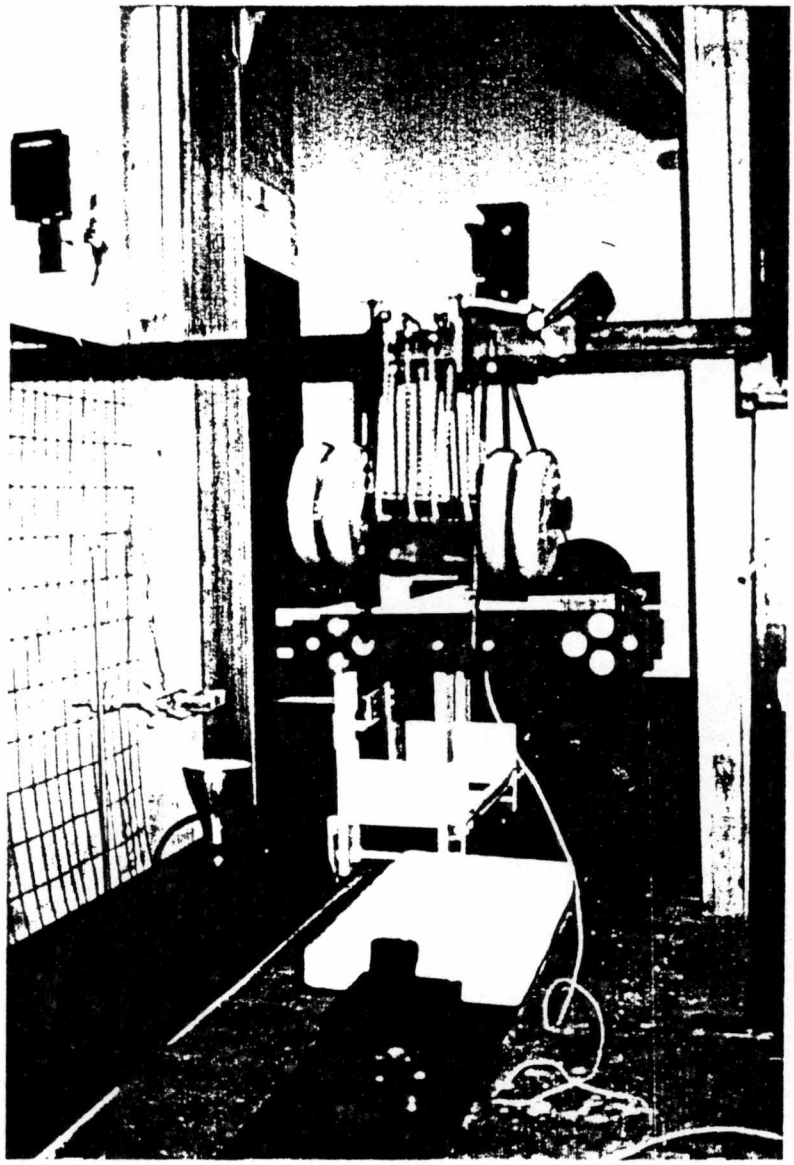
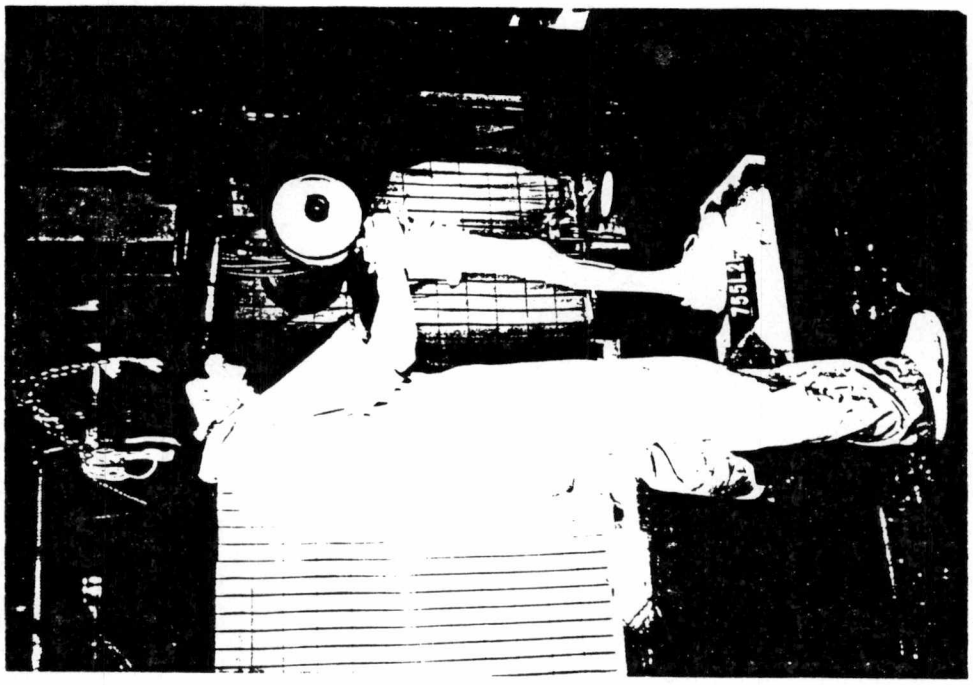
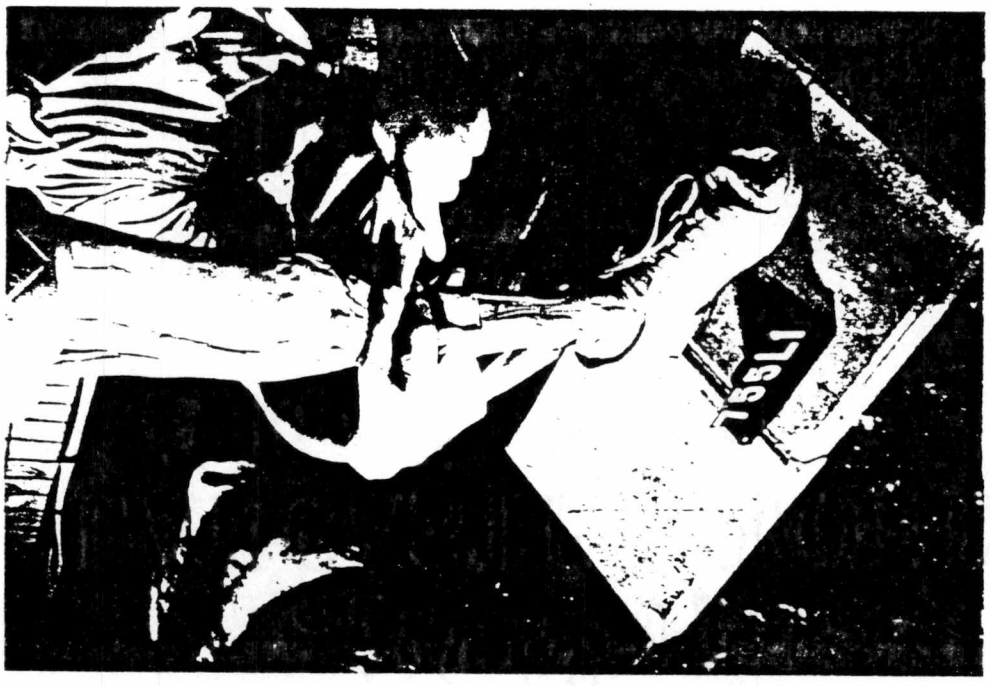


Figure APN-1.
Front view of the impact cart and the leg mounting device.

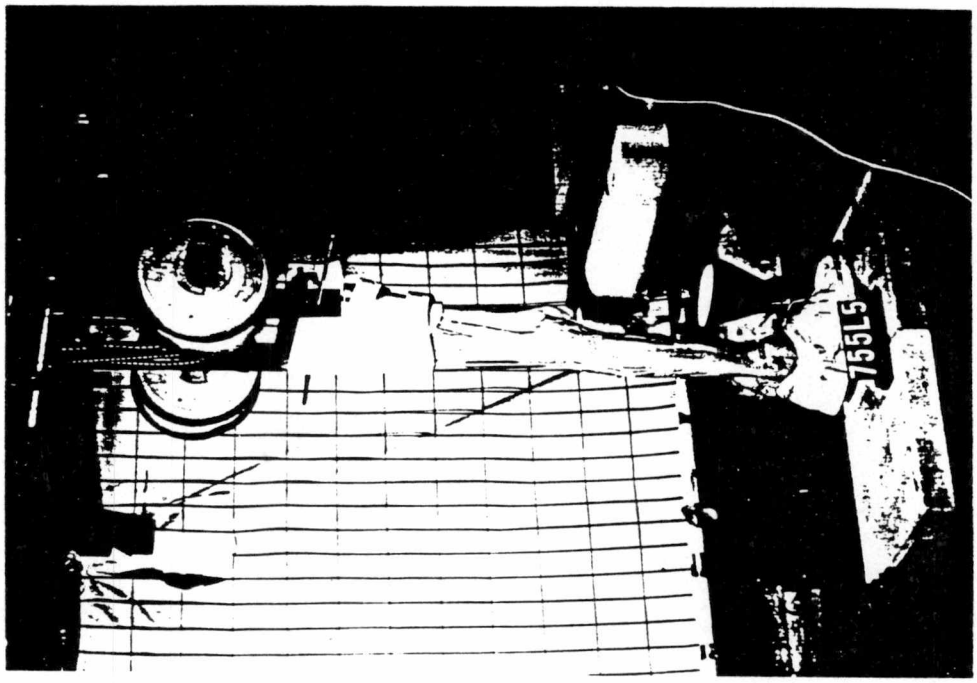


Balancing the leg specimen to keep the weight on top

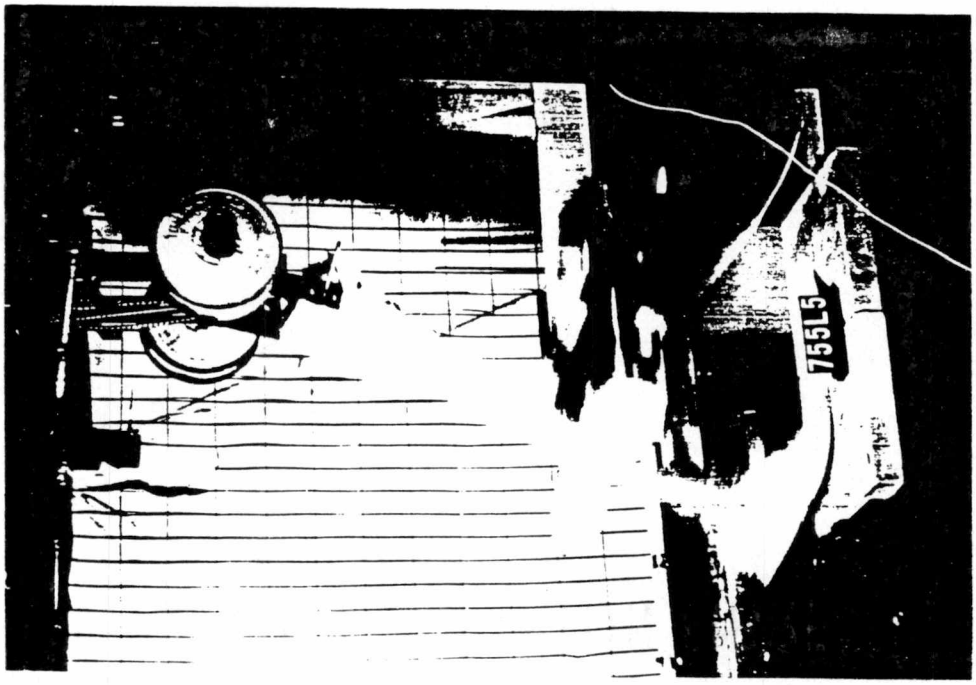


Checking the fracture generation on the bone under the skin

Figure APN-2.
Experimental setting and damage checking.



A photo snap just before the impact
(Specimen TL755L)



A photo snap during the impact
(Specimen TL755L)

Figure APN-3.

Snapshots of just before the impact and during the impact.

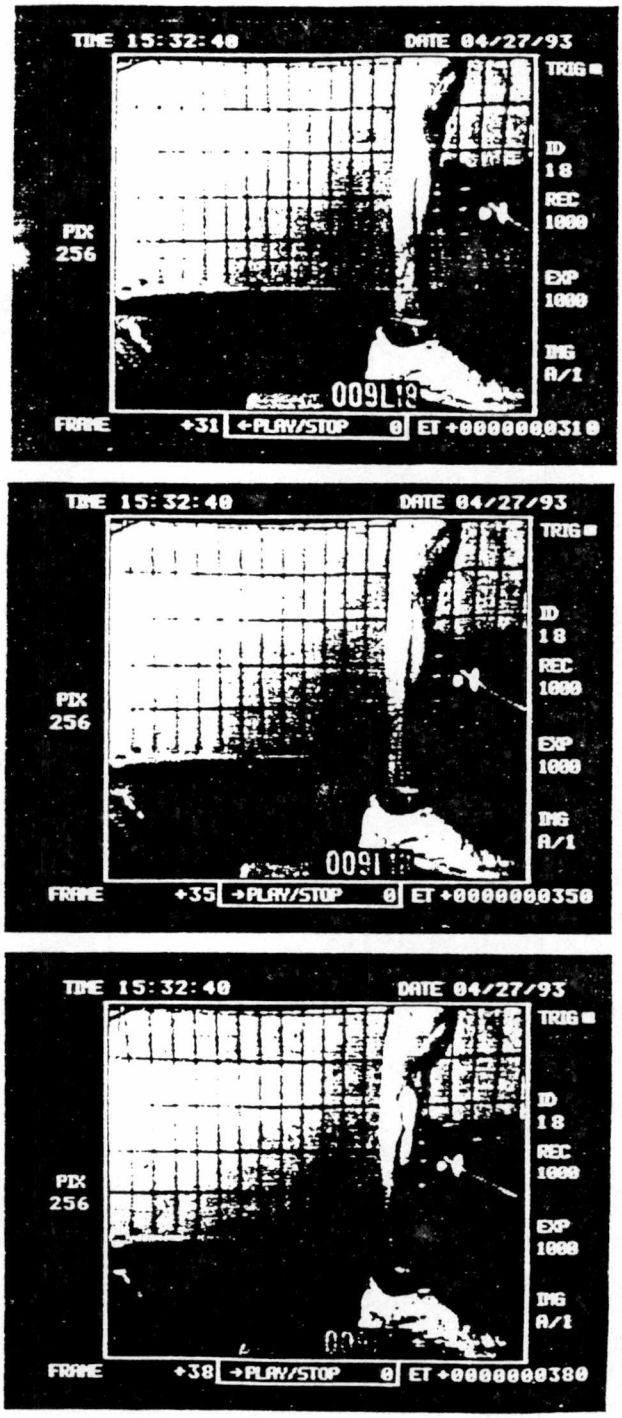


Figure APN-4.

Impact sequence filmed by the high-speed video camera.

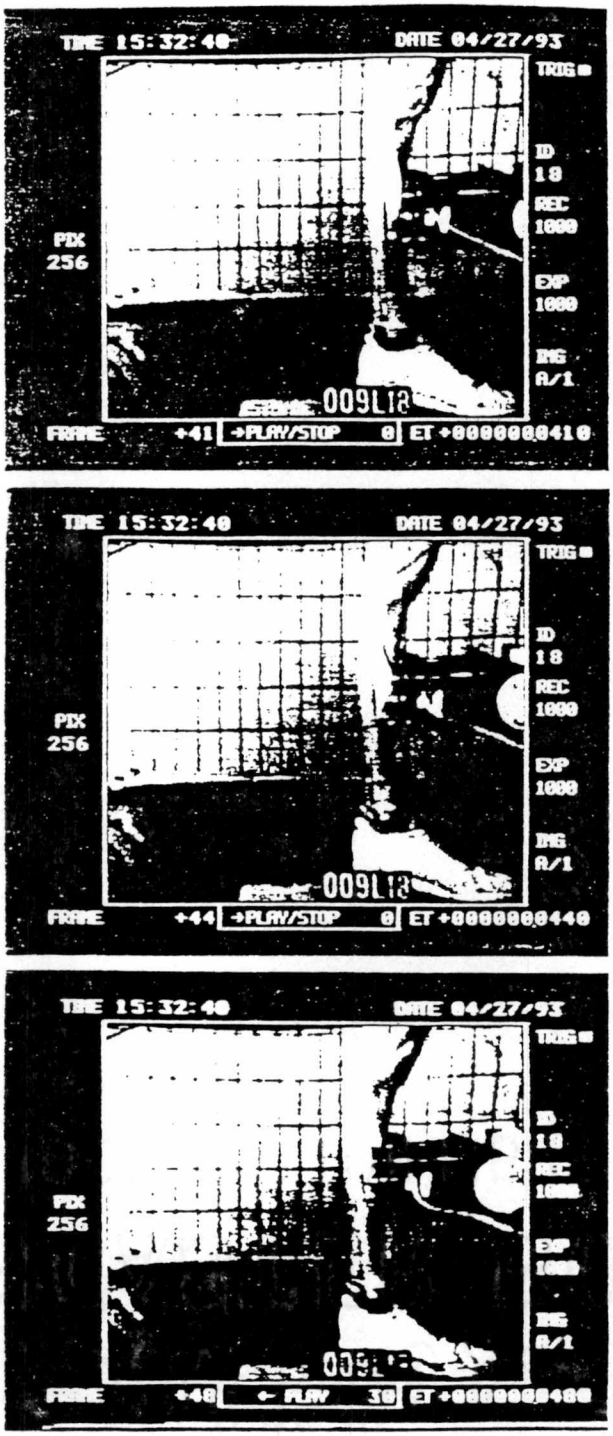


Figure APN-4. (continued)

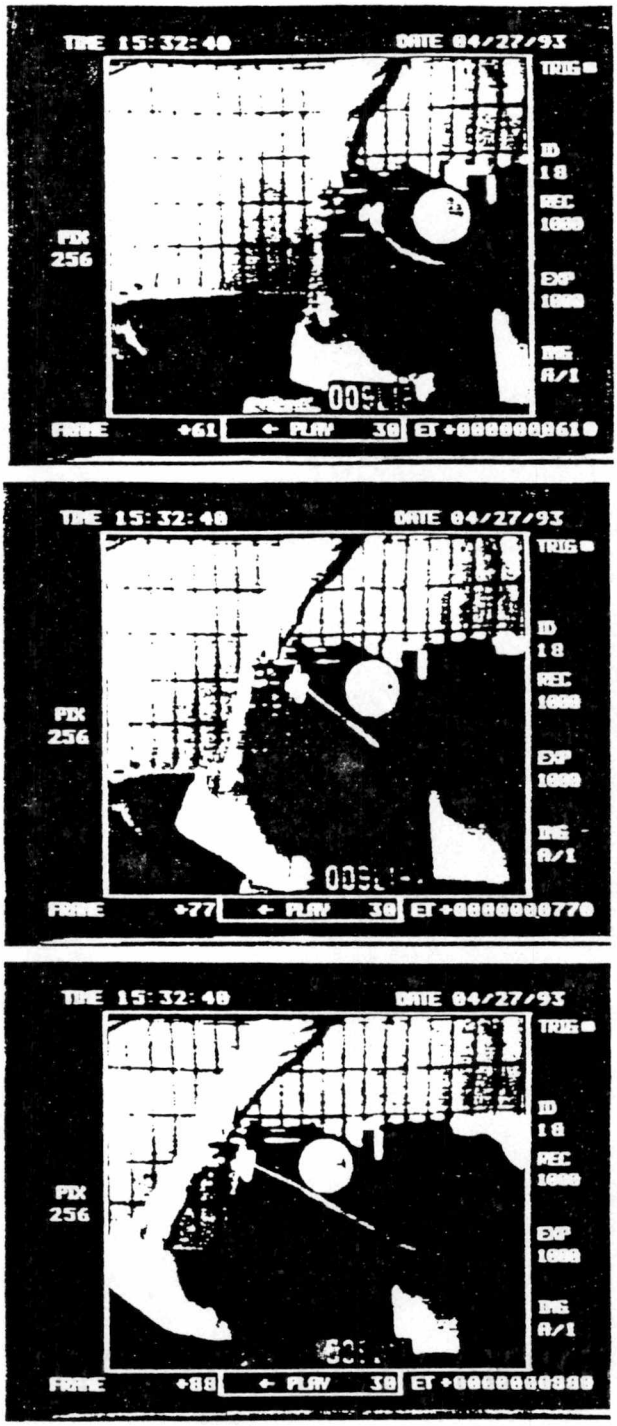


Figure APN-4. (continued)

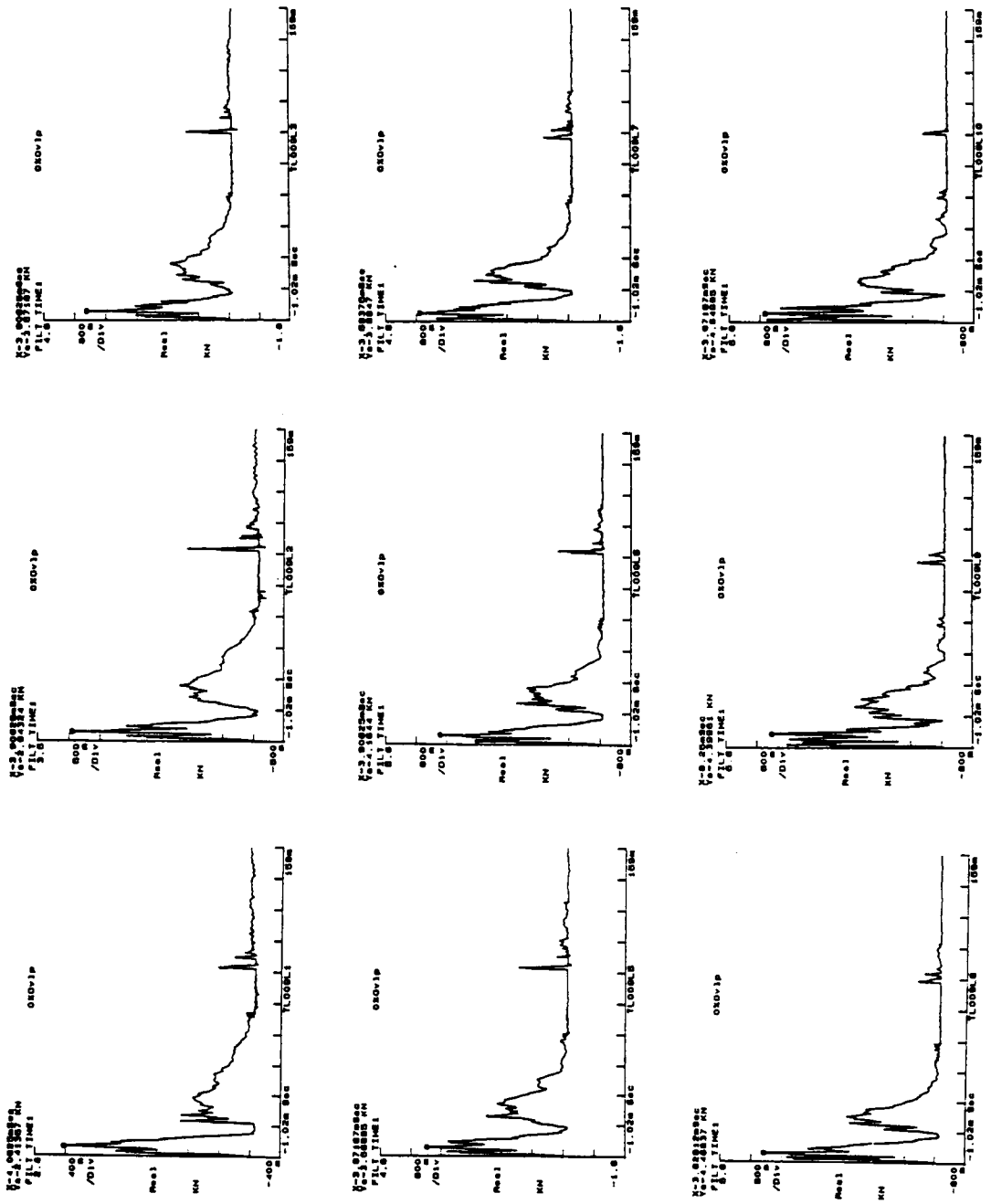


Figure APN-5.
Force vs. time plots
(TL009L1 through TL009L10)

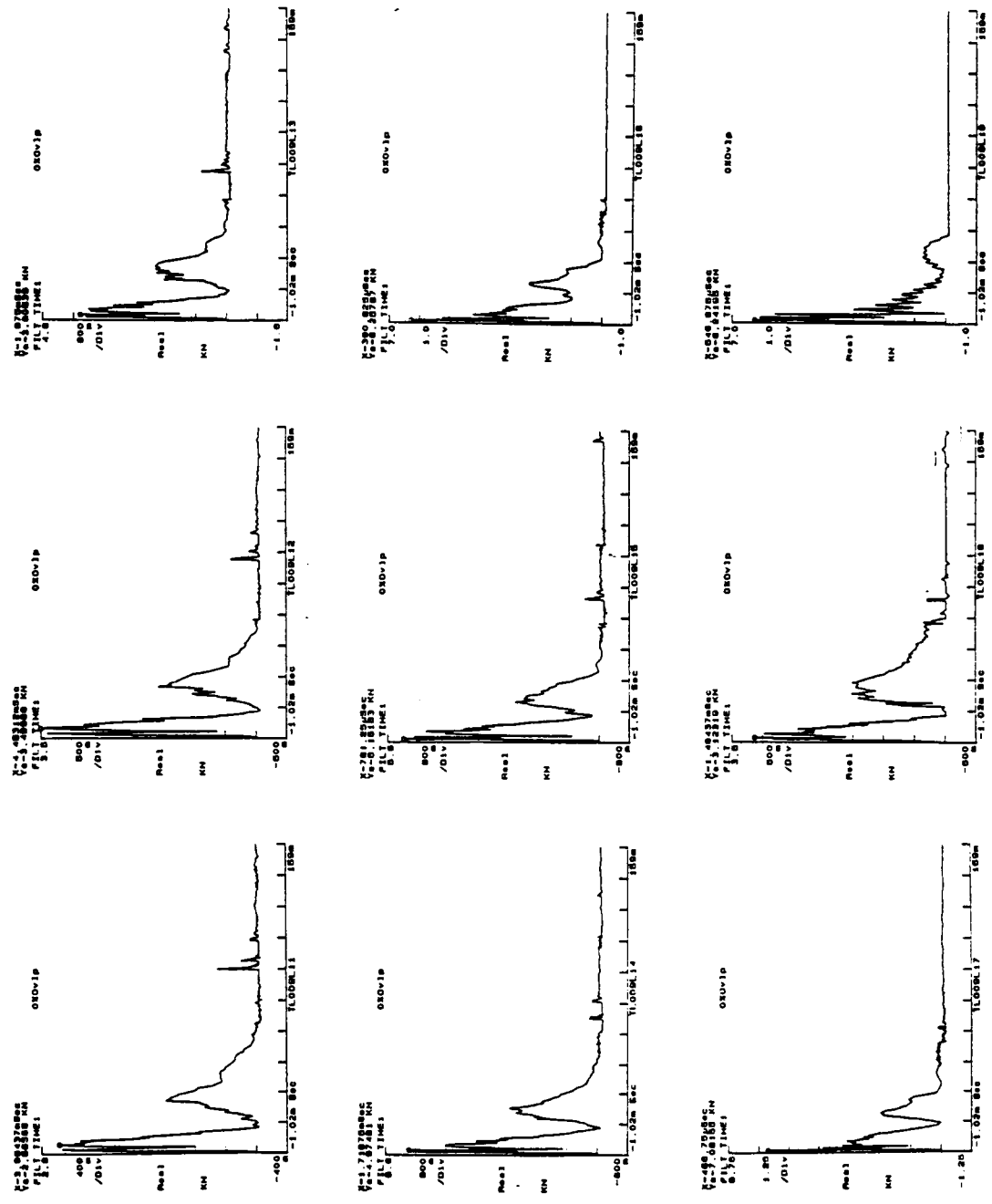


Figure APN-5. (continued)
(TL009L11 through TL009L19)

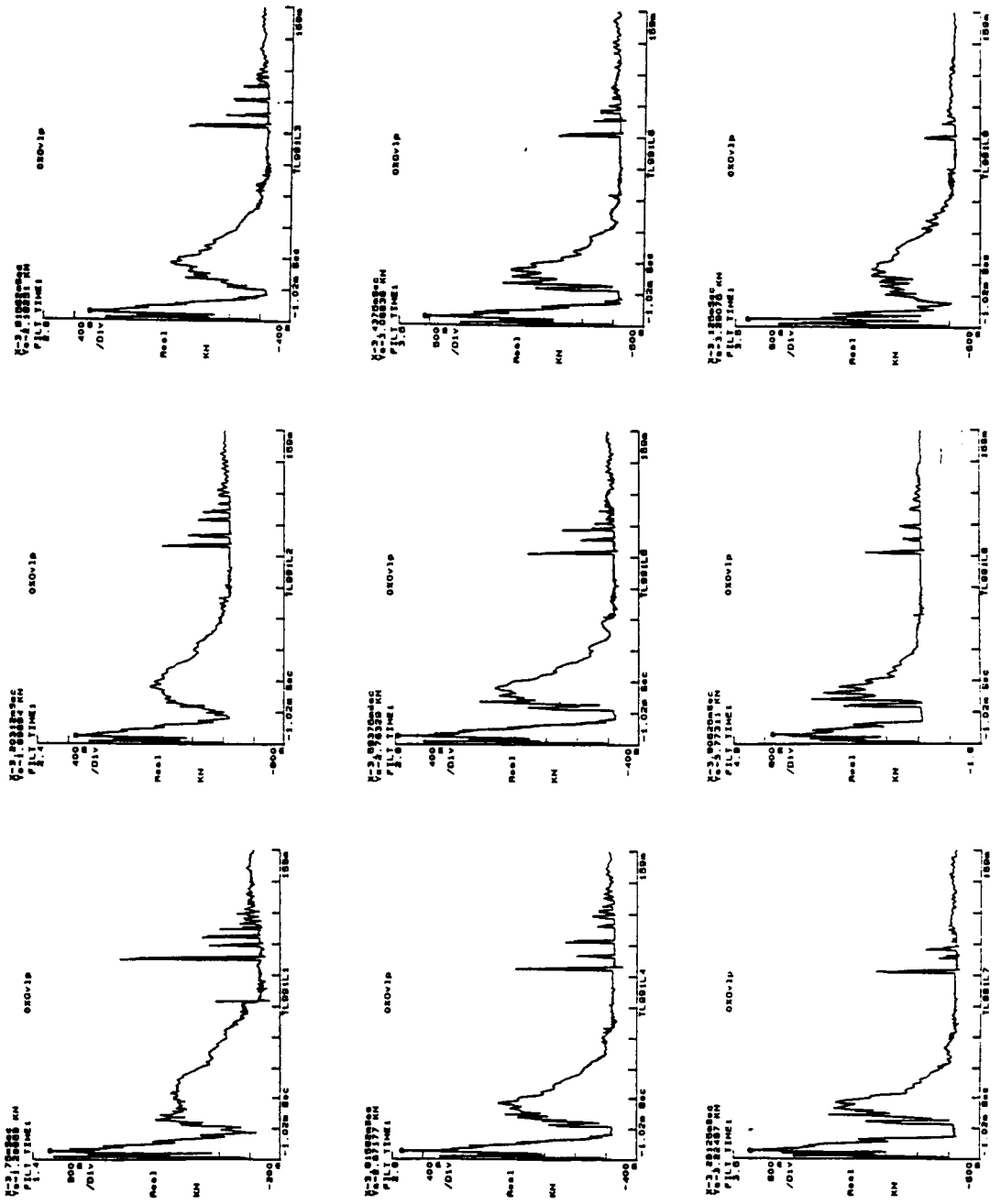


Figure APN-5. (continued)
(TL991L1 through TL991L9)

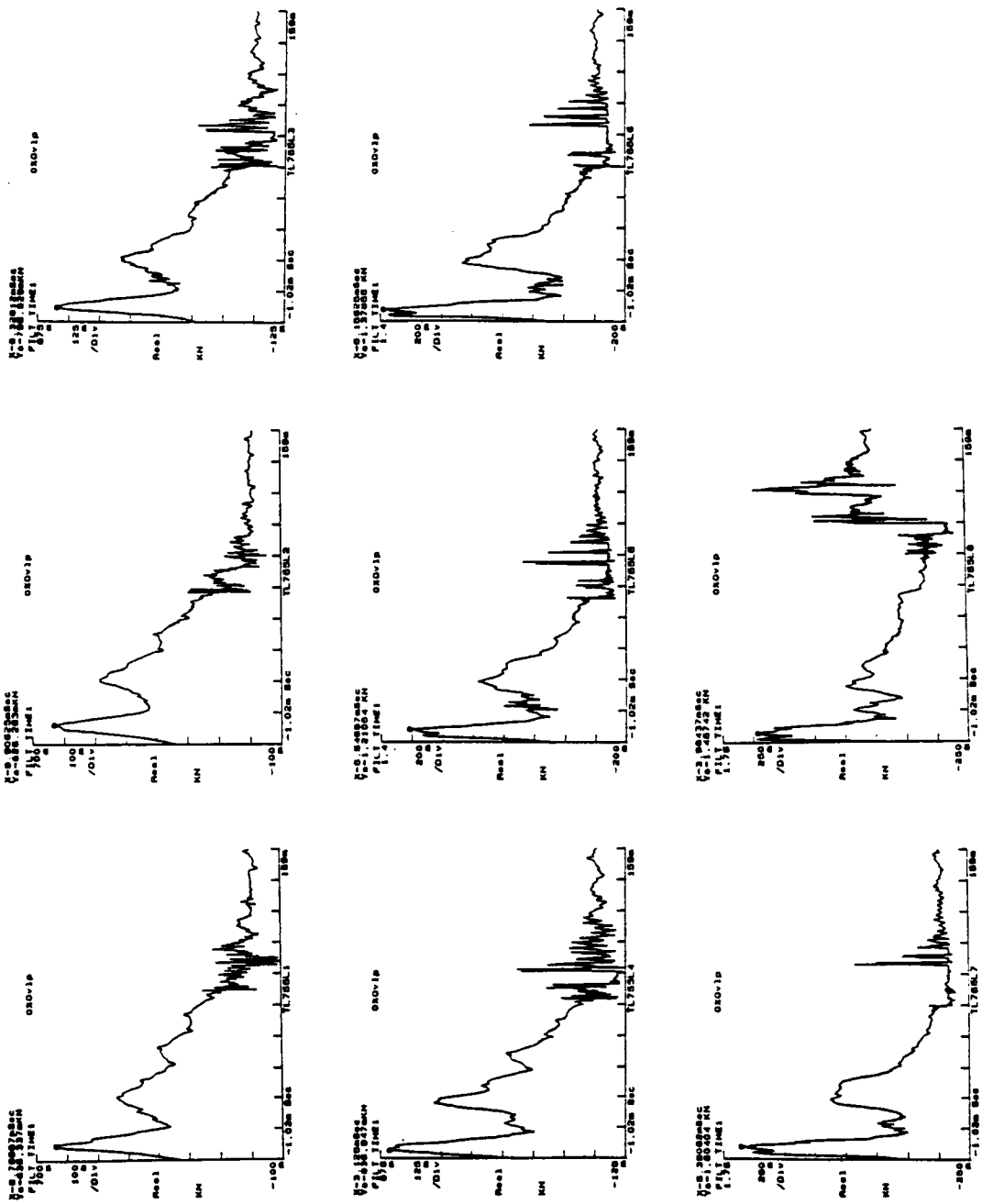


Figure APN-5. (continued)
(TL755L1 through TL755L8)

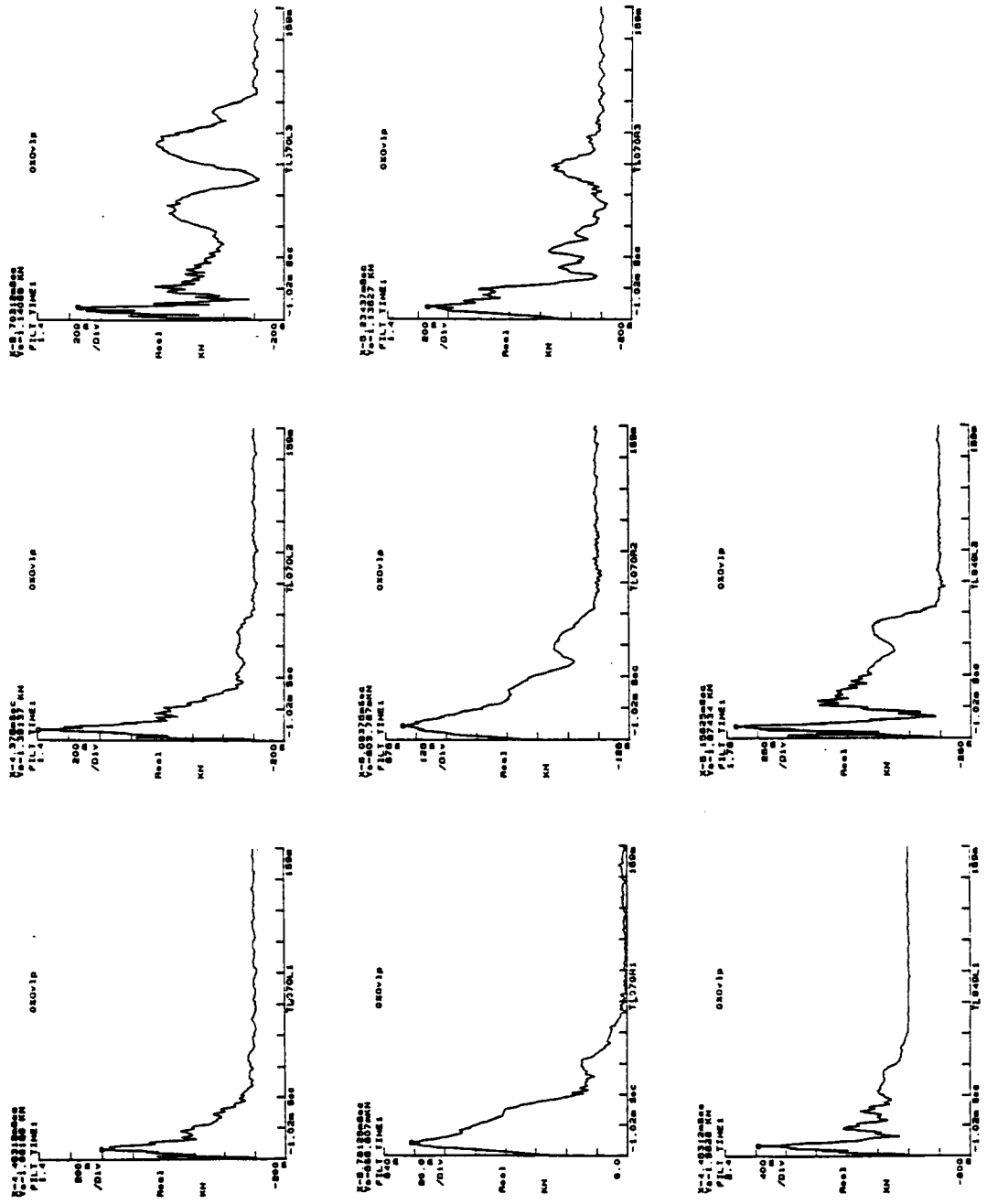


Figure APN-5. (continued)
(TL070L1 through TL070L3, TL070R1 through TL070R3, and TL949L1 through TL949L2)

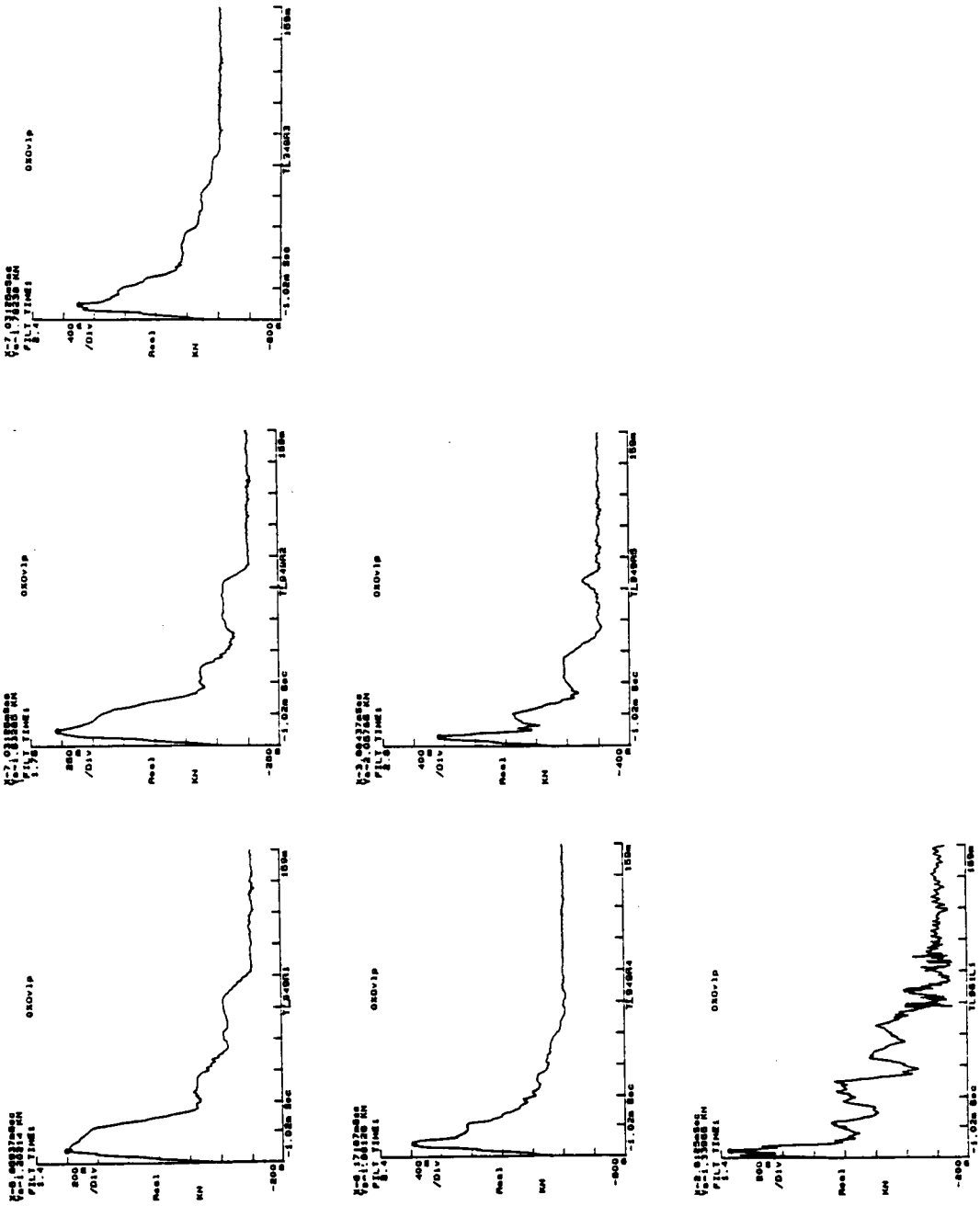
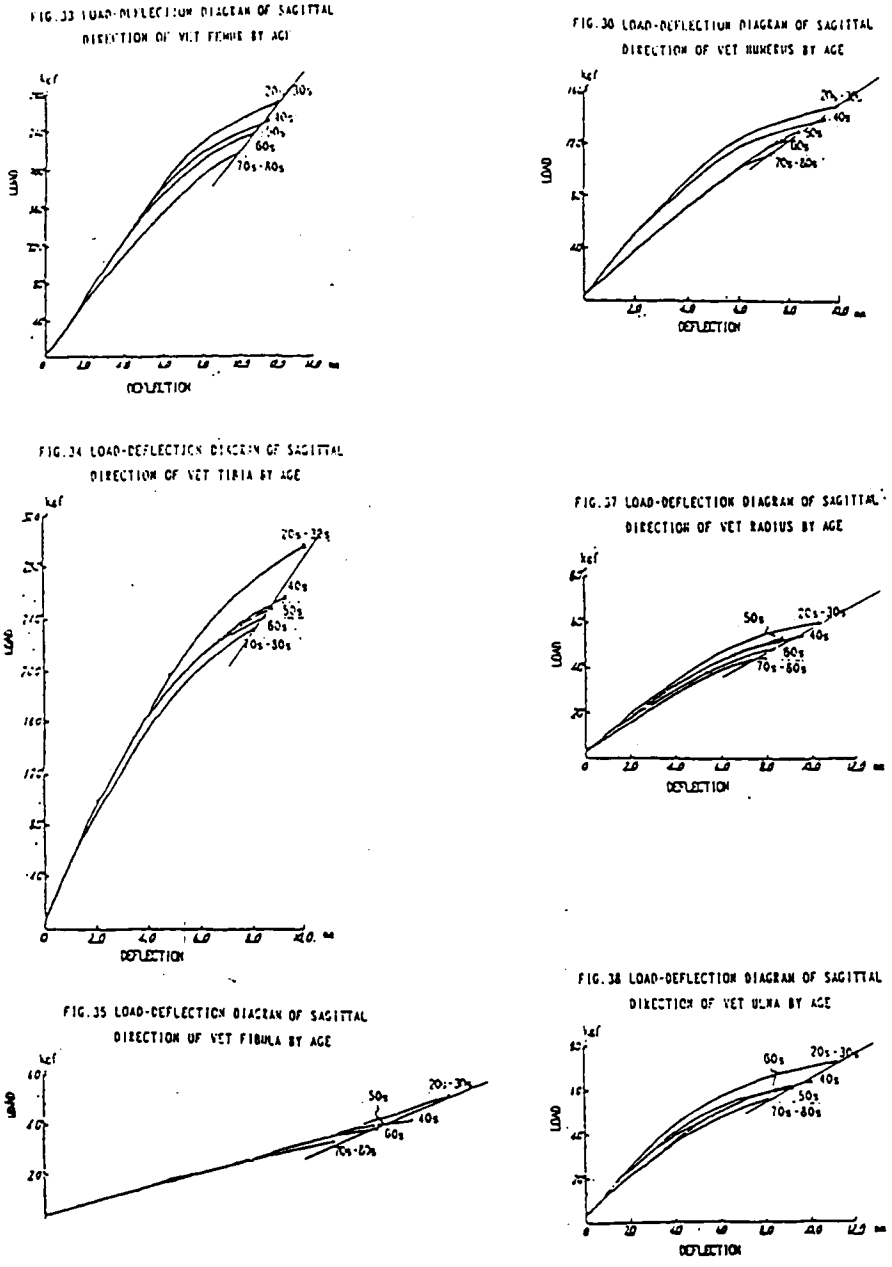


Figure APN-5. (continued)
(TL949R1 through TL949R5, and TL961L1)

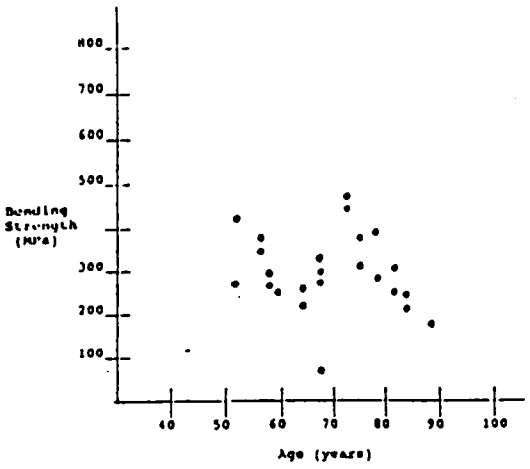


Clear linear correlations can be seen among the age group, the ultimate load and the ultimate deflection.

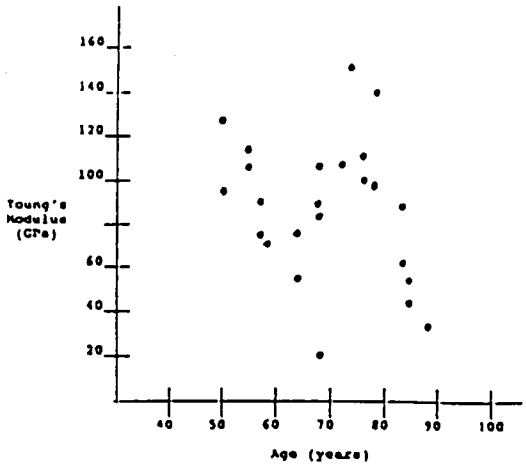
Figure APN-6.

Load vs. deflection of shaft bones.

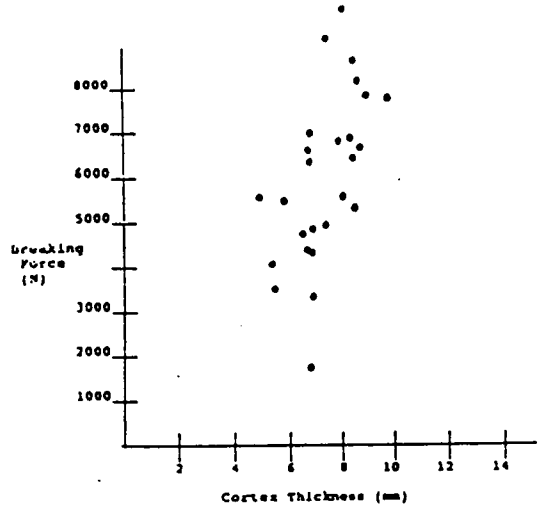
(Motishima, 1959)



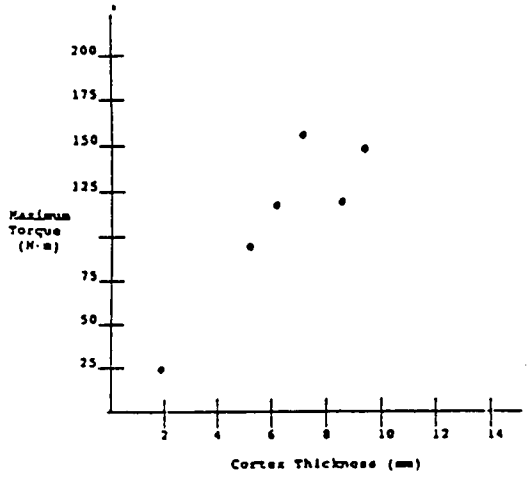
Plot of breaking strength vs. age for a-p impacted femur.



Plot Young's modulus vs. age for a-p impacted femur.



Plot of breaking force vs. cortex thickness for a-p impact on femur.



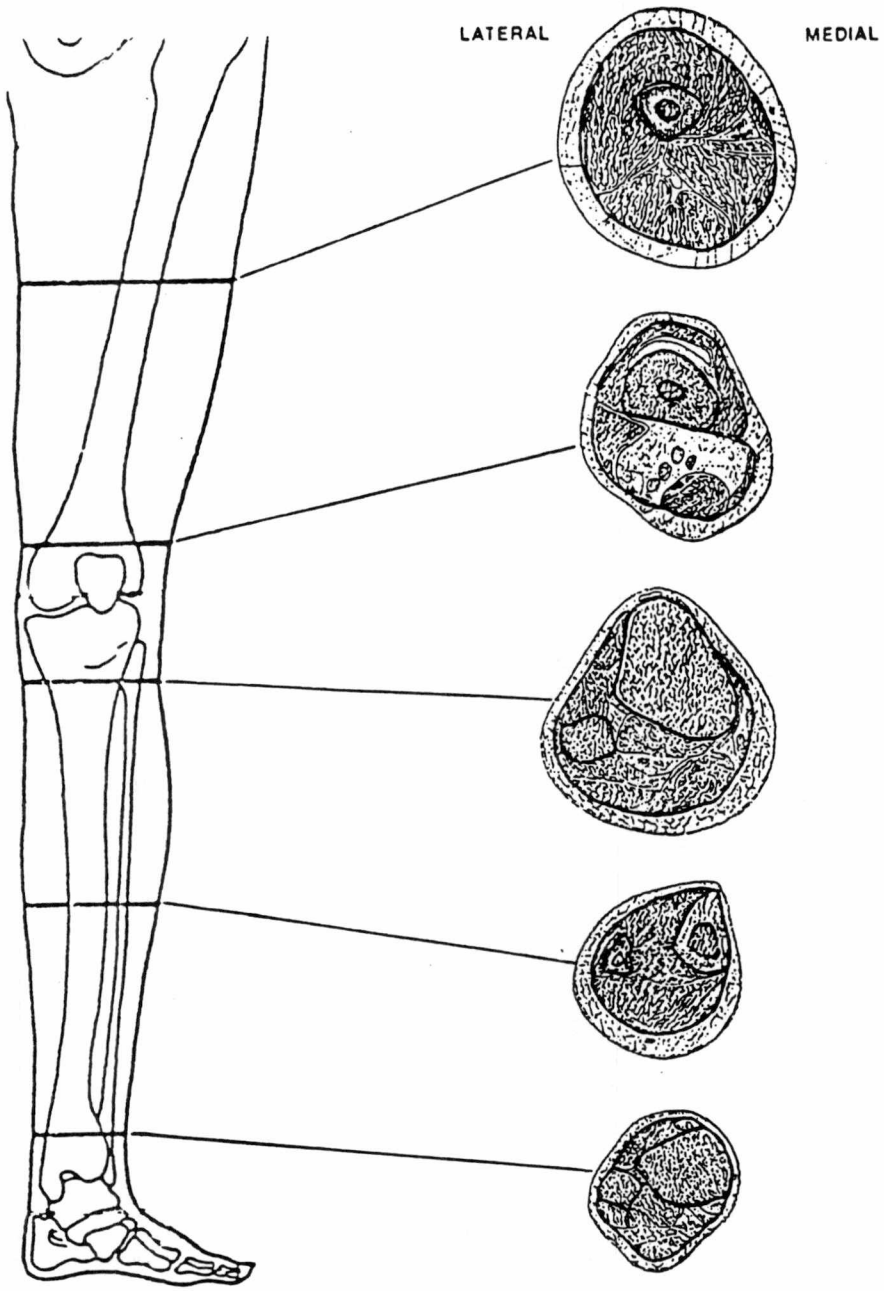
Plot of breaking torque vs. cortex thickness for femur loaded statically in torsion.

The fuzzy logic is appropriate to be used because the data points are scattered in some range.

Figure APN-7.

Distribution of bone fracture experiment data points.

(Tucker, 1991)



The change of muscle thickness effects to the impact force.

Figure APN-8.
The change of muscle thickness along the leg.

$$c_L = \sqrt{\frac{E}{\rho_0}} \quad \text{and} \quad c_T = \sqrt{\frac{G}{\rho_0}}$$

	Cast Iron	Carbon Steel	Brass	Copper	Lead	Alumi-nium	Glass
E N m^2	$114 . 10^9$	$204 . 10^9$	$93{\cdot}3 . 10^9$	$114 . 10^9$	$17{\cdot}6 . 10^9$	$69 . 10^9$	$55 . 10^9$
ρ_0 = kg/m^3	$0{\cdot}72 . 10^4$	$0{\cdot}775 . 10^4$	$0{\cdot}83 . 10^4$	$0{\cdot}887 . 10^4$	$1{\cdot}13 . 10^4$	$0{\cdot}266 . 10^4$	$0{\cdot}187 . 10^4$
$c_L = \sqrt{E/\rho_0}$ m s ($g \simeq 981$ m sec/sec)	3980	5150	3360	3690	1190	5100	5340
$c_T = \sqrt{G/\rho_0}$ m sec	2470	3230	2040	2290	700	3100	3260

Z = $\rho 0\, C$
Z = dynamic impedance
$\rho 0$ = density
C = speed of the impact wave (CT or CL)

CL = longitudinal wave speeed
CT = torsional wave speed

Table APN-1.

Dynamic impedance of various materials.

(Johnson, 1972)

```
c     PROGRAM TEST FUZZLE

c     Fuzzy inference routines were developed based on FUZZLE software
c     Rules and membership function design were done by Taisuke Akasaka
c     based on his series of experiments.

c     <<< This program does the following things. >>>

c 1.  Estimating the slope of the linear relationship between the impact
c     speed and the impact force from the distance between the pinned
c     point and the impact point, direction of the impact, and friction
c     condition.
c     The slope estimation can be done for two different pinned cases.
c     The first case is that a leg is pinned at the hip, and
c     the second case is that a leg is pinned at the knee.

c 2.  Computing the expected impact force from the impact speed and the
c     slope.
c     (Impact force = slope * impact speed within the linear range)

c 3.  Estimating the approximate maximum tolerable impact fracture force
c     for a leg from age, sex, and the mean cortex thickness.

c 4.  Estimating % fracture possibility from the difference between
c     the maximum tolerable impact force and the estimated impact force.

c     Program will ask input values step by step.
c     During the execution, results will be written in the output file.

          real radius, slope, frictn, direct, speed, age, sex, cortex
          real strng, force, diffrn, possib
          integer case, spring, ans
          character*30 fo
      write(*,*) '************************************************'
      write(*,*) '*                                              *'
      write(*,*) '*    FUZZY BONE FRACTURE PREDICTION PROGRAM    *'
      write(*,*) '*                                              *'
      write(*,*) '*          Designed by  Taisuke Akasaka        *'
      write(*,*) '*                July 17, 1993                 *'
      write(*,*) '*                                              *'
      write(*,*) '************************************************'
      write(*,*) ' '
      write(*,*) 'This program was written only to demonstrate the'
      write(*,*) 'effectiveness (easy application, modification'
      write(*,*) 'and expansibility) of the fuzzy logic to the'
      write(*,*) 'impact bone fracture prediction problems.'
      write(*,*) 'The validity of the output only be hold within'
      write(*,*) 'the indicated input variable range and points.'
      write(*,*) 'Due to the size of data which this program based on,'
      write(*,*) 'translation the output requires some caution.'
      write(*,*) ' '
c     Program will ask input values step by step.
c     During the execution, results will be written in the output file.
5     print *, 'Enter the output fine name.'
      read 10, fo
10    format (A)
      open(200, file=fo, status='UNKNOWN')
      write(*,*) 'Is the leg pinned at the hip or the knee ?'
      write(*,*) ' 1 = CASE1: pinned at the hip'
      write(*,*) ' 2 = CASE2: pinned at the knee'
      Read(*,*) case
```

```
write(*,*) 'Does the bumper has air springs ?'
write(*,*) '1 = yes : 0 = no'
write(*,*) 'If the bumper has no shock absorption capability,'
write(*,*) 'the linear range of impact speed vs impact force is'
write(*,*) 'cut off at the speed 7.7m/s. Just after that speed,'
write(*,*) 'the impact force will jump up like a sky rocket.'
Read(*,*) spring
write(*,*) 'Is there friction on the foot ?'
write(*,*) '1.0 = friction (by body weight) : -1.0 = No friction'
write(*,*) 'Numbers between -1.0 to 1.0 are all valid.'
write(*,*) 'For example, 0.0 can mean a half of the max friction.'
write(*,*) 'However, the effect of the parameter between'
write(*,*) '-1.0 and 1.0 has not been fine tuned yet'
write(*,*) 'due to the data shortage.'
Read(*,'(f16.8)') frictn
write(*,*) 'Age of the person ? (years old)'
write(*,*) 'The value must be a real number'
write(*,*) 'between 30.1 and 94.9.'
Read(*,'(f16.8)') age
write(*,*) 'What is the gender of the leg ?'
write(*,*) '1.0 = male : -1.0 = female'
write(*,*) 'Here, gender means masculinity or femininity.'
write(*,*) 'Real numbers between -1.0 and 1.0 are valid.'
Read(*,'(f16.8)') sex
write(*,*) 'What is the mean cortex at the point of impact ? (mm)'
write(*,*) 'The value must be a real number between 4.6 and 7.4.'
Read(*,'(f16.8)') cortex
write(*,*) 'Direction of impact ?'
write(*,*) '1.0 = A-P impact : -1.0 = P-A impact'
write(*,*) 'P-A option is only available for CASE2.'
write(*,*) 'No P-A impact data was collected for CASE1.'
write(*,*) 'Real numbers between -1.0 and 1.0 are all valid.'
write(*,*) 'This parameter reflects the reduction of'
write(*,*) 'the impact force due to the muscle thickness.'
write(*,*) 'Thus, the value 0.0 can mean the side impact.'
write(*,*) 'However, the effect of the parameter'
write(*,*) 'between -1.0 and 1.0 has not been fine tuned'
write(*,*) 'yet due to the data shortage.'
Read(*,'(f16.8)') direct
write(*,*) 'What is the distance between the pinned point and the'
write(*,*) 'impact point ? (cm)'
write(*,*) 'The value must be a real number between 49.1 and 55.4'
write(*,*) 'for CASE1 and between 10.1 and 32.9 for CASE2.'
Read(*,'(f16.8)')  radius
write(*,*) 'What is the speed of impact ? (m/s)'
write(*,*) 'A real number between 0.0 to 10.0'
Read(*,'(f16.8)')  speed
if (case .eq. 1) then
call test1(radius, slope)
else if (case .eq. 2) then
call test2 (radius, direct, frictn, slope)
end if

call test3 (age, cortex, sex, strng)
force = slope*speed
diffrn = force-strng

call test4 (diffrn, possib)
write(*,*) 'pinned point to impact point (cm) =',radius
write(200,*) 'pinned point to impact point (cm) =',radius
write(*,*) 'slope (Newton*sec/m) =',slope
```

```
      write(200,*) 'slope (Newton*sec/m) =',slope
      write(*,*) 'impact speed (m/s) =',speed
      write(200,*) 'impact speed (m/s) =',speed
      write(*,*) ' '
      write(200,*) ' '
      write(*,*) 'age (years old) =',age
      write(200,*) 'age (years old) =',age
      write(*,*) 'sex (1=male: -1=female) =',sex
      write(200,*) 'sex (1=male: -1=female) =',sex
      write(*,*) 'mean cortex thickness (mm) =',cortex
      write(200,*) 'mean cortex thickness (mm) =',cortex
      write(*,*) 'maximum tolerable impact force (Newton) = ',strng
      write(200,*) 'maximum tolerable impact force (Newton) = ',strng
      write(*,*) ' '
      write(200,*) ' '

      if (spring .eq. 0 .and. speed .gt. 7.7) then
      write(*,*) 'estimated impact force (Newton) = over 6500'
      write(200,*) 'estimated impact force (Newton) = over 6500N'
      possib=100.0

      else if (speed .le. 7.7 .or. spring .eq. 1) then
      write(*,*) 'estimated impact force (Newton) =',force
      write(200,*) 'estimated impact force (Newton) =',force
      write(*,*) 'difference in force (Newton) =',diffrn
      write(200,*) 'difference in force (Newton) =',diffrn
      end if
      write(*,*) 'fracture possibility (%) =',possib
      write(200,*) 'fracture possibility =',possib
      write(*,*) 'The output was written in the file ',fo
50    write(*,*) 'Repeat ? (yes=1: no=0)'
      read(*,*) ans
      if (ans .eq. 1) then
      go to 5
      else if (ans .eq. 0) then
      goto 100
      end if
100   stop
      end

c---------------------------------------------
            subroutine  test1 (radius, slope )
c---------------------------------------------
         real entry,exit
         real ymu( 5,50)
         real mmtrx( 5,50)
         real omtrx( 5,4)
         real uz( 5   )
         real r( 5   )
         real area( 5   )
         real radius
         real slope
c-----------------------------
       mmtrx( 1, 1)=     49.00000000
       mmtrx( 1, 2)=     49.00000000
       mmtrx( 1, 3)=     51.48333000
       mmtrx( 1, 4)=     52.56667000
       mmtrx( 2, 1)=     51.78333000
       mmtrx( 2, 2)=     52.44167000
       mmtrx( 2, 3)=     53.10000000
       mmtrx( 2, 4)=       .00000000
```

```
      mmtrx( 3, 1)=     52.41667000
      mmtrx( 3, 2)=     52.95000000
      mmtrx( 3, 3)=     53.48333000
      mmtrx( 3, 4)=       .00000000
      mmtrx( 4, 1)=     52.80000000
      mmtrx( 4, 2)=     53.48335000
      mmtrx( 4, 3)=     54.11667000
      mmtrx( 4, 4)=       .00000000
      mmtrx( 5, 1)=     53.33333000
      mmtrx( 5, 2)=     54.11667000
      mmtrx( 5, 3)=     55.50000000
      mmtrx( 5, 4)=     55.50000000
c-----------------------------
      omtrx( 1, 1)=    400.00000000
      omtrx( 1, 2)=    440.00000000
      omtrx( 1, 3)=    480.00000000
      omtrx( 1, 4)=    480.00000000
      omtrx( 2, 1)=    360.00000000
      omtrx( 2, 2)=    400.00000000
      omtrx( 2, 3)=    440.00000000
      omtrx( 2, 4)=       .00000000
      omtrx( 3, 1)=    320.00000000
      omtrx( 3, 2)=    360.00000000
      omtrx( 3, 3)=    400.00000000
      omtrx( 3, 4)=       .00000000
      omtrx( 4, 1)=    280.00000000
      omtrx( 4, 2)=    320.00000000
      omtrx( 4, 3)=    360.00000000
      omtrx( 4, 4)=       .00000000
      omtrx( 5, 1)=    240.00000000
      omtrx( 5, 2)=    240.00000000
      omtrx( 5, 3)=    280.00000000
      omtrx( 5, 4)=    320.00000000
c-----------------------------
        entry=radius
         icol= 1
         irow= 1
          exit=0.0
         call shape2test1 (mmtrx,icol,irow,entry,exit)
         ymu( 1, 1)=exit
c-----------------------------
        entry=radius
         icol= 2
         irow= 1
         exit=0.0
         call shape5test1 (mmtrx,icol,irow,entry,exit)
         ymu( 2, 1)=exit
c-----------------------------
        entry=radius
         icol= 3
         irow= 1
         exit=0.0
         call shape5test1 (mmtrx,icol,irow,entry,exit)
         ymu( 3, 1)=exit
c-----------------------------
        entry=radius
         icol= 4
         irow= 1
         exit=0.0
         call shape5test1 (mmtrx,icol,irow,entry,exit)
         ymu( 4, 1)=exit
```

```
c-----------------------------
         entry=radius
          icol= 5
          irow= 1
          exit=0.0
          call shape3test1 (mmtrx,icol,irow,entry,exit)
          ymu( 5, 1)=exit
c-----------------------------
        uz( 1)=ymu( 1,1)
        uz( 2)=ymu( 2,1)
        uz( 3)=ymu( 3,1)
        uz( 4)=ymu( 4,1)
        uz( 5)=ymu( 5,1)
c-----------------------------
c  -> Raw Output
        j=  1
            shot=uz(j)
            irow=j
        call cut4test1 (cmtrx,irow,shot,result,weight)
            r(j)=result
            area(j)=weight
c  -> Raw Output
        j=  2
            shot=uz(j)
            irow=j
        call cut3test1 (cmtrx,irow,shot,result,weight)
            r(j)=result
            area(j)=weight
c  -> Raw Output
        j=  3
            shot=uz(j)
            irow=j
        call cut3test1 (cmtrx,irow,shot,result,weight)
            r(j)=result
            area(j)=weight
c  -> Raw Output
        j=  4
            shot=uz(j)
            irow=j
        call cut3test1 (cmtrx,irow,shot,result,weight)
            r(j)=result
            area(j)=weight
c-------------------
c  -> Raw Output
        j=  5
            shot=uz(j)
            irow=j
        call cut4test1 (cmtrx,irow,shot,result,weight)
            r(j)=result
            area(j)=weight
c-------------------
c-- output fused --
c-------------------
        aall=
     + area( 1)+
     + area( 2)+
     + area( 3)+
     + area( 4)+
     + area( 5)+
     + 0.0
        aalu=
```

```
     + area( 1)*r( 1)+
     + area( 2)*r( 2)+
     + area( 3)*r( 3)+
     + area( 4)*r( 4)+
     + area( 5)*r( 5)+
     + 0.0
        slope =0.0
        if (aall.ne.0.0) then
        slope =aalu/aall
        end if
        return
        end
c=====================
       subroutine shape2test1 (mmtrx,icol,irow,entry,exit)
        real mmtrx( 5,50),entry,exit
          if ((entry.gt.mmtrx(icol,irow+2)).and.
     &      (entry.lt.mmtrx(icol,irow+3))) then
               exit=(mmtrx(icol,irow+3)-entry)/
     &  (mmtrx(icol,irow+3)-mmtrx(icol,irow+2))
          end if
          if ((entry.gt.mmtrx(icol,irow+1)).and.
     &      (entry.le.mmtrx(icol,irow+2))) then
           exit=1.0
          end if
              return
                 end
c=====================
       subroutine shape3test1 (mmtrx,icol,irow,entry,exit)
        real mmtrx( 5,50),entry,exit
          if ((entry.lt.mmtrx(icol,irow+1)).and.
     &        (entry.gt.mmtrx(icol,irow))) then
                  exit=(entry-mmtrx(icol,irow))/
     &    (mmtrx(icol,irow+1)-mmtrx(icol,irow))
          end if
          if ((entry.ge.mmtrx(icol,irow+1)).and.
     &      (entry.lt.mmtrx(icol,irow+2))) then
           exit=1.0
          end if
              return
                 end
c=====================
       subroutine shape5test1 (mmtrx,icol,irow,entry,exit)
        real mmtrx( 5,50),entry,exit
          if ((entry.le.mmtrx(icol,irow+1)).and.
     &        (entry.gt.mmtrx(icol,irow))) then
                  exit=(entry-mmtrx(icol,irow))/
     &    (mmtrx(icol,irow+1)-mmtrx(icol,irow))
          end if
          if ((entry.ge.mmtrx(icol,irow+1)).and.
     &      (entry.lt.mmtrx(icol,irow+2))) then
               exit=(mmtrx(icol,irow+2)-entry)/
     &  (mmtrx(icol,irow+2)-mmtrx(icol,irow+1))
          end if
              return
                 end
c-----------------------------------------------
       subroutine cut4test1 (omtrx,irow,shot,result,weight)
        real omtrx( 5,50)
           x2p=shot*(omtrx(irow,2)-omtrx(irow,1))+omtrx(irow,1)
           x3p=omtrx(irow,4)-shot*(omtrx(irow,4)-omtrx(irow,3))
           a1=shot*0.5*(x2p-omtrx(irow,1))
```

```
            a2=shot*(x3p-x2p)
            a3=shot*0.5*(omtrx(irow,4)-x3p)
            if(shot.ne.0.0) then
            result=0.5*(x2p+x3p)+(a3-a1)*0.5/shot
            if(a1.gt.a2+a3) then
            result=omtrx(irow,1)+(x2p-omtrx(irow,1))*(a2+a3)/a1
            end if
            if(a3.gt.a2+a1) then
            result=x3p+(omtrx(irow,4)-x3p)*(a1+a2)/a3
            end if
            end if
            weight=a1+a2+a3
             return
             end
c-----------------------------------------------
       subroutine cut3test1 (omtrx,irow,shot,result,weight)
        real omtrx( 5,50)
            x2p=shot*(omtrx(irow,2)-omtrx(irow,1))+omtrx(irow,1)
            x3p=omtrx(irow,3)-shot*(omtrx(irow,3)-omtrx(irow,2))
            a1=shot*0.5*(x2p-omtrx(irow,1))
            a2=shot*(x3p-x2p)
            a3=shot*0.5*(omtrx(irow,3)-x3p)
            if(shot.ne.0.0) then
            result=0.5*(x2p+x3p)+(a3-a1)*0.5/shot
            if(a1.gt.a2+a3) then
            result=omtrx(irow,1)+(x2p-omtrx(irow,1))*(a2+a3)/a1
            end if
            if(a3.gt.a2+a1) then
            result=x3p+(omtrx(irow,3)-x3p)*(a1+a2)/a3
            end if
            end if
            weight=a1+a2+a3
             return
             end

c-----------------------------------------
        subroutine  test2 (radius, direct, frictn, slope )
c-----------------------------------------
          real entry,exit
          real ymu( 9,50)
          real mmtrx( 9,50)
          real omtrx( 9,4)
          real uz( 9   )
          real r( 9   )
          real area( 9   )
          real radius
          real direct
          real frictn
          real slope
c---------------------------
       mmtrx( 1, 1)=     10.00000000
       mmtrx( 1, 2)=     10.00000000
       mmtrx( 1, 3)=     13.83333000
       mmtrx( 1, 4)=     17.66667000
       mmtrx( 2, 1)=     13.83333000
       mmtrx( 2, 2)=     17.66667000
       mmtrx( 2, 3)=     21.50000000
       mmtrx( 2, 4)=       .00000000
       mmtrx( 3, 1)=     17.66667000
       mmtrx( 3, 2)=     21.50000000
       mmtrx( 3, 3)=     25.33333000
```

```
      mmtrx( 3, 4)=       .00000000
      mmtrx( 4, 1)=     21.50000000
      mmtrx( 4, 2)=     25.33333000
      mmtrx( 4, 3)=     29.16667000
      mmtrx( 4, 4)=       .00000000
      mmtrx( 5, 1)=     25.33333000
      mmtrx( 5, 2)=     29.16667000
      mmtrx( 5, 3)=     33.00000000
      mmtrx( 5, 4)=     33.00000000
      mmtrx( 6, 1)=      -.66666670
      mmtrx( 6, 2)=       .66666660
      mmtrx( 6, 3)=      2.00000000
      mmtrx( 6, 4)=      2.00000000
      mmtrx( 6, 5)=      -.66666670
      mmtrx( 6, 6)=       .66666660
      mmtrx( 6, 7)=      2.00000000
      mmtrx( 6, 8)=      2.00000000
      mmtrx( 7, 1)=     -2.00000000
      mmtrx( 7, 2)=     -2.00000000
      mmtrx( 7, 3)=      -.66666660
      mmtrx( 7, 4)=       .66666670
      mmtrx( 7, 5)=      -.66666670
      mmtrx( 7, 6)=       .66666660
      mmtrx( 7, 7)=      2.00000000
      mmtrx( 7, 8)=      2.00000000
      mmtrx( 8, 1)=      -.66666670
      mmtrx( 8, 2)=       .66666660
      mmtrx( 8, 3)=      2.00000000
      mmtrx( 8, 4)=      2.00000000
      mmtrx( 8, 5)=     -2.00000000
      mmtrx( 8, 6)=     -2.00000000
      mmtrx( 8, 7)=      -.66666660
      mmtrx( 8, 8)=       .66666670
      mmtrx( 9, 1)=     -2.00000000
      mmtrx( 9, 2)=     -2.00000000
      mmtrx( 9, 3)=      -.66666660
      mmtrx( 9, 4)=       .66666670
      mmtrx( 9, 5)=     -2.00000000
      mmtrx( 9, 6)=     -2.00000000
      mmtrx( 9, 7)=      -.66666660
      mmtrx( 9, 8)=       .66666670
c-----------------------------
      cmtrx( 1, 1)=    460.00000000
      cmtrx( 1, 2)=    540.00000000
      cmtrx( 1, 3)=    630.00000000
      cmtrx( 1, 4)=    630.00000000
      cmtrx( 2, 1)=    385.00000000
      cmtrx( 2, 2)=    460.00000000
      cmtrx( 2, 3)=    535.00000000
      cmtrx( 2, 4)=       .00000000
      cmtrx( 3, 1)=    300.00000000
      cmtrx( 3, 2)=    370.00000000
      cmtrx( 3, 3)=    440.00000000
      cmtrx( 3, 4)=       .00000000
      cmtrx( 4, 1)=    240.00000000
      cmtrx( 4, 2)=    300.00000000
      cmtrx( 4, 3)=    360.00000000
      cmtrx( 4, 4)=       .00000000
      cmtrx( 5, 1)=    150.00000000
      cmtrx( 5, 2)=    150.00000000
      cmtrx( 5, 3)=    245.00000000
```

```
      omtrx( 5, 4)=    305.00000000
      omtrx( 6, 1)=    460.00000000
      omtrx( 6, 2)=    540.00000000
      omtrx( 6, 3)=    630.00000000
      omtrx( 6, 4)=    630.00000000
      omtrx( 7, 1)=    300.00000000
      omtrx( 7, 2)=    370.00000000
      omtrx( 7, 3)=    440.00000000
      omtrx( 7, 4)=       .00000000
      omtrx( 8, 1)=    385.00000000
      omtrx( 8, 2)=    460.00000000
      omtrx( 8, 3)=    535.00000000
      omtrx( 8, 4)=       .00000000
      omtrx( 9, 1)=    150.00000000
      omtrx( 9, 2)=    150.00000000
      omtrx( 9, 3)=    245.00000000
      omtrx( 9, 4)=    305.00000000
c-----------------------------
        entry=radius
         icol= 1
         irow= 1
          exit=0.0
         call shape2test2 (mmtrx,icol,irow,entry,exit)
         ymu( 1, 1)=exit
c-----------------------------
        entry=radius
         icol= 2
         irow= 1
         exit=0.0
         call shape5test2 (mmtrx,icol,irow,entry,exit)
         ymu( 2, 1)=exit
c-----------------------------
        entry=radius
         icol= 3
         irow= 1
         exit=0.0
         call shape5test2 (mmtrx,icol,irow,entry,exit)
         ymu( 3, 1)=exit
c-----------------------------
        entry=radius
         icol= 4
         irow= 1
         exit=0.0
         call shape5test2 (mmtrx,icol,irow,entry,exit)
         ymu( 4, 1)=exit
c-----------------------------
        entry=radius
         icol= 5
         irow= 1
         exit=0.0
         call shape3test2 (mmtrx,icol,irow,entry,exit)
         ymu( 5, 1)=exit
c-----------------------------
        entry=direct
         icol= 6
         irow= 1
         exit=0.0
         call shape3test2 (mmtrx,icol,irow,entry,exit)
         ymu( 6, 1)=exit
c-----------------------------
        entry=frictn
```

```
          icol= 6
          irow= 5
          exit=0.0
          call shape3test2 (mmtrx,icol,irow,entry,exit)
          ymu( 6, 2)=exit
c-----------------------------
         entry=direct
          icol= 7
          irow= 1
           exit=0.0
          call shape2test2 (mmtrx,icol,irow,entry,exit)
          ymu( 7, 1)=exit
c-----------------------------
         entry=frictn
          icol= 7
          irow= 5
          exit=0.0
          call shape3test2 (mmtrx,icol,irow,entry,exit)
          ymu( 7, 2)=exit
c-----------------------------
         entry=direct
          icol= 8
          irow= 1
          exit=0.0
          call shape3test2 (mmtrx,icol,irow,entry,exit)
          ymu( 8, 1)=exit
c-----------------------------
         entry=frictn
          icol= 8
          irow= 5
           exit=0.0
          call shape2test2 (mmtrx,icol,irow,entry,exit)
          ymu( 8, 2)=exit
c-----------------------------
         entry=direct
          icol= 9
          irow= 1
           exit=0.0
          call shape2test2 (mmtrx,icol,irow,entry,exit)
          ymu( 9, 1)=exit
c-----------------------------
         entry=frictn
          icol= 9
          irow= 5
           exit=0.0
          call shape2test2 (mmtrx,icol,irow,entry,exit)
          ymu( 9, 2)=exit
c-----------------------------
        uz( 1)=ymu( 1,1)
        uz( 2)=ymu( 2,1)
        uz( 3)=ymu( 3,1)
        uz( 4)=ymu( 4,1)
        uz( 5)=ymu( 5,1)
          r1001=min(ymu( 6, 1),ymu( 6, 2))
          uz( 6)=r1001
          r1002=min(ymu( 7, 1),ymu( 7, 2))
          uz( 7)=r1002
          r1003=min(ymu( 8, 1),ymu( 8, 2))
          uz( 8)=r1003
          r1004=min(ymu( 9, 1),ymu( 9, 2))
          uz( 9)=r1004
```

```
c----------------------------
c  -> Raw Output
         j=  1
             shot=uz(j)
             irow=j
         call cut4test2 (omtrx,irow,shot,result,weight)
             r(j)=result
             area(j)=weight
c  -> Raw Output
         j=  2
             shot=uz(j)
             irow=j
         call cut3test2 (omtrx,irow,shot,result,weight)
             r(j)=result
             area(j)=weight
c  -> Raw Output
         j=  3
             shot=uz(j)
             irow=j
         call cut3test2 (omtrx,irow,shot,result,weight)
             r(j)=result
             area(j)=weight
c  -> Raw Output
         j=  4
             shot=uz(j)
             irow=j
         call cut3test2 (omtrx,irow,shot,result,weight)
             r(j)=result
             area(j)=weight
c-------------------------------------
c  -> Raw Output
         j=  5
             shot=uz(j)
             irow=j
         call cut4test2 (omtrx,irow,shot,result,weight)
             r(j)=result
             area(j)=weight
c-------------------------------------
c  -> Raw Output
         j=  6
             shot=uz(j)
             irow=j
         call cut4test2 (omtrx,irow,shot,result,weight)
             r(j)=result
             area(j)=weight
c  -> Raw Output
         j=  7
             shot=uz(j)
             irow=j
         call cut3test2 (omtrx,irow,shot,result,weight)
             r(j)=result
             area(j)=weight
c  -> Raw Output
         j=  8
             shot=uz(j)
             irow=j
         call cut3test2 (omtrx,irow,shot,result,weight)
             r(j)=result
             area(j)=weight
c-------------------------------------
c  -> Raw Output
```

```
        j=  9
            shot=uz(j)
            irow=j
        call cut4test2 (omtrx,irow,shot,result,weight)
            r(j)=result
            area(j)=weight
c-------------------
c-- output fused --
c-------------------
        aall=
     + area( 1)+
     + area( 2)+
     + area( 3)+
     + area( 4)+
     + area( 5)+
     + area( 6)+
     + area( 7)+
     + area( 8)+
     + area( 9)+
     + 0.0
        aalu=
     + area( 1)*r( 1)+
     + area( 2)*r( 2)+
     + area( 3)*r( 3)+
     + area( 4)*r( 4)+
     + area( 5)*r( 5)+
     + area( 6)*r( 6)+
     + area( 7)*r( 7)+
     + area( 8)*r( 8)+
     + area( 9)*r( 9)+
     + 0.0
        slope =0.0
        if (aall.ne.0.0) then
        slope =aalu/aall
        end if
        return
        end
c=====================
       subroutine shape2test2 (mmtrx,icol,irow,entry,exit)
        real mmtrx( 9,50),entry,exit
          if ((entry.gt.mmtrx(icol,irow+2)).and.
     &      (entry.lt.mmtrx(icol,irow+3))) then
               exit=(mmtrx(icol,irow+3)-entry)/
     &  (mmtrx(icol,irow+3)-mmtrx(icol,irow+2))
          end if
          if ((entry.gt.mmtrx(icol,irow+1)).and.
     &      (entry.le.mmtrx(icol,irow+2))) then
           exit=1.0
          end if
              return
                 end
c=====================
       subroutine shape3test2 (mmtrx,icol,irow,entry,exit)
        real mmtrx( 9,50),entry,exit
          if ((entry.lt.mmtrx(icol,irow+1)).and.
     &        (entry.gt.mmtrx(icol,irow))) then
                  exit=(entry-mmtrx(icol,irow))/
     &    (mmtrx(icol,irow+1)-mmtrx(icol,irow))
          end if
          if ((entry.ge.mmtrx(icol,irow+1)).and.
     &      (entry.lt.mmtrx(icol,irow+2))) then
```

```
          exit=1.0
         end if
             return
                end
c=====================
       subroutine shape5test2 (mmtrx,icol,irow,entry,exit)
        real mmtrx( 9,50),entry,exit
          if ((entry.le.mmtrx(icol,irow+1)).and.
     &         (entry.gt.mmtrx(icol,irow))) then
                  exit=(entry-mmtrx(icol,irow))/
     &    (mmtrx(icol,irow+1)-mmtrx(icol,irow))
          end if
          if ((entry.ge.mmtrx(icol,irow+1)).and.
     &       (entry.lt.mmtrx(icol,irow+2))) then
                  exit=(mmtrx(icol,irow+2)-entry)/
     &  (mmtrx(icol,irow+2)-mmtrx(icol,irow+1))
          end if
              return
                 end
c-------------------------------------------------
       subroutine cut4test2 (omtrx,irow,shot,result,weight)
        real omtrx( 9,50)
           x2p=shot*(omtrx(irow,2)-omtrx(irow,1))+omtrx(irow,1)
           x3p=omtrx(irow,4)-shot*(omtrx(irow,4)-omtrx(irow,3))
           a1=shot*0.5*(x2p-omtrx(irow,1))
           a2=shot*(x3p-x2p)
           a3=shot*0.5*(omtrx(irow,4)-x3p)
           if(shot.ne.0.0) then
           result=0.5*(x2p+x3p)+(a3-a1)*0.5/shot
           if(a1.gt.a2+a3) then
           result=omtrx(irow,1)+(x2p-omtrx(irow,1))*(a2+a3)/a1
           end if
           if(a3.gt.a2+a1) then
           result=x3p+(omtrx(irow,4)-x3p)*(a1+a2)/a3
           end if
           end if
           weight=a1+a2+a3
            return
            end
c-------------------------------------------------
       subroutine cut3test2 (omtrx,irow,shot,result,weight)
        real omtrx( 9,50)
           x2p=shot*(omtrx(irow,2)-omtrx(irow,1))+omtrx(irow,1)
           x3p=omtrx(irow,3)-shot*(omtrx(irow,3)-omtrx(irow,2))
           a1=shot*0.5*(x2p-omtrx(irow,1))
           a2=shot*(x3p-x2p)
           a3=shot*0.5*(omtrx(irow,3)-x3p)
          if(shot.ne.0.0) then
           result=0.5*(x2p+x3p)+(a3-a1)*0.5/shot
           if(a1.gt.a2+a3) then
           result=omtrx(irow,1)+(x2p-omtrx(irow,1))*(a2+a3)/a1
           end if
           if(a3.gt.a2+a1) then
           result=x3p+(omtrx(irow,3)-x3p)*(a1+a2)/a3
           end if
           end if
           weight=a1+a2+a3
            return
            end

c-----------------------------------------
```

```
        subroutine  test3 (age, cortex, sex, strng )
c-------------------------------------------
          real entry,exit
          real ymu(14,50)
          real mmtrx(14,50)
          real omtrx(14,4)
          real uz(14   )
          real r(14   )
          real area(14   )
          real age
          real cortex
          real sex
          real strng
c-----------------------------
       mmtrx( 1, 1)=     73.33334000
       mmtrx( 1, 2)=     84.16666000
       mmtrx( 1, 3)=     95.00000000
       mmtrx( 1, 4)=     95.00000000
       mmtrx( 2, 1)=      4.50000000
       mmtrx( 2, 2)=      4.50000000
       mmtrx( 2, 3)=      5.30000000
       mmtrx( 2, 4)=      5.70000000
       mmtrx( 3, 1)=      5.30000000
       mmtrx( 3, 2)=      5.65000000
       mmtrx( 3, 3)=      6.00000000
       mmtrx( 3, 4)=       .00000000
       mmtrx( 4, 1)=      5.70000000
       mmtrx( 4, 2)=      6.00000000
       mmtrx( 4, 3)=      6.30000000
       mmtrx( 4, 4)=       .00000000
       mmtrx( 5, 1)=      6.00000000
       mmtrx( 5, 2)=      6.35000000
       mmtrx( 5, 3)=      6.70000000
       mmtrx( 5, 4)=       .00000000
       mmtrx( 6, 1)=      6.30000000
       mmtrx( 6, 2)=      6.70000000
       mmtrx( 6, 3)=      7.50000000
       mmtrx( 6, 4)=      7.50000000
       mmtrx( 7, 1)=     30.00000000
       mmtrx( 7, 2)=     30.00000000
       mmtrx( 7, 3)=     40.83333000
       mmtrx( 7, 4)=     51.66666000
       mmtrx( 7, 5)=      -.66666670
       mmtrx( 7, 6)=       .66666660
       mmtrx( 7, 7)=      2.00000000
       mmtrx( 7, 8)=      2.00000000
       mmtrx( 8, 1)=     30.00000000
       mmtrx( 8, 2)=     30.00000000
       mmtrx( 8, 3)=     40.83333000
       mmtrx( 8, 4)=     51.66666000
       mmtrx( 8, 5)=     -2.00000000
       mmtrx( 8, 6)=     -2.00000000
       mmtrx( 8, 7)=      -.66666660
       mmtrx( 8, 8)=       .66666670
       mmtrx( 9, 1)=     40.83333000
       mmtrx( 9, 2)=     51.66666000
       mmtrx( 9, 3)=     62.50000000
       mmtrx( 9, 4)=       .00000000
       mmtrx( 9, 5)=      -.66666670
       mmtrx( 9, 6)=       .66666660
       mmtrx( 9, 7)=      2.00000000
```

```
      mmtrx( 9, 8)=      2.00000000
      mmtrx(10, 1)=     40.83333000
      mmtrx(10, 2)=     51.66666000
      mmtrx(10, 3)=     62.50000000
      mmtrx(10, 4)=       .00000000
      mmtrx(10, 5)=     -2.00000000
      mmtrx(10, 6)=     -2.00000000
      mmtrx(10, 7)=      -.66666660
      mmtrx(10, 8)=       .66666670
      mmtrx(11, 1)=     51.66666000
      mmtrx(11, 2)=     62.50000000
      mmtrx(11, 3)=     73.33333000
      mmtrx(11, 4)=       .00000000
      mmtrx(11, 5)=      -.66666670
      mmtrx(11, 6)=       .66666660
      mmtrx(11, 7)=      2.00000000
      mmtrx(11, 8)=      2.00000000
      mmtrx(12, 1)=     51.66666000
      mmtrx(12, 2)=     62.50000000
      mmtrx(12, 3)=     73.33333000
      mmtrx(12, 4)=       .00000000
      mmtrx(12, 5)=     -2.00000000
      mmtrx(12, 6)=     -2.00000000
      mmtrx(12, 7)=      -.66666660
      mmtrx(12, 8)=       .66666670
      mmtrx(13, 1)=     62.50000000
      mmtrx(13, 2)=     73.33333000
      mmtrx(13, 3)=     84.16666000
      mmtrx(13, 4)=       .00000000
      mmtrx(13, 5)=      -.66666670
      mmtrx(13, 6)=       .66666660
      mmtrx(13, 7)=      2.00000000
      mmtrx(13, 8)=      2.00000000
      mmtrx(14, 1)=     62.50000000
      mmtrx(14, 2)=     73.33333000
      mmtrx(14, 3)=     84.16666000
      mmtrx(14, 4)=       .00000000
      mmtrx(14, 5)=     -2.00000000
      mmtrx(14, 6)=     -2.00000000
      mmtrx(14, 7)=      -.66666660
      mmtrx(14, 8)=       .66666670
C-----------------------------
      omtrx( 1, 1)=       .00000000
      omtrx( 1, 2)=       .00000000
      omtrx( 1, 3)=   1500.00000000
      omtrx( 1, 4)=   3000.00000000
      omtrx( 2, 1)=       .00000000
      omtrx( 2, 2)=       .00000000
      omtrx( 2, 3)=   1500.00000000
      omtrx( 2, 4)=   3000.00000000
      omtrx( 3, 1)=   1500.00000000
      omtrx( 3, 2)=   3000.00000000
      omtrx( 3, 3)=   4500.00000000
      omtrx( 3, 4)=       .00000000
      omtrx( 4, 1)=   3000.00000000
      omtrx( 4, 2)=   4500.00000000
      omtrx( 4, 3)=   6000.00000000
      omtrx( 4, 4)=       .00000000
      omtrx( 5, 1)=   4500.00000000
      omtrx( 5, 2)=   6000.00000000
      omtrx( 5, 3)=   7500.00000000
```

```
      omtrx( 5, 4)=       .00000000
      omtrx( 6, 1)=   6000.00000000
      omtrx( 6, 2)=   7500.00000000
      omtrx( 6, 3)=   9000.00000000
      omtrx( 6, 4)=   9000.00000000
      omtrx( 7, 1)=   6000.00000000
      omtrx( 7, 2)=   7500.00000000
      omtrx( 7, 3)=   9000.00000000
      omtrx( 7, 4)=   9000.00000000
      omtrx( 8, 1)=   4500.00000000
      omtrx( 8, 2)=   6000.00000000
      omtrx( 8, 3)=   7500.00000000
      omtrx( 8, 4)=       .00000000
      omtrx( 9, 1)=   6000.00000000
      omtrx( 9, 2)=   7500.00000000
      omtrx( 9, 3)=   9000.00000000
      omtrx( 9, 4)=   9000.00000000
      omtrx(10, 1)=   3000.00000000
      omtrx(10, 2)=   4500.00000000
      omtrx(10, 3)=   6000.00000000
      omtrx(10, 4)=       .00000000
      omtrx(11, 1)=   4500.00000000
      omtrx(11, 2)=   6000.00000000
      omtrx(11, 3)=   7500.00000000
      omtrx(11, 4)=       .00000000
      omtrx(12, 1)=   1500.00000000
      omtrx(12, 2)=   3000.00000000
      omtrx(12, 3)=   4500.00000000
      omtrx(12, 4)=       .00000000
      omtrx(13, 1)=   1500.00000000
      omtrx(13, 2)=   3000.00000000
      omtrx(13, 3)=   4500.00000000
      omtrx(13, 4)=       .00000000
      omtrx(14, 1)=       .00000000
      omtrx(14, 2)=       .00000000
      omtrx(14, 3)=   1500.00000000
      omtrx(14, 4)=   3000.00000000
c-----------------------------
        entry=age
         icol= 1
         irow= 1
         exit=0.0
         call shape3test3 (mmtrx,icol,irow,entry,exit)
         ymu( 1, 1)=exit
c-----------------------------
        entry=cortex
         icol= 2
         irow= 1
          exit=0.0
         call shape2test3 (mmtrx,icol,irow,entry,exit)
         ymu( 2, 1)=exit
c-----------------------------
        entry=cortex
         icol= 3
         irow= 1
         exit=0.0
         call shape5test3 (mmtrx,icol,irow,entry,exit)
         ymu( 3, 1)=exit
c-----------------------------
        entry=cortex
         icol= 4
```

```
          irow= 1
          exit=0.0
          call shape5test3 (mmtrx,icol,irow,entry,exit)
          ymu( 4, 1)=exit
c-----------------------------
         entry=cortex
          icol= 5
          irow= 1
          exit=0.0
          call shape5test3 (mmtrx,icol,irow,entry,exit)
          ymu( 5, 1)=exit
c-----------------------------
         entry=cortex
          icol= 6
          irow= 1
          exit=0.0
          call shape3test3 (mmtrx,icol,irow,entry,exit)
          ymu( 6, 1)=exit
c-----------------------------
         entry=age
          icol= 7
          irow= 1
           exit=0.0
          call shape2test3 (mmtrx,icol,irow,entry,exit)
          ymu( 7, 1)=exit
c-----------------------------
         entry=sex
          icol= 7
          irow= 5
          exit=0.0
          call shape3test3 (mmtrx,icol,irow,entry,exit)
          ymu( 7, 2)=exit
c-----------------------------
         entry=age
          icol= 8
          irow= 1
           exit=0.0
          call shape2test3 (mmtrx,icol,irow,entry,exit)
          ymu( 8, 1)=exit
c-----------------------------
         entry=sex
          icol= 8
          irow= 5
           exit=0.0
          call shape2test3 (mmtrx,icol,irow,entry,exit)
          ymu( 8, 2)=exit
c-----------------------------
         entry=age
          icol= 9
          irow= 1
          exit=0.0
          call shape5test3 (mmtrx,icol,irow,entry,exit)
          ymu( 9, 1)=exit
c-----------------------------
         entry=sex
          icol= 9
          irow= 5
          exit=0.0
          call shape3test3 (mmtrx,icol,irow,entry,exit)
          ymu( 9, 2)=exit
c-----------------------------
```

```
          entry=age
           icol=10
           irow= 1
           exit=0.0
           call shape5test3 (mmtrx,icol,irow,entry,exit)
           ymu(10, 1)=exit
c-----------------------------
          entry=sex
           icol=10
           irow= 5
            exit=0.0
           call shape2test3 (mmtrx,icol,irow,entry,exit)
           ymu(10, 2)=exit
c-----------------------------
          entry=age
           icol=11
           irow= 1
           exit=0.0
           call shape5test3 (mmtrx,icol,irow,entry,exit)
           ymu(11, 1)=exit
c-----------------------------
          entry=sex
           icol=11
           irow= 5
           exit=0.0
           call shape3test3 (mmtrx,icol,irow,entry,exit)
           ymu(11, 2)=exit
c-----------------------------
          entry=age
           icol=12
           irow= 1
           exit=0.0
           call shape5test3 (mmtrx,icol,irow,entry,exit)
           ymu(12, 1)=exit
c-----------------------------
          entry=sex
           icol=12
           irow= 5
            exit=0.0
           call shape2test3 (mmtrx,icol,irow,entry,exit)
           ymu(12, 2)=exit
c-----------------------------
          entry=age
           icol=13
           irow= 1
           exit=0.0
           call shape5test3 (mmtrx,icol,irow,entry,exit)
           ymu(13, 1)=exit
c-----------------------------
          entry=sex
           icol=13
           irow= 5
           exit=0.0
           call shape3test3 (mmtrx,icol,irow,entry,exit)
           ymu(13, 2)=exit
c-----------------------------
          entry=age
           icol=14
           irow= 1
           exit=0.0
           call shape5test3 (mmtrx,icol,irow,entry,exit)
```

```
          ymu(14, 1)=exit
c-----------------------------
          entry=sex
           icol=14
           irow= 5
            exit=0.0
           call shape2test3 (mmtrx,icol,irow,entry,exit)
           ymu(14, 2)=exit
c-----------------------------
         uz( 1)=ymu( 1,1)
         uz( 2)=ymu( 2,1)
         uz( 3)=ymu( 3,1)
         uz( 4)=ymu( 4,1)
         uz( 5)=ymu( 5,1)
         uz( 6)=ymu( 6,1)
           r1001=min(ymu( 7, 1),ymu( 7, 2))
           uz( 7)=r1001
           r1002=min(ymu( 8, 1),ymu( 8, 2))
           uz( 8)=r1002
           r1003=min(ymu( 9, 1),ymu( 9, 2))
           uz( 9)=r1003
           r1004=min(ymu(10, 1),ymu(10, 2))
           uz(10)=r1004
           r1005=min(ymu(11, 1),ymu(11, 2))
           uz(11)=r1005
           r1006=min(ymu(12, 1),ymu(12, 2))
           uz(12)=r1006
           r1007=min(ymu(13, 1),ymu(13, 2))
           uz(13)=r1007
           r1008=min(ymu(14, 1),ymu(14, 2))
           uz(14)=r1008
c-----------------------------
c  -> Raw Output
         j=  1
             shot=uz(j)
             irow=j
         call cut4test3 (omtrx,irow,shot,result,weight)
             r(j)=result
             area(j)=weight
c--------------------------------------
c  -> Raw Output
         j=  2
             shot=uz(j)
             irow=j
         call cut4test3 (omtrx,irow,shot,result,weight)
             r(j)=result
             area(j)=weight
c  -> Raw Output
         j=  3
             shot=uz(j)
             irow=j
         call cut3test3 (omtrx,irow,shot,result,weight)
             r(j)=result
             area(j)=weight
c  -> Raw Output
         j=  4
             shot=uz(j)
             irow=j
         call cut3test3 (omtrx,irow,shot,result,weight)
             r(j)=result
             area(j)=weight
```

```
c  -> Raw Output
        j=  5
            shot=uz(j)
            irow=j
        call cut3test3 (omtrx,irow,shot,result,weight)
            r(j)=result
            area(j)=weight
c---------------------------------------
c  -> Raw Output
        j=  6
            shot=uz(j)
            irow=j
        call cut4test3 (omtrx,irow,shot,result,weight)
            r(j)=result
            area(j)=weight
c---------------------------------------
c  -> Raw Output
        j=  7
            shot=uz(j)
            irow=j
        call cut4test3 (omtrx,irow,shot,result,weight)
            r(j)=result
            area(j)=weight
c  -> Raw Output
        j=  8
            shot=uz(j)
            irow=j
        call cut3test3 (omtrx,irow,shot,result,weight)
            r(j)=result
            area(j)=weight
c---------------------------------------
c  -> Raw Output
        j=  9
            shot=uz(j)
            irow=j
        call cut4test3 (omtrx,irow,shot,result,weight)
            r(j)=result
            area(j)=weight
c  -> Raw Output
        j= 10
            shot=uz(j)
            irow=j
        call cut3test3 (omtrx,irow,shot,result,weight)
            r(j)=result
            area(j)=weight
c  -> Raw Output
        j= 11
            shot=uz(j)
            irow=j
        call cut3test3 (omtrx,irow,shot,result,weight)
            r(j)=result
            area(j)=weight
c  -> Raw Output
        j= 12
            shot=uz(j)
            irow=j
        call cut3test3 (omtrx,irow,shot,result,weight)
            r(j)=result
            area(j)=weight
c  -> Raw Output
        j= 13
```

```
            shot=uz(j)
            irow=j
          call cut3test3 (omtrx,irow,shot,result,weight)
            r(j)=result
            area(j)=weight
c---------------------------------------
c  -> Raw Output
          j= 14
            shot=uz(j)
            irow=j
          call cut4test3 (omtrx,irow,shot,result,weight)
            r(j)=result
            area(j)=weight
c-------------------
c-- output fused --
c-------------------
          aall=
     + area( 1)+
     + area( 2)+
     + area( 3)+
     + area( 4)+
     + area( 5)+
     + area( 6)+
     + area( 7)+
     + area( 8)+
     + area( 9)+
     + area(10)+
     + area(11)+
     + area(12)+
     + area(13)+
     + area(14)+
     + 0.0
          aalu=
     + area( 1)*r( 1)+
     + area( 2)*r( 2)+
     + area( 3)*r( 3)+
     + area( 4)*r( 4)+
     + area( 5)*r( 5)+
     + area( 6)*r( 6)+
     + area( 7)*r( 7)+
     + area( 8)*r( 8)+
     + area( 9)*r( 9)+
     + area(10)*r(10)+
     + area(11)*r(11)+
     + area(12)*r(12)+
     + area(13)*r(13)+
     + area(14)*r(14)+
     + 0.0
          strng =0.0
          if (aall.ne.0.0) then
          strng =aalu/aall
          end if
          return
          end
c=====================
        subroutine shape2test3 (mmtrx,icol,irow,entry,exit)
          real mmtrx(14,50),entry,exit
            if ((entry.gt.mmtrx(icol,irow+2)).and.
     &        (entry.lt.mmtrx(icol,irow+3))) then
                exit=(mmtrx(icol,irow+3)-entry)/
     &   (mmtrx(icol,irow+3)-mmtrx(icol,irow+2))
```

```
          end if
          if ((entry.gt.mmtrx(icol,irow+1)).and.
     &      (entry.le.mmtrx(icol,irow+2))) then
           exit=1.0
          end if
              return
                 end
c=======================
        subroutine shape3test3 (mmtrx,icol,irow,entry,exit)
         real mmtrx(14,50),entry,exit
           if ((entry.lt.mmtrx(icol,irow+1)).and.
     &         (entry.gt.mmtrx(icol,irow))) then
                   exit=(entry-mmtrx(icol,irow))/
     &    (mmtrx(icol,irow+1)-mmtrx(icol,irow))
          end if
          if ((entry.ge.mmtrx(icol,irow+1)).and.
     &      (entry.lt.mmtrx(icol,irow+2))) then
           exit=1.0
          end if
              return
                 end
c=======================
        subroutine shape5test3 (mmtrx,icol,irow,entry,exit)
         real mmtrx(14,50),entry,exit
           if ((entry.le.mmtrx(icol,irow+1)).and.
     &         (entry.gt.mmtrx(icol,irow))) then
                   exit=(entry-mmtrx(icol,irow))/
     &    (mmtrx(icol,irow+1)-mmtrx(icol,irow))
          end if
          if ((entry.ge.mmtrx(icol,irow+1)).and.
     &      (entry.lt.mmtrx(icol,irow+2))) then
                   exit=(mmtrx(icol,irow+2)-entry)/
     &  (mmtrx(icol,irow+2)-mmtrx(icol,irow+1))
           end if
              return
                 end
c-------------------------------------------------
        subroutine cut4test3 (omtrx,irow,shot,result,weight)
         real omtrx(14,50)
            x2p=shot*(omtrx(irow,2)-omtrx(irow,1))+omtrx(irow,1)
            x3p=omtrx(irow,4)-shot*(omtrx(irow,4)-omtrx(irow,3))
            a1=shot*0.5*(x2p-omtrx(irow,1))
            a2=shot*(x3p-x2p)
            a3=shot*0.5*(omtrx(irow,4)-x3p)
            if(shot.ne.0.0) then
            result=0.5*(x2p+x3p)+(a3-a1)*0.5/shot
            if(a1.gt.a2+a3) then
            result=omtrx(irow,1)+(x2p-omtrx(irow,1))*(a2+a3)/a1
            end if
            if(a3.gt.a2+a1) then
            result=x3p+(omtrx(irow,4)-x3p)*(a1+a2)/a3
            end if
            end if
            weight=a1+a2+a3
             return
             end
c-------------------------------------------------
        subroutine cut3test3 (omtrx,irow,shot,result,weight)
         real omtrx(14,50)
            x2p=shot*(omtrx(irow,2)-omtrx(irow,1))+omtrx(irow,1)
            x3p=omtrx(irow,3)-shot*(omtrx(irow,3)-omtrx(irow,2))
```

```
          a1=shot*0.5*(x2p-omtrx(irow,1))
          a2=shot*(x3p-x2p)
          a3=shot*0.5*(omtrx(irow,3)-x3p)
         if(shot.ne.0.0) then
          result=0.5*(x2p+x3p)+(a3-a1)*0.5/shot
          if(a1.gt.a2+a3) then
          result=omtrx(irow,1)+(x2p-omtrx(irow,1))*(a2+a3)/a1
          end if
          if(a3.gt.a2+a1) then
          result=x3p+(omtrx(irow,3)-x3p)*(a1+a2)/a3
          end if
          end if
          weight=a1+a2+a3
           return
           end

c-------------------------------------------
        subroutine  test4 (diffrn, possib)
c-------------------------------------------
          real entry,exit
          real ymu( 5,50)
          real mmtrx( 5,50)
          real omtrx( 5,4)
          real uz( 5   )
          real r( 5   )
          real area( 5   )
          real diffrn
          real possib
c----------------------------
       mmtrx( 1, 1)=  -7500.00000000
       mmtrx( 1, 2)=  -7500.00000000
       mmtrx( 1, 3)=  -4000.00000000
       mmtrx( 1, 4)=  -2000.00000000
       mmtrx( 2, 1)=  -4000.00000000
       mmtrx( 2, 2)=  -2000.00000000
       mmtrx( 2, 3)=       .00000000
       mmtrx( 2, 4)=       .00000000
       mmtrx( 3, 1)=  -2000.00000000
       mmtrx( 3, 2)=       .00000000
       mmtrx( 3, 3)=   2000.00000000
       mmtrx( 3, 4)=       .00000000
       mmtrx( 4, 1)=       .00000000
       mmtrx( 4, 2)=   2000.00000000
       mmtrx( 4, 3)=   4000.00000000
       mmtrx( 4, 4)=       .00000000
       mmtrx( 5, 1)=   2000.00000000
       mmtrx( 5, 2)=   4000.00000000
       mmtrx( 5, 3)=   7500.00000000
       mmtrx( 5, 4)=   7500.00000000
c----------------------------
       omtrx( 1, 1)=    -16.66666000
       omtrx( 1, 2)=    -16.66666000
       omtrx( 1, 3)=      5.55555900
       omtrx( 1, 4)=     27.77778000
       omtrx( 2, 1)=      5.55555900
       omtrx( 2, 2)=     27.77778000
       omtrx( 2, 3)=     50.00000000
       omtrx( 2, 4)=       .00000000
       omtrx( 3, 1)=     27.77778000
       omtrx( 3, 2)=     50.00000000
       omtrx( 3, 3)=     72.22221000
```

```
       omtrx( 3, 4)=       .00000000
       omtrx( 4, 1)=     50.00000000
       omtrx( 4, 2)=     72.22221000
       omtrx( 4, 3)=     94.44444000
       omtrx( 4, 4)=       .00000000
       omtrx( 5, 1)=     72.22221000
       omtrx( 5, 2)=     94.44444000
       omtrx( 5, 3)=    116.66670000
       omtrx( 5, 4)=    116.66670000
c-----------------------------
         entry=diffrn
          icol= 1
          irow= 1
           exit=0.0
          call shape2test4 (mmtrx,icol,irow,entry,exit)
          ymu( 1, 1)=exit
c-----------------------------
         entry=diffrn
          icol= 2
          irow= 1
          exit=0.0
          call shape5test4 (mmtrx,icol,irow,entry,exit)
          ymu( 2, 1)=exit
c-----------------------------
         entry=diffrn
          icol= 3
          irow= 1
          exit=0.0
          call shape5test4 (mmtrx,icol,irow,entry,exit)
          ymu( 3, 1)=exit
c-----------------------------
         entry=diffrn
          icol= 4
          irow= 1
          exit=0.0
          call shape5test4 (mmtrx,icol,irow,entry,exit)
          ymu( 4, 1)=exit
c-----------------------------
         entry=diffrn
          icol= 5
          irow= 1
          exit=0.0
          call shape3test4 (mmtrx,icol,irow,entry,exit)
          ymu( 5, 1)=exit
c-----------------------------
        uz( 1)=ymu( 1,1)
        uz( 2)=ymu( 2,1)
        uz( 3)=ymu( 3,1)
        uz( 4)=ymu( 4,1)
        uz( 5)=ymu( 5,1)
c-----------------------------
c  -> Raw Output
        j=  1
            shot=uz(j)
            irow=j
        call cut4test4 (omtrx,irow,shot,result,weight)
            r(j)=result
            area(j)=weight
c  -> Raw Output
        j=  2
            shot=uz(j)
```

```
            irow=j
          call cut3test4 (omtrx,irow,shot,result,weight)
              r(j)=result
              area(j)=weight
c  -> Raw Output
          j=  3
              shot=uz(j)
              irow=j
          call cut3test4 (omtrx,irow,shot,result,weight)
              r(j)=result
              area(j)=weight
c  -> Raw Output
          j=  4
              shot=uz(j)
              irow=j
          call cut3test4 (omtrx,irow,shot,result,weight)
              r(j)=result
              area(j)=weight
c-------------------------------------
c  -> Raw Output
          j=  5
              shot=uz(j)
              irow=j
          call cut4test4 (omtrx,irow,shot,result,weight)
              r(j)=result
              area(j)=weight
c-------------------
c-- output fused --
c-------------------
          aall=
     + area( 1)+
     + area( 2)+
     + area( 3)+
     + area( 4)+
     + area( 5)+
     + 0.0
          aalu=
     + area( 1)*r( 1)+
     + area( 2)*r( 2)+
     + area( 3)*r( 3)+
     + area( 4)*r( 4)+
     + area( 5)*r( 5)+
     + 0.0
          possib=0.0
          if (aall.ne.0.0) then
          possib=aalu/aall
          end if
          return
          end
c=====================
        subroutine shape2test4 (mmtrx,icol,irow,entry,exit)
          real mmtrx( 5,50),entry,exit
            if ((entry.gt.mmtrx(icol,irow+2)).and.
     &        (entry.lt.mmtrx(icol,irow+3))) then
                  exit=(mmtrx(icol,irow+3)-entry)/
     &   (mmtrx(icol,irow+3)-mmtrx(icol,irow+2))
            end if
            if ((entry.gt.mmtrx(icol,irow+1)).and.
     &        (entry.le.mmtrx(icol,irow+2))) then
           exit=1.0
          end if
```

```
            return
               end
c=====================
      subroutine shape3test4 (mmtrx,icol,irow,entry,exit)
       real mmtrx( 5,50),entry,exit
         if ((entry.lt.mmtrx(icol,irow+1)).and.
     &        (entry.gt.mmtrx(icol,irow))) then
                exit=(entry-mmtrx(icol,irow))/
     &    (mmtrx(icol,irow+1)-mmtrx(icol,irow))
         end if
         if ((entry.ge.mmtrx(icol,irow+1)).and.
     &      (entry.lt.mmtrx(icol,irow+2))) then
          exit=1.0
         end if
            return
               end
c=====================
      subroutine shape5test4 (mmtrx,icol,irow,entry,exit)
       real mmtrx( 5,50),entry,exit
         if ((entry.le.mmtrx(icol,irow+1)).and.
     &        (entry.gt.mmtrx(icol,irow))) then
                exit=(entry-mmtrx(icol,irow))/
     &    (mmtrx(icol,irow+1)-mmtrx(icol,irow))
         end if
         if ((entry.ge.mmtrx(icol,irow+1)).and.
     &      (entry.lt.mmtrx(icol,irow+2))) then
                exit=(mmtrx(icol,irow+2)-entry)/
     &  (mmtrx(icol,irow+2)-mmtrx(icol,irow+1))
         end if
            return
               end
c-----------------------------------------------
      subroutine cut4test4 (omtrx,irow,shot,result,weight)
       real omtrx( 5,50)
          x2p=shot*(omtrx(irow,2)-omtrx(irow,1))+omtrx(irow,1)
          x3p=omtrx(irow,4)-shot*(omtrx(irow,4)-omtrx(irow,3))
          a1=shot*0.5*(x2p-omtrx(irow,1))
          a2=shot*(x3p-x2p)
          a3=shot*0.5*(omtrx(irow,4)-x3p)
          if(shot.ne.0.0) then
          result=0.5*(x2p+x3p)+(a3-a1)*0.5/shot
          if(a1.gt.a2+a3) then
          result=omtrx(irow,1)+(x2p-omtrx(irow,1))*(a2+a3)/a1
          end if
          if(a3.gt.a2+a1) then
          result=x3p+(omtrx(irow,4)-x3p)*(a1+a2)/a3
          end if
          end if
          weight=a1+a2+a3
           return
           end
c-----------------------------------------------
      subroutine cut3test4 (omtrx,irow,shot,result,weight)
       real omtrx( 5,50)
          x2p=shot*(omtrx(irow,2)-omtrx(irow,1))+omtrx(irow,1)
          x3p=omtrx(irow,3)-shot*(omtrx(irow,3)-omtrx(irow,2))
          a1=shot*0.5*(x2p-omtrx(irow,1))
          a2=shot*(x3p-x2p)
          a3=shot*0.5*(omtrx(irow,3)-x3p)
         if(shot.ne.0.0) then
          result=0.5*(x2p+x3p)+(a3-a1)*0.5/shot
```

```
if(a1.gt.a2+a3) then
result=omtrx(irow,1)+(x2p-omtrx(irow,1))*(a2+a3)/a1
end if
if(a3.gt.a2+a1) then
result=x3p+(omtrx(irow,3)-x3p)*(a1+a2)/a3
end if
end if
weight=a1+a2+a3
 return
 end
```

VITA

Taisuke Akasaka was born on July 5, 1964 in Misawa city, Japan. Misawa is located at the northern end of Honshyu, the main island of Japan. In Misawa, U.S. Air Force base and Japanese Self Defence Air Force are stationed side by side. Being raised in Misawa, he was always curious about the United States and their people. After graduating from Hachinohe High School, he entered Nihon University at Chiba Japan in 1983. During the summer of that year, he gained a chance to go to the University of Tennessee at Martin as one of the exchange students. That was his first experience abroad. Although he had no relatives in the states and spoke no fluent English, he had no difficulties making friends because of the sincere welcome of the town people. With the help of teachers and friends at UTM, he was able to pass the English proficiency examination required for foreign students before returning to Japan. In the winter of 1985, he returned to UTM to be a regular student. In 1986, he transferred to the University of Tennessee, Knoxville. He graduated from the University of Tennessee with a Bachelor of Science degree in the spring of 1989. During his undergraduate years, he was awarded by Tau Bata Pi Society and Golden Key Society. In the fall of 1989, he entered the graduate school program to join the research project sponsored by Japan Automobile Manufacturers' Association at Engineering Science Department. In December of 1993, he received his Master of Science Degree in Engineering Science.